Mathematisches Forschungsinstitut Oberwolfach

Report No. 07/2010

DOI: 10.4171/OWR/2010/07

New Directions in Simulation, Control and Analysis for Interfaces and Free Boundaries

Organised by
Charles M. Elliott, Warwick
Yoshikazu Giga, Tokyo
Michael Hinze, Hamburg
Vanessa Styles, Brighton

January 31st – February 6th, 2010

Abstract. The field of mathematical and numerical analysis of systems of nonlinear partial differential equations involving interfaces and free boundaries is a flourishing area of research. Many such systems arise from mathematical models in material science, fluid dynamics and biology, for example phase separation in alloys, epitaxial growth, dynamics of multiphase fluids, evolution of cell membranes and in industrial processes such as crystal growth. The governing equations for the dynamics of the interfaces in many of these applications involve surface tension expressed in terms of the mean curvature and a driving force. Here the forcing terms depend on variables that are solutions of additional partial differential equations which hold either on the interface itself or in the surrounding bulk regions. Often in applications of these mathematical models, suitable performance indices and appropriate control actions have to be specified. Mathematically this leads to optimization problems with partial differential equation constraints including free boundaries. Because of the maturity of the field of computational free boundary problems it is now timely to consider such control problems.

In order to carry out design, control and simulation of such problems interaction is required between distinct mathematical fields such as analysis, modeling, computation and optimization. By bringing together leading experts and young researchers from these separate fields we intended to develop novel research directions in applied and computational mathematics. The aim of the workshop here was to focus on emerging new themes and developments in these fields and to establish and extend links between them.

Mathematics Subject Classification (2000): MSC: 35-XX, 49-XX, 65-XX IMU: 11, 16, 17.

Introduction by the Organisers

The meeting was attended by 53 participants from Austria, Belgium, China, France, Germany, Great Britain, Japan, Portugal, Spain and the United States, with expertise from three main areas: optimal control of partial differential equations, modeling involving free boundary problems and mathematical and numerical analysis of free boundary problems. Apart from discussing current problems, techniques and issues across the differing communities the focus of the workshop was set on developing the necessary analytical and numerical techniques required to successfully tackle new emerging classes of problems related to the following themes:

(1) Computational and analytical approaches to interfaces and free boundaries,
(2) Control and optimization of interfaces and free boundaries,
(3) Numerical treatment and control of surface partial differential equations.

The presentations of Abels, Asai, Bellettini, Bothe, Garcke, Giga, Kohsaka, Niethammer, Röger and Santosa concerned analytical approaches to interfaces and free boundaries. While Feng, Kornhuber, Nürnberg, Pozzi, Reusken, A. Schmidt, Stoll, and Tobiska gave talks on numerical approaches to interfaces and free boundaries. Control and optimization with focus on interfaces and free boundaries was the subject of the talks of Bernauer, Casas, Deckelnick, Günther, Hintermüller, Raymond, S. Schmidt, Siebert, Vierling and Yan. Elliott gave a survey talk on the treatment of surface partial differential equations with surface finite elements, and Voigt, in his talk, introduced a diffuse-interface approach for the numerical treatment of coupled bulk/surface partial differential equations. Finally, Sprekels, in his talk, reported on the state of the art of mathematical and technical achievements in Czochralski crystal growth. This method may be considered a model application containing many of the topics considered within the workshop.

To offer young researchers a stage for presenting their research, a young researcher session was organized on Wednesday evening where the Heizaemon Honda Scholar Asai together with the Oberwolfach Leibniz Graduate Students Bernauer, Günther, S. Schmidt, and Vierling took this opportunity and gave talks on their current research results.

Surveys and articles concerning mathematical and numerical approaches to interfaces and free boundary problems may be found in the conference proceedings [5, 6, 2, 8]. The level set approach to related problems of optimal design are surveyed in [3]. The book [1] contains theoretical results for optimal control of variational inequalities. Modern mathematical concepts of control and optimization with partial differential equation constraints are developed in the book [7]. Also we mention a survey of numerical methods for interface evolution involving curvature, [4]. Finally we remark that many recent references concerning the issues of the workshop are provided at the end of the each extended abstract.

Acknowledgement: The organizers would like to thank Professor Karl Heinz Hoffmann for many fruitful discussions in the run-up to the application for this Oberwolfach workshop.

References

[1] V. Barbu *Optimal control of Variational Inequalities* Pitman Research Notes in Mathematics **100** Pitman Boston London Melbourne (1984).

[2] A. Bossavit, A. Damlamian and M. Fremond (editors) *Free Boundary Problems: applications and theory* Pitman Research Notes in Mathematics **121** Pitman Boston London Melbourne (1985).

[3] M. Burger and S. Osher *A survey on level set methods for inverse problems and optimal design* Euro. J. Appl. Math. **16** (2005) 263–301.

[4] K.P. Deckelnick, G. Dziuk and C.M. Elliott *Computation of Geometric PDEs and Mean Curvature Flow* Acta Numerica (2005) 139–232.

[5] C.M. Elliott and J.R. Ockendon *Weak and variational methods for moving boundary problems.* Pitman Research Notes in Mathematics **59** Pitman Boston London Melbourne (1982).

[6] A. Fasano and M. Primicerio (editors) *Free Boundary Problems, Theory Applications* Pitman Research Notes in Mathematics **79** Pitman Boston London Melbourne (1983).

[7] M. Hinze, R. Pinnau, M. Ulbrich, S. Ulbrich *Optimization with PDE constraints* MMTA 23, Springer (2009).

[8] K.H. Hoffman and J. Sprekels (editors) *Free Boundary Problems, Theory and Applications* Pitman Research Notes in Mathematics **186** Pitman Boston London Melbourne (1990).

Workshop: New Directions in Simulation, Control and Analysis for Interfaces and Free Boundaries

Table of Contents

T. Asai, M. Bernauer, A. Günther, S. Schmidt, M. Vierling
Young researcher Session 261

Helmut Abels
Sharp and Diffuse Interface Models for Two-Phase Flows of Viscous Incompressible Fluids 262

Giovanni Bellettini (joint with M. Novaga and G. Orlandi)
Minimal timelike lorentzian submanifolds as limits of singularly perturbed wave equations 265

Dieter Bothe (joint with Jan Prüss)
Transport processes at fluidic interfaces 266

Eduardo Casas
Optimal Control of PDEs. Topics and Methods 268

Klaus Deckelnick (joint with C.M. Elliott and V. Styles)
An arrival time inverse problem for the eikonal equation 269

Charlie Elliott (joint with Bjoern Stinner)
Surface finite elements for two phase geometric biomembranes 271

Xiaobing Feng (joint with Andreas Prohl, Haijun Wu)
Exponential-free a priori and a posteriori error estimates for finite element approximations of diffuse interface equations for surface evolution 272

Harald Garcke (joint with Stefan Schaubeck)
The Stefan Problem with anisotropic Gibbs–Thomson law 275

Yoshikazu Giga (joint with Robert V. Kohn, Courant–NYU)
On scale–independent extinction time estimates for total variation flows 278

M. Hintermüller (joint with I. Kopacka)
Optimal Control of Variational Inequalties: Stationarity; -ies and Numerics 279

Yoshihito Kohsaka (joint with Harald Garcke, Kazuo Ito)
Motion of phase boundaries by geometric evolution equations 283

Ralf Kornhuber (joint with Carsten Gräser, Uli Sack)
Nonsmooth Schur Newton Methods for Nonsmooth Saddle Point Problems 286

Barbara Niethammer (joint with A. Münch, D. Peschka)
Self-similar rupture in thin films with slip 287

Robert Nürnberg (joint with John W. Barrett, Harald Garcke)
Parametric approximation of geometric evolution equations and applications to the modelling of snowflake growth 288

Takeshi Ohtsuka
Level set method for spiral crystal growth and surface evolution 291

P. Pozzi
FEM approximation of the anisotropic mean curvature flow in higher codimension 295

Jean-Pierre Raymond
Stabilization of a fluid – structure model 295

Arnold Reusken (joint with P. Esser, J. Grande, S. Groß, M. Olshanskii)
Numerical methods for surfactant transport in two-phase incompressible flows 298

Matthias Röger (joint with L. Mugnai)
The Allen–Cahn action functional and forced mean curvature flow 301

Fadil Santosa (joint with Selim Esedoḡlu)
An Analysis of a Bar Code Deconvolution Problem 302

Alfred Schmidt (joint with Eberhard Bänsch, Thilo Moshagen, and Jordi Paul)
Finite element simulation of solid-liquid phase transitions with a free melt surface 304

Stephan Schmidt (joint with Volker Schulz)
Large Scale Aerodynamic Shape Optimization 307

Kunibert G. Siebert (joint with Kristina Kohls and Arnd Rösch)
Analysis of Adaptive Finite Elements for Control Constrained Optimal Control Problems 308

Jürgen Sprekels (joint with Wolfgang Dreyer (WIAS Berlin), P.-E. Druet (WIAS Berlin), O. Klein (WIAS Berlin), F. Tröltzsch (TU Berlin), I. Yousept (TU Berlin))
Technical and Mathematical Problems in the Czochralski Growth of Single Crystals 312

Martin Stoll (joint with Lavinia Sarbu, Luise Blank)
Preconditioning for Allen-Cahn variational inequalities with non-local constraints 314

Lutz Tobiska (joint with Sashikumaar Ganesan)
Finite element methods for interface flows with surfactants 315

Ningning Yan (joint with Duan Wang and Ruo Li)
Anisotropic adaptive finite element methds for interface problems 317

Axel Voigt (joint with Sebastian Aland, Andreas Rätz, John Lowengrub)
A diffuse-interface approach for solving coupled bulk/surface PDEs in complex evolving domains 319

Abstracts

Young researcher Session

T. Asai, M. Bernauer, A. Günther, S. Schmidt, M. Vierling

Tomoro Asai: *On the smoothing effect for higher order curvature flow equations* We constructed a local unique smooth solution starting from a rough initial curve for higher order curvature flow equations including the surface diffusion flow and the Willmore flow. The initial curvature is allowed to be discontinuous. For this purpose we develop an abstract theory for quasilinear parabolic equations based on the theory of analytic semigroups. We estimate lower order terms in a careful way which leads a strong smoothing effect of higher order curvature flow equations.

Martin K. Bernauer (joint with Roland Herzog & Karl Kunisch): *Optimal Control of the Two-Phase Stefan Problem in Level Set Formulation* Motion planning problems for the two-phase Stefan problem are considered. A level set representation of the moving interface is used. First order optimality conditions are derived using shape calculus. The approximation of the forward and adjoint systems relies on the X-FEM and discontinuous Galerkin schemes. Numerical examples are included.

Andreas Günther (joint with M.H. Tber): *A goal-oriented adaptive Moreau-Yosida algorithm for control- and state-constrained elliptic optimal control problems* We consider adaptive finite elements for distributed optimal control problems governed by elliptic partial differential equations. Of particular interest is the tailored design of goal-oriented adaptive meshes under additional control- and state-constraints. The latter ones are regularized by a Moreau-Yosida penalization. Throughout our investigations we use piecewise linear finite elements for the state variable while the control is not discretized. This technique in particular results in the absence of control residuals in error representations. Our findings are confirmed by numerical experiments.

Stephan Schmidt (joint with Volker Schulz): *Large Scale Aerodynamic Shape Optimization* The talk presents the problem of aerodynamic shape optimization as a free boundary problem. First, a very brief overview on shape optimization is given. Next, incompressible fluids are considered. The gradient in Hadamard form is derived for a general incompressible Navier-Stokes problem. Afterwards, the shape Hessian is analyzed and found to have an operator symbol similar to the Dirichlet-to-Neumann map. The talk concludes with the optimization of an Onera M6 flying wing using the compressible Euler equations to model the fluid. Due to using the Hadamard form of the gradient, a very large scale morphing of shapes is possible.

Morten Vierling: *An optimal order error bound for state constrained optimal control problems* We consider the variational discretization of a linear–quadratic optimal control problem with pointwise control and state constraints. In order to allow for a Fréchet smooth norm, the problem is reformulated by means of the

reflexive space $W^{1,p}(\Omega)$ instead of $C(\bar{\Omega})$. The discretization of the state equation yields a family of perturbed optimal control problems, whose solutions can be computed numerically. Assuming a Slater condition, we apply an implicit multifunction theorem to the first order necessary conditions to proof a bound on the perturbation error for these solutions. In the special case of an elliptic state equation in $\Omega \subset \mathbb{R}^2$ undergoing a simple finite element discretization we obtain convergence of order $O(h)$.

Sharp and Diffuse Interface Models for Two-Phase Flows of Viscous Incompressible Fluids

Helmut Abels

We consider a two-phase flow of two viscous incompressible Newtonian fluids of the same density filling a domain $\Omega \subseteq \mathbb{R}^d$, $d = 2, 3$. In classical models the interface between both fluids is modeled as a $(d-1)$-dimensional surface $\Gamma(t)$. – Such a model will be called *sharp interface model* in the following. – The surface energy associated to the interface is $\sigma \mathcal{H}^{d-1}(\Gamma(t))$, where $\mathcal{H}^{d-1}$ denotes the $(d-1)$-dimensional Hausdorff measure and σ is a (constant) surface tension coefficient. The presence of a surface energy causes an extra contribution to the inner forces/the stress tensor, which is proportional to the mean curvature of the interface and described by the Young-Laplace law (7) below.

On the other hand in so-called diffuse interface model for such a two-phase flow a partial mixing of the macroscopically immiscible fluids in a small interfacial region is assumed in the model. Additionally, diffusion of both components is taken into account. This leads to a coupled Navier-Stokes/Cahn-Hilliard system, which is capable to describe the evolution of droplet formation and collision during the flow consistently and reads as follows:

$$\partial_t v + v \cdot \nabla v - \underbrace{\operatorname{div}(\nu(c) Dv)}_{\text{inner friction}} + \nabla p = \underbrace{-\varepsilon \operatorname{div}(\nabla c \otimes \nabla c)}_{\text{surface tension}} \tag{1}$$

$$\operatorname{div} v = 0 \tag{2}$$

$$\partial_t c + v \cdot \nabla c = m \Delta \mu \tag{3}$$

$$\mu = \frac{\delta E_\varepsilon}{\delta c} = -\varepsilon \Delta c + \varepsilon^{-1} \phi'(c) \tag{4}$$

Here v is the mean velocity, $Dv = \frac{1}{2}(\nabla v + \nabla v^T)$, p is the pressure, c is an order parameter related to the concentration of the fluids (e.g. the concentration difference or the concentration of one component), μ is a chemical potential, and Ω is a suitable bounded domain. Moreover, $\nu(c) > 0$ is the viscosity of the mixture, $\varepsilon > 0$ is a (small) parameter, which will be related to the "thickness" of the interfacial region, $m > 0$ is a mobility coefficient, and $\phi = \Phi'$ for some suitable energy density Φ. The latter model first appeared in [9] with the name "model H". A rigorous derivation was given in [8].

The system is dissipative and sufficiently smooth solution satisfy

$$\frac{d}{dt}E(c(t),v(t)) \quad = \quad -\int_\Omega \nu(c)|Dv|^2\,dx - \int_\Omega m|\nabla\mu|^2\,dx$$

where $E(c(t),v(t)) = E_\varepsilon(c(t)) + \frac{1}{2}\int_\Omega |v(t)|^2\,dx$, and

$$E_\varepsilon(c) = \frac{\varepsilon}{2}\int_\Omega |\nabla c(x)|^2\,dx + \varepsilon^{-1}\int_\Omega \Phi(c(x))\,dx$$

describes the energy of the mixture. Here Φ is a double well potential as e.g. $\Phi(c) = \frac{1}{8}(1-c^2)^2$ if $c = c_1 - c_2$ is the difference of the mass concentrations.

For the mathematical analysis it is essential that both the interface thickness ε *and* the mobility m are positive. Under this assumption and suitable assumptions on Φ, the domain and the initial conditions, one can prove the existence of weak solutions of (1)-(4) in two and three space dimension. Furthermore, strong unique solutions exist in two dimensions globally in time and in three dimensions locally in time. Moreover, for large times any weak solution becomes regular and converges to a solution of the associated stationary system. We refer to [3] for these results and further references. In the case $\varepsilon > 0$ and $m = 0$ existence of weak solutions is an open problem and so far only short-time existence of strong solutions was shown, cf. [5].

In applications the parameter $\varepsilon > 0$ is often very small. Therefore a rigorous understanding of the limit $\varepsilon \to 0$ and the relation to classical sharp interface models is of interest. But the limit system as $\varepsilon \to 0$ depends on the choice of the scaling of $m = m(\varepsilon)$. We expect that, if $m(\varepsilon) \to_{\varepsilon\to 0} m_0 \geq 0$ and c is the concentration of one fluid, then the limit system is

$$\partial_t v + v\cdot\nabla v - \operatorname{div}(\nu^\pm Dv) + \nabla p = 0 \qquad \text{in } \Omega^\pm(t) \tag{5}$$

$$\operatorname{div} v = \Delta\mu = 0 \qquad \text{in } \Omega^\pm(t) \tag{6}$$

$$-\left[n\cdot(\nu^\pm Dv - pI)\right] = \sigma H n \qquad \text{on } \Gamma(t) \tag{7}$$

$$V = n\cdot v|_{\Gamma(t)} - m_0[n\cdot\nabla\mu] \qquad \text{on } \Gamma(t) \tag{8}$$

$$[v] = 0, \quad \mu|_{\Gamma(t)} = \sigma H \qquad \text{on } \Gamma(t) \tag{9}$$

Here [.] denotes the jump of a function across the interface $\Gamma(t)$. In the case $m_0 = 0$, the equations for the chemical potential μ decouple from the rest and the system coincides with the classical sharp interface model. In the case $m_0 > 0$ it was shown that weak solutions of (1)-(4) converge (modulo subsequences) to *varifold solutions* of (5)-(9) in the sense of [6]. In the case $m_0 = 0$ convergence was shown by formally matched asymptotics in [12] and it was observed numerically in [10] for some scalings of $m(\varepsilon)$.

In the case $m_0 > 0$ existence of weak solutions for large times was shown in [4]. In the case $m_0 = 0$ this is an open problem. So far only short time existence of strong solutions and existence of varifold solutions globally in time are known, cf. [7, 13], [1, 2], respectively. In order to obtain weak solutions using methods from geometric measure theory, it is essential that sufficiently smooth solutions of

(5)-(9) satisfy

$$\frac{d}{dt}E(v(t),\Gamma(t)) \quad = \quad -\int_\Omega \nu(\chi)|Dv|^2\,dx - m_0\int_\Omega |\nabla\mu|^2\,dx$$

where $E(v(t),\Gamma(t)) = \frac{1}{2}\|v(t)\|_2^2 + \sigma\mathcal{H}^{d-1}(\Gamma(t))$. In the case $m_0 > 0$ this gives some control of μ and the curvature of the interface $\Gamma(t)$, which is sufficient to apply a result by Schätzle [11] and to obtain weak solutions.

Conclusion: Comparing diffuse and sharp interface models it is important to realize that there are *two new parameters* $\varepsilon > 0$, which measure the interface thickness, and $m > 0$, which is a mobility coefficient. In particular, since $m > 0$, new diffusion effects occur in comparison with the classical sharp interface model, which corresponds to the case $\varepsilon = m = 0$. More precisely, in the case $m = 0$, the interface is just transported by mean velocity of the mixture v, while in the case $m > 0$ the evolution of the interface is given by a (non-local) transport-diffusion equation. Therefore the choice of $m = m(\varepsilon) > 0$ influences the behavior of the diffuse interface model a lot and the scaling of $m(\varepsilon)$ as $\varepsilon \to 0$ influences the limit system. Moreover, we note that in the case $m > 0$ new effects like Ostwald ripening occur, which was observed numerically. On the other hand the existence of global weak solutions was only shown in the case $m > 0$ (both for $\varepsilon > 0$ and $\varepsilon = 0$). In this case the energy estimate provides an estimate of the chemical potential μ, which gives some control of the ("diffuse") curvature of the interface. This control is essential for the construction of global weak solutions. Therefore in the case $m > 0$ the system has much better analytical properties. (It is a completely parabolic system in this case.) But choosing $m = m(\varepsilon) > 0$ new phenomena related to diffusion in the system occur, which still have to be understood more rigorously.

References

[1] H. Abels. On generalized solutions of two-phase flows for viscous incompressible fluids. *Interfaces Free Bound.*, 9:31–65, 2007.

[2] H. Abels. On the notion of generalized solutions of two-phase flows for viscous incompressible fluids. *RIMS Kôkyûroku Bessatsu*, B1:1–15, 2007.

[3] H. Abels. On a diffuse interface model for two-phase flows of viscous, incompressible fluids with matched densities. *Arch. Rat. Mech. Anal.*, 194(2):463–506, 2009.

[4] H. Abels and M. Röger. Existence of weak solutions for a non-classical sharp interface model for a two-phase flow of viscous, incompressible fluids. *Ann. Inst. H. Poincaré Anal. Non Linéaire*, 26:2403–2424, 2009.

[5] H. Abels and Y. Terasawa. Non-homogeneous navier-stokes systems with order-parameter dependent stresses. *Preprint, Max Planck Institute for Mathematics in the Sciences, No. 19/2009, to appear in Math. Math. Methods Appl. Sci.*, 2009.

[6] X. Chen. Global asymptotic limit of solutions of the Cahn-Hilliard equation. *J. Differential Geom.*, 44(2):262–311, 1996.

[7] I. V. Denisova and V. A. Solonnikov. Solvability in Hölder spaces of a model initial-boundary value problem generated by a problem on the motion of two fluids. *Zap. Nauchn. Sem. Leningrad. Otdel. Mat. Inst. Steklov. (LOMI)*, 188(Kraev. Zadachi Mat. Fiz. i Smezh. Voprosy Teor. Funktsii. 22):5–44, 186, 1991.

[8] M. E. Gurtin, D. Polignone, and J. Viñals. Two-phase binary fluids and immiscible fluids described by an order parameter. *Math. Models Methods Appl. Sci.*, 6(6):815–831, 1996.

[9] P.C. Hohenberg and B.I. Halperin. Theory of dynamic critical phenomena. *Rev. Mod. Phys.*, 49:435–479, 1977.
[10] D. Jacqmin. Calculation of two-phase Navier-Stokes flows using phase-field modeling. *J. Comput. Phys.*, 155(1):96–127, 1999.
[11] R. Schätzle. Hypersurfaces with mean curvature given by an ambient Sobolev function. *J. Differential Geom.*, 58(3):371–420, 2001.
[12] V. N. Starovoĭtov. A model of the motion of a two-component fluid taking into account capillary forces. *Prikl. Mekh. Tekhn. Fiz.*, 35(6):85–92, 1994.
[13] N. Tanaka. Global existence of two phase nonhomogeneous viscous incompressible fluid flow. *Comm. Partial Differential Equations*, 18(1-2):41–81, 1993.

Minimal timelike lorentzian submanifolds as limits of singularly perturbed wave equations

Giovanni Bellettini
(joint work with M. Novaga and G. Orlandi)

I have described a recent convergence result [2] as $\epsilon \to 0^+$ of solutions of the hyperbolic problems

$$\mathbf{u}_{tt} - \Delta \mathbf{u} + \frac{1}{\epsilon^2} \nabla W(\mathbf{u}) = 0. \tag{1}$$

Here

$$\mathbf{u} : \mathbb{R} \times \mathbb{R}^n \to \mathbb{R}^k, \qquad n \geq 1,\ k = 1, 2,$$

and $W(\mathbf{u})$ is a suitable potential vanishing only on the unit circle if $k = 2$ and on ± 1 if $k = 1$, for instance $W(\mathbf{u}) = \frac{1}{4}(1 - |\mathbf{u}|^2)^2$ if $n \leq 4$ and $k = 2$. Our starting point was a computation made by Neu in [8] where he showed, using a formal argument and assuming $k = 1$, that there are solutions of (1) which take the constant values ± 1 out of a transition region of thickness ϵ, provided such a region is close to a timelike lorentzian minimal surface (of codimension one), also called classical string.

Given a solution $\mathbf{u}_\epsilon$ to (1) a relevant quantity to be analyzed in the limit $\epsilon \to 0^+$ is the rescaled lagrangian density

$$\ell_\epsilon(\mathbf{u}_\epsilon) := c_k(\epsilon) \left(\frac{-|\mathbf{u}_{\epsilon t}|^2 + |\nabla \mathbf{u}_\epsilon|^2}{2} + \frac{W(\mathbf{u}_\epsilon)}{\epsilon^2} \right) \text{ where } c_k(\epsilon) := \begin{cases} \epsilon & \text{if } k = 1, \\ \frac{1}{|\log \epsilon|} & \text{if } k = 2. \end{cases}$$

Our convergence result shows that $\ell_\epsilon(\mathbf{u}_\epsilon)$ concentrates on a k-codimensional set as $\epsilon \to 0^+$, which is a timelike lorentzian stationary varifold. This theorem is obtained under rather strong assumptions (see [2] for the details) and its proof is based on a strategy used by Ambrosio and Soner [1] for the $k = 2$ corresponding parabolic problems, which in turn is related to the paper [5] of Ilmanen for the $k = 1$ parabolic case. Convergence results for solutions to (1) were also obtained by Jerrard, see [6], [7].

Neu [8] also exhibited an example showing that suitably perturbing an initial circle with small oscillations (not dissipated in time) may cause the corresponding sequence of lorentzian minimal surfaces not to converge to a lorentzian minimal surface as the oscillation scale tends to zero. Our assumptions on the initial data

of (1), stated at the approximate ϵ-level, should prevent such phenomena. See also the paper [4] of Brenier for related results. In the paper [3] we continue the analysis of Brenier, and discuss an example of lorentzian minimal surface starting from a square with zero initial velocity. Being this latter surface only Lipschitz, still a notion of weak solution should be used, in order to describe the stationarity condition.

References

[1] L. Ambrosio, H.M. Soner. *A measure-theoretic approach to higher codimension mean curvature flows*, Ann. Scuola Norm. Sup. Pisa Cl. Sci. **25** (1998), 27–49.

[2] G. Bellettini, M. Novaga, G. Orlandi, *Time-like lorentzian minimal submanifolds as singular limits of nonlinear wave equations*, Physica D, to appear.

[3] G. Bellettini, J. Hoppe, M. Novaga, G. Orlandi, *Closure and convexity properties of closed relativistic strings*, Complex Anal. Oper. Theory, to appear.

[4] Y. Brenier *Non relativistic strings may be approximated by relativistic strings*, Methods Appl. Anal. **12** (2005), 153–167.

[5] T. Ilmanen, *Convergence of the Allen-Cahn equation to Brakke's motion by mean curvature*, J. Differential Geom. **38** (1993), 417–461.

[6] R.L. Jerrard, *Dynamics of topological defects in nonlinear field theories*, Oberwolfach Reports 27/2008, 16–18.

[7] R.L. Jerrard *Defect in semilinear wave equations and timelike minimal surfaces in Minkowski space*, available at http://arxiv.org/abs/0909.3548

[8] J.C. Neu. *Kinks and the minimal surface equation in Minkowski space*, Physica D **43** (1990), 421–434.

Transport processes at fluidic interfaces

Dieter Bothe

(joint work with Jan Prüss)

Fluidic interfaces are mobile and deformable phase boundaries between a liquid phase and another liquid or gas phase. They appear as free boundaries of fluidic particles such as drops or bubbles, or as free surfaces of liquids and play a prominent role in numerous applications like multiphase chemical reactors, fuel engines, atomization, drying of liquid sprays, heat exchange and ink-jet printing etc.

We consider sharp-interface models, where the hydrodynamics is described by the two-phase balances of mass and momentum which read as

$$\partial_t \rho + \operatorname{div}(\rho \mathbf{u}) = 0 \qquad \text{in } \Omega \setminus \Gamma(t), \quad [\![\mathbf{u}]\!] = [\![\tfrac{1}{\rho}]\!]\, j \mathbf{n}_\Gamma \qquad \text{on } \Gamma(t),$$

$$\partial_t(\rho\mathbf{u}) + \nabla\cdot(\rho\mathbf{u}\otimes\mathbf{u}) = \nabla\cdot\mathbf{T} \quad \text{in } \Omega \setminus \Gamma(t), \quad [\![\mathbf{u}]\!]\, j - [\![\mathbf{T}]\!]\cdot \boldsymbol{n}_\Gamma = \sigma\kappa_\Gamma \boldsymbol{n}_\Gamma \quad \text{on } \Gamma(t),$$

where ρ is the mass density, $\mathbf{u}$ the velocity and σ the surface tension assumed to be constant here. The interface is denoted as Γ which depends on time and is to be found as part of the solution. The interface normal is $\boldsymbol{n}_\Gamma$ and $\kappa_\Gamma := \operatorname{div}_\Gamma(-\boldsymbol{n}_\Gamma)$ is the sum of the principal curvatures. The relations on Γ are transmission conditions which involve the jump of certain quantities across Γ which is defined as

$$[\![\phi]\!](t,\, x) := \lim_{h\to 0+} \left(\phi(t,\, x + h\boldsymbol{n}_\Gamma) - \phi(t,\, x - h\boldsymbol{n}_\Gamma)\right) \text{ for } x \in \Gamma(t).$$

The two fluids are assumed to be Newtonian and we focus on the case of incompressible flows, i.e. $\mathbf{T} = -p\mathbf{I} + \mathbf{S}$ with the viscous stress $\mathbf{S} = \eta(\nabla\mathbf{u} + \nabla\mathbf{u}^\mathsf{T})$ and the first equation reduces to $\operatorname{div}\mathbf{u} = 0$. Note that the material parameters ρ and η depend on the phase. We allow for phase change and therefore the transmission conditions involve the mass transfer flux density j defined on Γ as

$$j = \rho(\mathbf{u} - \mathbf{u}_\Gamma) \cdot \boldsymbol{n}_\Gamma,$$

where $\mathbf{u}_\Gamma$ is the interface velocity. The latter differs from the adjacent bulk velocities if mass and, hence, phase transfer occurs and this leads to a so-called Stefan flow. In this situation the normal velocity V_Γ of the interface is related to the phase velocities through

$$V_\Gamma = \mathbf{u} \cdot \boldsymbol{n}_\Gamma + j/\rho.$$

We are interested in sharp-interface models for mass transfer driven by deviations from chemical equilibrium. For this purpose the above model has to be extended to multicomponent two-phase fluid mixtures. Such a mixture is composed of chemical components $A_1, \ldots, A_n$, say, which are partially miscible. As an example consider air bubbles in water: then the gas phase contains oxygen, nitrogen, carbon dioxide but also water vapor. The liquid phase is mainly water, but with dissolved quantities of oxygen, nitrogen and carbon dioxide. If the gas components dissolve, the bubble shrinks and may finally even disappear.

The continuum thermodynamical sharp-interface model is based on the mass and momentum balances of the individual components. Still, a single common momentum balance is usually employed. Hence the two-phase Navier-Stokes system above is complemented by species equations of the form

$$\rho(\partial_t y_i + \mathbf{u} \cdot \nabla y_i) + \operatorname{div}\mathbf{J}_i = 0 \text{ in } \Omega \setminus \Gamma(t), \quad [\![y_i]\!]\, j + [\![\mathbf{J}_i]\!] \cdot \mathbf{n}_\Gamma = 0 \text{ on } \Gamma(t),$$

where $\mathbf{J}_i$ denotes the diffusive (molecular) fluxes which have to be modeled by means of constitutive equations and $y_i := \rho_i/\rho$ are the mass fractions.

The model is not complete and a constitutive interfacial relation is missing, where our argumentation essentially follows the line on given in [1]. Consider the total energy

$$E = \int_\Omega \rho\big(\frac{1}{2}|\mathbf{u}|^2 + \psi\big)\,dx + \int_\Gamma \sigma\, do$$

of the system, where $\rho\psi(T, \rho_1, \ldots, \rho_n)$ is the free (available) energy density with T the absolute temperature. The chemical potentials of the components are then given as

$$\mu_i = \frac{\partial(\rho\psi)}{\partial\rho_i}.$$

For simplicity, let us focus on the isothermal case. Assuming no-slip and no-flux boundary conditions, direct computation of $\partial_t E$ displays an interfacial contribution to the energy dissipation of the form

$$\int_\Gamma j\big([\![\frac{1}{2\rho^2}]\!]\, j^2 - [\![\mathbf{n}_\Gamma \cdot \mathbf{S}\mathbf{n}_\Gamma/\rho]\!]\big)\,do + \int_\Gamma \sum_i [\![\mu_i]\!]\, j_i\, do.$$

Now, since the interface is considered massless, we assume no dissipation on Γ. Elimination of one of the individual mass transfer fluxes j_i by means of the relation $\sum_i j_i = j$, this yields the additional jump condition

$$[\![\mu_i]\!] = [\![\mathbf{n}_\Gamma \cdot \mathbf{S}\mathbf{n}_\Gamma/\rho]\!] - [\![\frac{1}{2\rho^2}]\!]\, j^2 \quad \text{for all } i.$$

In many technically relevant cases, the right-hand side is negligible, i.e. the assumption of continuity of chemical potentials across the interface results.

A thermodynamically consistent closure of the diffusive fluxes is not trivial. For instance, naive usage of Fick's law of the form $\mathbf{J}_i = -d_i \nabla y_i$ with constant D_i leads to contradictions in the multicomponent case unless all diffusion coefficients are equal; cf. [2]. We employ the Maxwell-Stefan approach to multicomponent diffusion (see, e.g., [3]). Formulated in terms of mass densities, the fluxes are then implicitly given by the system

$$\rho \frac{y_i}{M_i R T} \nabla \mu_i = -\sum_{j \neq i} \frac{y_j \mathbf{J}_i - y_i \mathbf{J}_j}{M_i M_j\, D_{ij}} \quad \text{for } i = 1, \ldots, n$$

with molar mass M_i and Maxwell-Stefan diffusivities D_{ij} which are symmetric. Here R is the universal gas constant. The fluxes are not independent but satisfy the relation $\sum_i \mathbf{J}_i = 0$.

With this thermodynamically consistent model of cross-diffusion effects, the aim of our current work in progress is local-in-time wellposedness and stability properties of the full multicomponent two-phase system, allowing for mass transfer across the fluidic interface. We currently focus on the incompressible and isothermal case, where we are able to prove that the differential operator associated to the cross-diffusion system with Maxwell-Stefan constitutive relations is normally elliptic and that the transmission and jump conditions at the interface satisfy the Lopatinskii-Shapiro conditions.

References

[1] W. Dreyer, On jump conditions at phase boundaries for ordered and disordered phases, WIAS preprint No. 869 (2003).
[2] V. Giovangigli, *Multicomponent Flow Modeling*, Birkhäuser, Boston 1999.
[3] R. Krishna, J.A. Wesselingh: The Maxwell-Stefan approach to mass transfer. Chem. Eng. Sci. **52**, 861-911 (1997).

Optimal Control of PDEs. Topics and Methods

Eduardo Casas

In this talk I give an introduction to the Optimal Control Theory. The elements of an optimal control problem are stated: the control, the state, the state equation and the cost functional. Then, the goals of the theory are pointed out as follows

- Existence of a solution
- First and second order optimality conditions
- Numerical approximation

- Numerical resolution of the discrete control problem

Only the first three points are analyzed in this talk, which is done through the following model control problem

$$(\mathrm{P}) \begin{cases} \text{Minimize } \ J(u) = \displaystyle\int_\Omega L(x, y_u(x), u(x))dx \\ \\ u \in \mathcal{K} = \{u \in L^\infty(\Omega) : \alpha \le u(x) \le \beta \ \text{ a.e. } x \in \Omega\}, \end{cases}$$

where $-\infty < \alpha < \beta < +\infty$ and y_u is the solution of the state equation

$$Ay = -\sum_{i,j=1}^{n} \partial_{x_j} \left(a_{ij}(x)\partial_{x_i} y(x)\right) + a_0(x)y(x),$$

with $a_{ij} \in C^{0,1}(\bar{\Omega})$ and $a_0 \in L^\infty(\Omega)$ satisfy

$$\begin{cases} \exists m > 0 \text{ s.t. } \displaystyle\sum_{i,j=1}^{n} a_{ij}(x)\xi_i\xi_j \ge m|\xi|^2 \ \ \forall \xi \in \mathbb{R}^n \ \forall x \in \Omega, \\ \\ a_0(x) \ge 0 \ \text{ a.e. } x \in \Omega. \end{cases}$$

We state a theorem of existence of a solution, then we derive the first and second order optimality conditions and finally, we apply the previous results to prove the convergence of the numerical discretization of the control problem and to deduce some error estimates for the optimal control as well as for the optimal state and adjoint state.

An arrival time inverse problem for the eikonal equation

Klaus Deckelnick
(joint work with C.M. Elliott and V. Styles)

We are concerned with the formulation and numerical approximation of an optimal control problem for the eikonal equation. Our work is motivated by applications in transmission travel-time tomography, where one tries to estimate the wave-speed distribution in a subsurface region from measured first arrival times of acoustic, seismic or electromagnetic signals. In order to formulate a mathematical problem we consider the following eikonal equation

$$|\nabla u| = a(x), \ x \in \Omega \setminus \{x_0\}; \tag{1}$$

$$u(x_0) = 0; \quad u(x) = +\infty, x \in \partial\Omega. \tag{2}$$

Here, $\Omega \subset \mathbb{R}^n$ is a bounded domain with a Lipschitz boundary and $x_0 \in \Omega$ represents the location of the signal source. For a given positive function $a \in C^0(\bar{\Omega})$ problem (1), (2) is solved uniquely by the function

$$u_a(x) = \inf\{\int_0^t a(\xi(r))|\xi'(r)|dr \mid \xi \in W^{1,\infty}([0,t],\bar{\Omega}), \\ \xi(0) = x_0, \xi(t) = x \text{ for some } t \ge 0\}$$

representing the travel time of the signal to go from x_0 to x with velocity $\frac{1}{a}$. The function u_a is a viscosity subsolution on Ω and a viscosity supersolution on $\bar{\Omega}$, see [3], [1].
Let us suppose that first arrival time measurements are given in terms of a function $u_{obs} : \partial\Omega \to \mathbb{R}_{>0}$. Furthermore, let $0 < A_m < A_M < \infty$ and choose functions $\{\phi_i\}_{i=1}^L \subset W^{1,\infty}(\Omega)$ satisfying $\phi_i(x) \geq 0, i = 1, \ldots, L$ and $\sum_{i=1}^L \phi_i(x) = 1, x \in \Omega$. We introduce the set

$$K := \{a : \Omega \to \mathbb{R} \,|\, a(x) = \sum_{i=1}^{L} a_i \phi_i(x),\ A_m \leq a_i \leq A_M, i = 1, \ldots, L\}$$

as a velocity model and consider the optimization problem

$$\min_{a \in K} \mathcal{J}(a) = \frac{1}{2} \int_{\partial\Omega} |u_a(x) - u_{obs}(x)|^2 do. \tag{3}$$

It can be shown that (3) has at least one solution $a^* \in K$. A numerical approach to minimize $\mathcal{J}$ with the help of the adjoint method is presented in [2] and it is the aim of the present work to analyze and justify this approach.
Our starting point is a discretization of (1), (2). For simplicity we assume that $\Omega = (0, b_1) \times (0, b_2) \subset \mathbb{R}^2$ and consider the regular grid $\mathbb{Z}_h^2 := \{x_\alpha = (h_1\alpha_1, h_2\alpha_2) \,|\, \alpha_i \in \mathbb{Z}, i = 1, 2\}$ with $b_i = h_i N_i, i = 1, 2$ for some $N_1, N_2 \in \mathbb{N}$. We set $\Omega_h = \Omega \cap \mathbb{Z}_h^2, \Gamma_h = (\partial\Omega \cap \mathbb{Z}_h^2) \setminus \{(0,0), (b_1, 0), (0, b_2), (b_1, b_2)\}$ as well as $G_h = \Omega_h \cup \Gamma_h$. For a grid point $x_\alpha \in G_h$ we denote by N_α its four neighbours if $x_\alpha \in \Omega_h$; if $x_\alpha \in \Gamma_h$, then N_α only consists of the neighbour which belongs to Ω_h. Given a positive function $a \in C^0(\bar{\Omega})$ we approximate (1), (2) as follows: Find $U : G_h \to \mathbb{R}$ such that $U(x_0) = 0$ and

$$\sum_{x_\beta \in N_\alpha} \Big\{ \Big(\frac{U(x_\alpha) - U(x_\beta)}{h_{\alpha\beta}} \Big)^+ \Big\}^2 = a(x_\alpha)^2, \quad x_\alpha \in G_h \setminus \{x_0\},$$

where $h_{\alpha\beta} = |x_\alpha - x_\beta|$ and where we have assumed that x_0 is a grid point. It can be shown that the above problem has a unique solution $U = U_a$. Assuming in addition that a is Lipschitz, we obtain the error bound

$$\max_{x_\alpha \in G_h} |u(x_\alpha) - U_a(x_\alpha)| \leq C\sqrt{h},$$

where C depends on $\Omega, \min_{\bar{\Omega}} a$ and the Lipschitz constant of a. Hence it is natural to approximate (3) by

$$\min_{a \in K} \mathcal{J}_h(a) = \frac{1}{2} \Big(h_1 \sum_{x_\alpha \in \Gamma_2 \cap G_h} + h_2 \sum_{x_\alpha \in \Gamma_1 \cap G_h} \Big) |U_a(x_\alpha) - u_{obs}(x_\alpha)|^2, \tag{4}$$

where $\Gamma_k = \{(x_1, x_2) \in \partial\Omega \,|\, x_k = 0 \text{ or } x_k = b_k\}, k = 1, 2$. We can show that (4) has a solution $a_h^* \in K$ and that there exists a sequence $h \searrow 0$ such that (a_h^*) converges to a solution of (3). The actual minimization of $\mathcal{J}_h$ can be carried out with the help of a projected gradient method. Here, derivatives of $\mathcal{J}_h$ are given by

$$\frac{\partial \mathcal{J}_h}{\partial a_m}(a) = -h_1 h_2 \sum_{x_\alpha \in G_h \setminus \{x_0\}} P(x_\alpha) a(x_\alpha) \phi_m(x_\alpha), \qquad m = 1, \ldots, L$$

where the discrete adjoint $P : G_h \setminus \{x_0\} \to \mathbb{R}$ is the solution of

$$P(x_\alpha) = \frac{\sum_{x_\beta \in N_\alpha} \frac{P(x_\beta)}{h_{\alpha\beta}} \left(\frac{U(x_\beta)-U(x_\alpha)}{h_{\alpha\beta}}\right)^+}{\sum_{x_\beta \in N_\alpha} \frac{1}{h_{\alpha\beta}} \left(\frac{U(x_\alpha)-U(x_\beta)}{h_{\alpha\beta}}\right)^+}, \quad x_\alpha \in \Omega_h \setminus \{x_0\} \tag{5}$$

$$P(x_\alpha) = \frac{u_{obs}(x_\alpha) - U(x_\alpha)}{\sum_{x_\beta \in N_\alpha} \left(\frac{U(x_\alpha)-U(x_\beta)}{h_{\alpha\beta}}\right)^+}, \qquad x_\alpha \in \Gamma_h. \tag{6}$$

From (5) we see that the values of P can be successively calculated by ordering the grid points with respect to the size of $U(x_\alpha)$ starting with the largest value. This information is available if the forward problem is solved with the help of the Fast Marching Method.

References

[1] I. Capuzzo Dolcetta, P.L. Lions *Hamilton-Jacobi equations with state constraints*, Trans. Amer. Soc. **318** (1990), 643–683.

[2] S. Leung, J. Qian *An adjoint state method for three–dimensional transmission traveltime tomography using first–arrivals*, Comm. Math. Sci. **4** (2006), 249–266.

[3] H.M. Soner *Optimal control problems with state constraints I and II*, SIAM J. Control Optim. **24** (1986), 551–561 and 1110–1122.

Surface finite elements for two phase geometric biomembranes

Charlie Elliott

(joint work with Bjoern Stinner)

Biomembranes consisting of multiple lipids may involve phase separation phenomena leading to coexisting domains of different lipid compositions. The modelling of such biomembranes involves an elastic or bending energy together with a line energy associated with the phase interfaces. This leads to a free boundary problem for the phase interface on the unknown equilibrium surface which minimizes an energy functional subject to volume and area constraints. In this talk we presented a new computational tool for computing equilibria based on an L^2 relaxation flow for the total energy in which the line energy is approximated by a surface Ginzburg-Landau phase field functional. The relaxation dynamics couple a nonlinear fourth order geometric evolution equation of Willmore flow type for the membrane with a surface Allen-Cahn equation describing the lateral decomposition. A novel system is derived involving second order elliptic operators and in which the field variables are the positions of material points of the surface, the mean curvature vector and the surface phase field function. The resulting variational formulations use H^1 spaces. We use triangulated surfaces and the surface finite element method with H^1 conforming surface finite elements. Quadratic surface finite elements are employed together with a semi-implicit time discretisation of the evolution equations yielding an iterative scheme for computing stationary solutions using linear solvers. Numerical experiments are presented which exhibit convergence and the power of

this new method for two component geometric biomembranes by computing equilibria such as dumbells, discocytes and starfish with lateral phase separation. The work described in the talk is based on [1, 2].

References

[1] C. M. Elliott and B. Stinner *Modelling and computation of two phase geometric biomembranes using surface finite elements* J. Comp. Phys. (submitted)
[2] C. M. Elliott and B. Stinner *A surface phase field model for two- phase biological membranes* SIAM J. Applied Math. (submitted)

Exponential-free a priori and a posteriori error estimates for finite element approximations of diffuse interface equations for surface evolution

Xiaobing Feng
(joint work with Andreas Prohl, Haijun Wu)

Let Γ_0 be a given hypersurface (i.e., a codimension one manifold) in $\mathbf{R}^{n+1}$, the geometric evolution of surfaces is a family of one-parameter hypersurfaces $\{\Gamma_t\}_{t\geq 0}$ which are governed by the geometric law $V_n = F_{\rm int}(\lambda_1, \lambda_2, \cdots, \lambda_n) + F_{\rm ext}$. Where V_n stands for the normal velocity of Γ_t, $\{\lambda_j\}_{j=1}^n$ denote the principal curvatures of Γ_t. $F_{\rm int}$ and $F_{\rm ext}$ are two given functions and $F_{\rm ext}$ depends on some external variable(s)/field(s). Well-known examples of the geometric evolution of surfaces (also known as moving interface problems) include the mean curvature flow ($F_{\rm int} = -H =: -(\lambda_1 + \lambda_2 \cdots + \lambda_n)$, $F_{\rm ext} \equiv 0$), the inverse mean curvature flow ($F_{\rm int} = \frac{1}{H}$, $F_{\rm ext} \equiv 0$), the surface diffusion flow ($F_{\rm int} = -\Delta_\Gamma H$, $F_{\rm ext} \equiv 0$), the Willmore flow ($F_{\rm int} = -\Delta_\Gamma H - 2H(H^2 - K)$, $K := \lambda_1\lambda_2\cdots\lambda_n$, $F_{\rm ext} \equiv 0$), the Hele-Shaw flow ($F_{\rm int} \equiv 0$, $F_{\rm ext} = \frac{1}{2}[\partial_n \mathbf{u}]_{\Gamma_t}$, the jump of the normal derivative of the velocity of the fluids across Γ_t, $\mathbf{u}|_{\Gamma_t} = \sigma H$), and the generalized Stefan problem ($F_{\rm int} \equiv 0$, $F_{\rm ext} = \frac{1}{2}[\partial_n \mathbf{u}]_{\Gamma_t}$, $\mathbf{u}|_{\Gamma_t} = \gamma(H - \alpha V_n)$).

To analytically and numerically study such a geometric evolution (or moving interface) problem, one first needs to adopt some formulation to describe the problem. Different formulations not only lead to different mathematical solution theories but also lead to different numerical methods and algorithms for approximating and computing the solutions. The best known types of formulations include (i) the parametric formulation; (ii) the level set formulation (and method); (iii) the diffuse interface (or phase field) formulation (and method). It is self-explained that the parametric formulation describes the points on the hypersurface by a set of parametric equations. The level set formulation expresses the hypersurface as the zero-level set of a level set function and the evolution of the hypersurface is sought indirectly through evolving the level set function. The diffuse interface formulation is based on the idea of using a non-zero width interface to approximate the hypersurface and using the zero-level set of a phase function, which is contained in the diffuse interface, as the representation of the diffuse interface. Like in the

level set method, the evolution of the hypersurface is sought indirectly through evolving the phase function (cf. [24, 25, 23, 19, 28, 10, 11]).

In the past thirty years extensive studies have been carried out on developing the diffuse interface (or phase field) theory and on developing various types of numerical methods, in particular, adaptive grid methods, for computing the solutions of the diffuse interface models. Rigorous and formal connections have been established for many well-known geometric evolution problems and their diffuse interface models, among them are the mean curvature flow and the Allen-Cahn equation [20, 8], the Hele-Shaw flow and the Cahn-Hilliard equation [27, 2], the surface diffusion flow and the Cahn-Hilliard equation with concentration-dependent mobility [3], and the generalized Stefan problem and the classical phase field model [18, 4]. On the other hand, there were very few results on convergence of numerical methods and numerical interfaces obtained based on the diffuse interface methodology [26, 7, 22], although there have had a very large amount of literature on numerical simulations and computer implementations of various numerical methods for diffuse interface models. As the convergence results of [26, 7, 22] were established using the discrete maximum principle, it is not feasible to extend these results to the diffuse interface models which involve the Cahn-Hilliard equations or systems of equations because the maximum principle does not hold for these equations.

To overcome the difficulty, a new approach/technique, which was first proposed in [12], has emerged and developed in the past ten years. The key to this approach is so-called *exponential-free error estimates*, which means to derive (a priori and/or a posteriori) error bounds for $u^\varepsilon - u_h^\varepsilon$ that depend on ε^{-1} only polynomially (instead of exponentially). Where u^ε and u_h^ε denote respectively the solutions of the diffuse interface model and its numerical approximation. Such an exponential-free error estimate and the triangle inequality $\|u^0 - u_h^\varepsilon\| \le \|u^0 - u^\varepsilon\| + \|u^\varepsilon - u_h^\varepsilon\|$ immediately infer the convergence of u_h^ε to the solution u^0 of the limiting sharp interface problem, which in turn implies the convergence of the numerical interface to the sharp interface. To establish the desired exponential-free error estimates, the key idea is to utilize (and to establish its discrete analogue) the spectrum estimate result [1, 9, 5] for the linearized operator (at the diffuse interface solution) associated with the diffuse interface model.

In the past ten years, exponential-free a priori and a posteriori error estimates and convergence of numerical interfaces have been established for the following pairs of sharp-diffuse interface problems: the Allen-Cahn equation and the mean curvature flow [12, 21, 16], the Cahn-Hilliard equation and the Hele-Shaw flow [13, 14, 17], the classical phase field model and the generalized Stefan problem [15]. This talk intends to give an overview of these results and the main ideas behind of these results. Moreover, recent attempts and ideas for extending these results past the singularities (or topological changes) are also reviewed and commented.

References

[1] N. D. Alikakos and G. Fusco, *The spectrum of the Cahn-Hilliard operator for generic interface in higher space dimensions*, Indiana Univ. Math. J., **42** (1993), 637–674.

[2] N. D. Alikakos, X. Chen and P. Bates, *Convergence of the Cahn-Hilliard equation to the Hele-Shaw model*, Arch. Rational Mech. Anal., **128** (1994), 165–205.

[3] J. W. Cahn, C. M. Elliott, and A. Novick-Cohen, *The Cahn-Hilliard equation with a concentration dependent mobility: motion by minus the Laplacian of the mean curvature*, European J. Appl. Math., **7** (1996), 287–301.

[4] G. Caginalp and X. Chen, *Convergence of the phase field model to its sharp interface limits*, European J. Appl. Math., **9** (1998), 417–445.

[5] X. Chen. *Spectrum for the Allen-Cahn, Cahn-Hilliard, and phase-field equations for generic interfaces*, Comm. PDEs, **19** (1994), 1371–1395.

[6] X. Chen, *Global asymptotic limit of solutions of the Cahn-Hilliard equation*, J. Diff. Geom., **44** (1996), 262–311.

[7] X. Chen, C. M. Elliott, A. Gardiner, and J. Zhao, *Convergence of numerical solutions to the Allen-Cahn equation*, Appl. Anal., **69** (1998), 47–56.

[8] L. C. Evans, H. M. Soner, and P. E. Souganidis, *Phase transitions and generalized motion by mean curvature*, Comm. Pure Appl. Math., **45** (1992), 1097–1123.

[9] P. de Mottoni and M. Schatzman, *Geometrical evolution of developed interfaces*, Trans. Amer. Math. Soc., **347** (1995), 1533–1589.

[10] X. Feng, *Fully discrete finite element approximations of the Navier-Stokes-Cahn-Hilliard diffuse interface model for two phase fluid flows*, SIAM J. Numer. Anal., **44** (2006), 1049–1072.

[11] X. Feng, Y. He, and C. Liu, *Analysis of finite element approximations of a phase field model for two phase fluids*, Math. Comp., **76** (2007), 539–571.

[12] X. Feng and A. Prohl, *Numerical analysis of the Allen-Cahn equation and approximation of the mean curvature flows*, Numer. Math., **94** (2003), 33–65.

[13] X. Feng and A. Prohl, *Error analysis of a mixed finite element method for the Cahn-Hilliard equation*, Numer. Math., **99** (2004), 47–84.

[14] X. Feng and A. Prohl, *Numerical analysis of the Cahn-Hilliard equation and approximation for the Hele-Shaw problem*, Interfaces and Free Boundaries, **7** (2004), 1–28.

[15] X. Feng and A. Prohl, *Analysis of a fully discrete finite element method for the phase field model and approximation of its sharp interface limits*, Math. Comp., **73** (2006), 541–567.

[16] X. Feng and H. Wu, *A posteriori error estimates and an adaptive finite element method for the Allen-Cahn equation and the mean curvature flow*, J. Sci. Comput., **24** (2005), 121–146.

[17] X. Feng and H. Wu, *A posteriori error estimates and adaptive finite element methods for the Cahn-Hilliard equation and the Hele-Shaw flow*, J. Comp. Math., **26** (2008), 767–796.

[18] G. Fix, *Phase field method for free boundary problems*, in A. Fasano and M. Primicerio, editors, Free Boundary Problems, Pitman, London (1983), 580–589.

[19] D. Jacqmin, *Calculation of two-phase Navier-Stokes flows using phase-field modeling*, J. Comp. Phys., **115** (1999), 96–127.

[20] J. Rubinstein, P. Sternberg, and J. B. Keller, *Fast reaction, slow diffusion, and curve shortening*, SIAM J. Appl. Math., **49** (1989), 116–133.

[21] D. Kessler, R. H. Nochetto, and A. Schmidt, *A posteriori error control for the Allen-Cahn problem: circumventing Gronwall's inequality*, Math. Model. Numer. Anal., **38** (2004), 129–142.

[22] T. Kühn, *Convergence of a fully discrete approximation for advected mean curvature flows*, IMA J. Numer. Anal., **18** (1998), 595–634.

[23] J. Lowengrub and I. Truskinovsky, *Cahn-Hilliard fluids and topological transitions*, Proc. R. Soc. London A, **454** (1998), 2617–2654.

[24] G. B. McFadden, *Phase field models of solidification*, in Recent Advances in Numerical Methods for Partial Differential Equations and Applications, Contemp. Math., **306** (2002), 107–145.
[25] G. B. McFadden, A. A. Wheeler, R. J. Braun, S. R. Coriell, and R. F. Sekerka, *Phase-field models for anisotropic interfaces*, Phys. Rev. E (3), **48** (1993), 2016–2024.
[26] R. H. Nochetto, M. Paolini, and C. Verdi, *Optimal interface error estimates for the mean curvature flow*, Ann. Scuola Norm. Sup. Pisa Cl. Sci., **21** (1994), 193–212.
[27] R. L. Pego, *Front migration in the nonlinear Cahn-Hilliard equation*, Proc. Roy. Soc. London Ser. A, **422** (1989), 261–278.
[28] N. Provatas, N. Goldenfeld, and J. Dantzig, *Adaptive mesh refinement computation of solidification microstructures using dynamic data structures*, J. Comput. Phys., **148** (1999), 265–290.

The Stefan Problem with anisotropic Gibbs–Thomson law

Harald Garcke
(joint work with Stefan Schaubeck)

The Stefan problem is a free boundary problem in which one seeks a temperature distribution u together with the interface between a liquid and a solid phase. In the bulk a diffusion equation for the temperature has to hold and at the interface the Stefan condition guarantees energy conservation across the interface taking latent heat release into account. In addition a thermodynamical equilibrium condition has to hold. If surface energy effects are important this condition is given by the Gibbs–Thomson law. As most materials have an anisotropic surface energy also the Gibbs–Thomson law should take anisotropy into account. But most known results for the Stefan problem consider an isotropic Gibbs–Thomson law. As a pioneering work we mention in particular a result by Luckhaus [4] who was able to show a global existence result for the Stefan problem with Gibbs–Thomson law. The arguments of Luckhaus relied on the isotropy of the surface energy and it is the goal of this contribution to present a result which generalizes the work of Luckhaus to the anisotropic situation.

Given a time interval $(0,T)$ and a bounded domain $\Omega \subset \mathbb{R}^n$ with C^1–boundary we define $\Omega_T := (0,T) \times \Omega$. We now seek for the temperature $u : \Omega_T \to \mathbb{R}$ and a phase function $\chi : \Omega_T \to \{0,1\}$ where the liquid phase is given as the set $\{(t,x) \in \Omega_T \,|\, \chi(t,x) = 1\}$ and the solid phase is given as $\{(t,x) \in \Omega_T \,|\, \chi(t,x) = 0\}$. Denoting by $f : \Omega_T \to \mathbb{R}$ given heat sources, the energy balance law is now given as

$$\partial_t(u + \chi) - \Delta u = f \tag{1}$$

where this identity has to be understood in its distributional form.

To formulate the Gibbs-Thomson law in its anisotropic form we need to introduce the anisotropic interfacial free energy

$$\mathcal{F}(\Gamma) := \int_\Gamma \gamma(\nu)\, d\mathcal{H}^{n-1}$$

for a hypersurface Γ with unit normal ν pointing into the solid phase. We assume that γ is a one-homogeneous, convex function.

The L^2–gradient of $\mathcal{F}$ is now given as

$$H_\gamma := \operatorname{div}_\Gamma (D\gamma(\nu))$$

where $D\gamma$ is the gradient of γ and the anisotropic Gibbs-Thomson law is given as

$$u = H_\gamma \quad \text{on} \quad \Gamma\,.$$

The anisotropic Gibbs-Thomson law $u = H_\gamma$ has the weak formulation

$$\int_\Omega (\operatorname{div}\xi\,\gamma(\nu) - \nu \cdot D\xi D\gamma(\nu))\, d|\nabla\chi| = \int_\Omega \operatorname{div}(u\xi)\chi\, dx$$

which has to hold for all $\xi \in C^1(\overline{\Omega}, \mathbb{R}^n)$ with $\xi \cdot \nu_{\partial\Omega} = 0$.

Our approach will be based on a distributional definition of the anisotropic surface energy $\int_\Gamma \gamma(\nu) d\mathcal{H}^{n-1}$. Introducing a function $\gamma^0 : \mathbb{R}^n \to \mathbb{R}^+_0$ with the properties

(2) $\gamma^0 \in C^2(\mathbb{R}^n \setminus \{0\})$, $\gamma^0(p) > 0$ for all $p \in \mathbb{R}^n \setminus \{0\}$,
γ^0 is positively homogeneous of degree 1, i.e.:

(3) $\gamma^0(\lambda p) = \lambda\gamma^0(p)$ for all $\lambda > 0$ and $p \in \mathbb{R}^n \setminus \{0\}$,
there exists a $d_0 > 0$ such that

(4) $(D^2\gamma^0)(p)q \cdot q \geq d_0|q|^2$ for all $p, q \in \mathbb{R}^n$, $|p| = 1$, $p \cdot q = 0$,

we define for $f \in BV(\Omega)$

$$\int_\Omega |\nabla f|_\gamma := \sup\left\{ \int_\Omega f \operatorname{div}\varphi dx \mid \varphi \in C^1_0(\Omega, \mathbb{R}^n),\ \gamma^0(\varphi(x)) \leq 1 \text{ a.e.} \right\}. \tag{5}$$

We now assume that γ is given as

$$\gamma(q) = \sup_{p \in \mathbb{R}^n \setminus \{0\}} \frac{p \cdot q}{\gamma^0(p)}\,, \tag{6}$$

and it turns out, see [1], that for all $f \in BV(\Omega)$ we obtain

$$\int_\Omega |\nabla f|_\gamma = \int_\Omega \gamma(\nu_f)\, d|\nabla f| \tag{7}$$

where $\nu_f = -\frac{\nabla f}{|\nabla f|}$ for $|\nabla f|$ a.e. $x \in \Omega$. It turns out that (5) and (7) will be crucial in the existence proof.

The existence result is now given as follows.

Theorem (see [3]). *Let the following assumptions hold:*

(A1) $\Omega \subset \mathbb{R}^n$ *is a bounded domain with* C^1*–boundary,* $T > 0$.

(A2) *The initial data u_0, χ_0, the boundary data u^D and the right hand side f fulfill*

$$\begin{aligned} u_0 &\in L^\infty(\Omega) \cap H^{1,2}(\Omega)\,, \\ \chi_0 &\in BV(\Omega;\{0,1\})\,, \\ u^D &\in H^{1,2}(\Omega), \\ f &\in L^\infty(\Omega_T)\,. \end{aligned}$$

(A3) *The anisotropy γ is given by (6), where $\gamma^0 : \mathbb{R}^n \to \mathbb{R}$ fulfills (2)-(4).*

Then there exist functions

$$\chi \in L^1(\Omega_T, \{0,1\})$$

such that $\operatorname*{ess\,sup}_{t\in(0,T)} \int_\Omega |\nabla\chi|(t) < \infty$ *and*

$$u \in [u^D + L^2(0,T;H_0^{1,2}(\Omega))] \cap L^\infty(0,T;L^2(\Omega))$$

such that

$$(i) \quad \int_{\Omega_T} (u+\chi)\partial_t\varphi \, d(t,x) + \int_\Omega (u_0+\chi_0)\varphi(0)\,dx = \int_{\Omega_T} \nabla u\cdot\nabla\varphi \, d(t,x) - \int_{\Omega_T} f\varphi \, d(t,x)$$

for all $\varphi \in C_0^\infty([0,T)\times\Omega)$, and

$$(ii) \quad \int_0^T \int_\Omega (div\ \xi D\gamma(\nu)\cdot\nu - \nu\cdot D\xi D\gamma(\nu))\, d|\nabla\chi(t)|dt - \int_{\Omega_T} div\,(u\xi)\chi \, d(t,x) = 0$$

for all $\xi \in C^1(\overline{\Omega}_T, \mathbb{R}^n)$ with $\xi\cdot\nu_{\partial\Omega} = 0$ on $\partial\Omega$.

As in the paper of Luckhaus [4] we use an implicit time discretization to construct approximate solutions. In order to show that time discrete solutions converge to solutions of the continuous problem it is easy to handle the discrete version of the diffusion equation (1).

It will turn out that the main difficulty will be to pass to the limit in the discrete version of the term

$$\int_\Omega (\operatorname{div}\xi\gamma(\nu) - \nu\cdot D\xi D\gamma(\nu))\, d|\nabla\chi|\,.$$

In the isotropic case a lemma of Reshetnyak can be used to show that the approximate normals from the time discrete problems converge, see Luckhaus [4]. In the anisotropic case such a reasoning is not possible and we will use the crucial fact that

$$\int_\Omega \gamma(\nu^h)\, d|\nabla\chi^h| \to \int_\Omega \gamma(\nu)\, d|\nabla\chi|\,,$$

ν_h being approximate normals, implies that $D\gamma(\nu^h) \to D\gamma(\nu)$ in some appropriate sense. This fact will be important in order to pass to the limit in an approximate version of the weak form of the Gibbs-Thomson law.

Numerical computations showing the importance of anisotropy in the Gibbs–Thomson law can be found in [2] or in the abstract of Robert Nürnberg for the same workshop.

References

[1] M. Amar and G. Bellettini, *A notion of total variation depending on a metric with discontinuous coefficients*, Ann. Inst. H. Poincaré, Analyse Non-Linéaire 11 (1994), 91–133.
[2] J.W. Barrett, H. Garcke, and R. Nürnberg, *On stable parametric finite element methods for the Stefan problem and the Mullins–Sekerka problem with applications to dendritic growth*, 2009, Preprint No. 21/2009, University Regensburg.
[3] H. Garcke and S. Schaubeck, *Existence of weak solutions for the Stefan problem with anisotropic Gibbs-Thomson law*, Preprint 2010, University of Regensburg.
[4] S. Luckhaus, *Solutions for the two-phase Stefan problem with the Gibbs-Thomson law for the melting temperature*, European J. Appl. Math. 1 (1990), 101–111.

On scale–independent extinction time estimates for total variation flows

Yoshikazu Giga
(joint work with Robert V. Kohn, Courant–NYU)

A total variation flow is a gradient flow of the total variation and is often used in image analysis for denoising and restoring image. It is often used in materials science to describe evolution of crystal surface.

We consider two models. One is an L^2-gradient flow of the total variation, i.e.,

$$u_t = \text{ div } (\nabla u/|\nabla u|) \tag{1}$$

and the other is an H^{-1}-gradient flow, i.e.,

$$u_t = -\Delta \text{ div } (\nabla u/|\nabla u|). \tag{2}$$

Both equations have a strong diffusivity effect for the surface with slope zero and the solution becomes flat in finite time. For (1) it is known but for (2) it was not yet proved rigrously. We are interested in estimating extinction time both for (1) and (2). To fix idea we impose for example a periodic boundary condition with zero average condition. In this talk for a given initial data u_0 we derive on upper bound for the extinction time $T^*(u_0)$, the first time when the solution u vanishes indetically zero. Such a time is important since it is the time that all pattern disappears.

Our goal is to derive a scale-independent estimate for $T^*(u_0)$ from above both (1) and (2). The estimate for (1) is more or less known. The extinction time is estimated by

$$T^*(u_0) \le S_n ||u_0||_{L^n},$$

where S_n is the best Sobolev constant when the space dimension is n. For (2) the estimate is more involved and we are only successful for lower dimensions $1 \le n \le 4$. Even $T^*(u_0) < \infty$ is a new result. Our estimate for $n = 4$ is

$$T^*(u_0) \le C||u_0||_{\dot{H}^{-1}}$$

while for $1 \le n \le 3$

$$T^*(u_0) \le C||u_0||^{1/\theta-1}_{\dot{W}^{-3,p}} ||u_0||^{2-1/\theta}_{\dot{H}^{-1}}$$

with $(4-n+n/p)\theta = 2-n/2+n/p,\ 1/2<\theta\le 1,\ 1\le p<\infty$. Here the norm $||\cdot||_{\dot{W}^{-m,p}}$ denotes the dual norm of homogeneous $W^{m,p'}$ space with $1/p+1/p'=1$ so that $\dot{H}^{-1}=\dot{W}^{-1,2}$. The constant C is of course independent of u_0 and moreover, it is dilation invariant. The constant C depends only on θ (and blows up as $\theta\downarrow 1/2$). The exponents θ and p are chosen so that the estimate is invariant under all scaling transformations which makes the equation (2) invariant.

A key observation is a new interpolation inequality

$$||u||_{\dot{H}^{-1}} \le C_* ||(-\Delta)^{-1}u||^{1-\theta}_{\dot{W}^{-1,p}} \left(\int |\nabla u|\right)^{\theta}$$

and the growth estimate of the solution

$$\frac{d}{dt}\,||(-\Delta)^{-1}u||_{\dot{W}^{-1,p}} \le \text{ (volume of periodic cell)}^{1/p}$$

together with an energy estimate

$$\frac{1}{2}\,\frac{d}{dt}\,||u||^2_{\dot{H}^{-1}} = -\int |\nabla u|,$$

where $\int|\nabla u|$ denotes the total variation of the measure ∇u.

Optimal Control of Variational Inequalties: Stationarity; -ies and Numerics

M. Hintermüller
(joint work with I. Kopacka)

1. Problem formulation

We focus on a new stationarity concept and the design of multigrid algorithms for the following minimization problem $(\mathcal{P})$:

$$\min J(y,u) = \frac{1}{2}\|y-y_d\|^2_{L^2} + \frac{\nu}{2}\|u\|^2_{L^2} \ \text{ over } y\in V,\ u\in L^2(\Omega)$$

(1.1a) s.t. (subject to) $y\in K,\ a(y,v-y)\ge (f+u,v-y)\ \forall v\in K,$

(1.1b) $u\in U_{ad}$

where $U_{ad}=\{v\in L^2(\Omega): a\le v\le b \text{ a.e. in } \Omega\}$, and $\Omega\subset\mathbb{R}^n$, $n\le 3$, is an open, bounded domain that is either convex and polygonal or has a $C^{1,1}$-boundary $\partial\Omega$. Further $a(\cdot,\cdot): V\times V\to\mathbb{R}$, with $V=H^1_0(\Omega)$, denotes the bilinear form

$$a(v,w)=\sum_{i,j=1}^n \int_\Omega a_{ij}\frac{\partial v}{\partial x_j}\frac{\partial w}{\partial x_i}d\boldsymbol{x} + \sum_{i=1}^n\int_\Omega b_i\frac{\partial v}{\partial x_i}w\,d\boldsymbol{x} + \int_\Omega cvw\,d\boldsymbol{x},$$

for all $v,w\in V$, where $b_i,\ c\in L^\infty(\Omega),\ a_{ij}\in C^{0,1}(\bar\Omega)$ and $c\ge 0$. We assume that $a(\cdot,\cdot)$ is bounded and coercive, and denote by $\mathcal{A}: V\to V^*=H^{-1}(\Omega)$ the associated operator. The variational inequality (VI) constraint (1.1a) involves the cone $K=\{v\in V: v\ge 0 \text{ a.e. in } \Omega\}$. By $(\cdot,\cdot)$ and $\|\cdot\|$ we denote the scalar product

and norm, respectively, in $L^2(\Omega)$ and by $\langle\cdot,\cdot\rangle$ the duality pairing between V and V^*. Moreover, $y_d, f \in L^2(\Omega)$ are given, $\nu > 0$ is fixed, and the bounds on the control variable u are $a, b \in L^2(\Omega) \cup \{-\infty, \infty\}$ with $(b-a) > 0$. The state variable is denoted by y. Note that our notation allows us to choose $a \equiv -\infty$, $b \equiv \infty$ if no lower or upper bound acts on the control. Further, the cone K may be replaced by $K_\psi = \{v \in V : v \geq \psi \text{ a.e. in } \Omega\}$, with $\psi \in H^2(\Omega)$, $\psi|_{\partial\Omega} \leq 0$, and the subsequent results remain true.

2. Penalization of the variational inequality

A common technique for solving a VI of the form (1.1a) is by penalization, where the VI is approximated by a sequence of nonlinear boundary value problems. In our case, the approximating problems read

$$a(y, v) + \frac{1}{\alpha}\langle -\max(0, -y), v\rangle = (f + u, v)\ \forall v \in V, \tag{2.2}$$

with $\alpha > 0$ being the *penalty parameter*. Due to the monotonicity of the max-operator, (2.2) has a unique solution $y_\alpha(u)$. Furthermore, it is well known that

$$y_\alpha(u) \to y(u) \text{ in } V \text{ as } \alpha \downarrow 0, \tag{2.3}$$

where $y(u)$ denotes the unique solution of the original VI.

For a fixed *smoothing parameter* $\varepsilon > 0$ we define the following regularized or smoothed max-operators:

(2.4)

$$\max{}^g_\varepsilon(0,r) := \begin{cases} r - \frac{\varepsilon}{2} & \text{if } r \geq \varepsilon \\ \frac{r^2}{2\varepsilon} & \text{if } r \in (0,\varepsilon), \\ 0 & \text{if } r \leq 0 \end{cases} \quad \max{}^l_\varepsilon(0,r) := \begin{cases} r & \text{if } r \geq \varepsilon \\ \frac{r^2}{4\varepsilon} + \frac{r}{2} + \frac{\varepsilon}{4} & \text{if } r \in (-\varepsilon,\varepsilon), \\ 0 & \text{if } r \leq -\varepsilon \end{cases}$$

Both regularizations are C^1-functions that smooth the kink of the max-operator. Concering the involved parameters we invoke the following assumption .

Assumption 2.1. *For each $\alpha > 0$ let $\varepsilon(\alpha) > 0$ be given such that*

(i) $\{\varepsilon(\alpha)\}$ *is bounded if* $\max^g_\varepsilon$ *or* $\max^G_\varepsilon$ *is used and*
(ii) $\frac{\varepsilon(\alpha)}{\alpha} \to 0$ *for* $\alpha \to 0$ *if* $\max^l_\varepsilon$ *is used.*

3. The optimal control problem

We solve $(\mathcal{P})$ by approximating the lower-level problem, i.e., the variational inequality, using the techniques developed in the previous section. For each set of parameters $(\alpha, \varepsilon) > 0$ we therefore consider $(\mathcal{P}_{\alpha,\varepsilon})$

$$\begin{aligned} \min J(y,u) &= \frac{1}{2}\|y - y_d\|^2_{L^2} + \frac{\nu}{2}\|u\|^2_{L^2} \ \text{ over } y \in V,\ u \in L^2(\Omega) \\ \text{s.t. } & \mathcal{A}y - \frac{1}{\alpha}\max{}_\varepsilon(0,-y) = u + f, \\ & a \leq u \leq b \ \text{ a.e. in } \Omega, \end{aligned} \tag{3.5}$$

where $\max_\varepsilon$ is a generic notation that stands for either of the regularizations introduced in Section 2. The existence of a solution of (3.5) can be established by standard arguments. Moreover, under Assumption 2.1 it can be shown that a sequence of global solutions of (3.5) converges to a global solution of (1.1) as $\alpha \to 0$.

Next we study stationarity principles. For the sake of brevity we set $\Omega^+ := \{\boldsymbol{x} \in \Omega : y(\boldsymbol{x}) > 0\}$ and introduce the notion of $\mathscr{E}$-almost *C-stationarity*.

Definition 3.1. *The point $(y, u) \in V \times L^2(\Omega)$ is called $\mathscr{E}$-almost* C-stationary *for problem* (1.1)*, if there exist $\xi \in L^2(\Omega)$, $p \in V$ and $\lambda \in V^*$ such that the following system is satisfied:*

$$y - \lambda + \mathcal{A}^* p = y_d, \tag{3.6a}$$

$$\mathcal{A}y - u - \xi = f, \tag{3.6b}$$

$$u \in U_{ad},\ (\nu u - p, v - u) \geq 0 \quad \forall v \in U_{ad}, \tag{3.6c}$$

$$\xi \geq 0 \text{ a.e., } y \geq 0,\ (y, \xi) = 0, \tag{3.6d}$$

$$p = 0 \text{ a.e. in } \{\xi > 0\}, \tag{3.6e}$$

$$\langle \lambda, p \rangle \leq 0,\ \langle \lambda, y \rangle = 0, \tag{3.6f}$$

and furthermore for every $\tau > 0$ there exists a subset $E_\tau \subset \Omega^+$ with $meas(\Omega^+ \setminus E_\tau) \leq \tau$ such that

$$\langle \lambda, \phi \rangle = 0\ \forall \phi \in V,\ \phi = 0 \text{ a.e. in } \Omega \setminus E_\tau. \tag{3.7}$$

We now state the main result describing the convergence properties of stationary points of the smoothed penalized problem with respect to the penalty and smoothing parameters.

Theorem 3.2. *Consider the smooth penalized problem with bounds $a, b \in L^2(\Omega)$ and a C^1-regularization of the* max*-operator. Let $\{\alpha\}$ and $\{\varepsilon(\alpha)\}$ satisfy Assumption 2.1. For every $\alpha > 0$ let $(y_\alpha, u_\alpha) \in V \times L^2(\Omega)$ be stationary points of the smooth penalized problem* (3.5) *with corresponding adjoint state $p_\alpha \subset V$.*

Then there exist $(\tilde{y}, \tilde{u}, \tilde{\xi}, \tilde{p}, \tilde{\lambda}) \in V \times L^2(\Omega) \times L^2(\Omega) \times V \times V^*$ and a subsequence (again denoted by $\{\alpha\}$) such that $y_\alpha \to \tilde{y}$ in V, $u_\alpha \to \tilde{u}$ in $L^2(\Omega)$, $\frac{1}{\alpha} \max_{\varepsilon(\alpha)}(0, -y_\alpha) \to \tilde{\xi}$ in V^*, $p_\alpha \rightharpoonup \tilde{p}$ in V and $-\frac{1}{\alpha} \max'_{\varepsilon(\alpha)}(0, -y_\alpha) p_\alpha \rightharpoonup \tilde{\lambda}$ in V^*, where $(\tilde{y}, \tilde{u})$ is $\mathscr{E}$-almost C-stationary for the MPEC (1.1).

4. The Algorithm

The constructive nature of Theorem 3.2 implies an infinite dimensional solution algorithm for the MPEC problem $(\mathcal{P})$, where the solution is approximated by the solution of the smoothed penalized problems $(\mathcal{P}_{\alpha,\varepsilon})$ along a sequence $\{(\alpha, \varepsilon(\alpha))\}$. This outer algorithm is described in Algorithm 1. Theorem 3.2 then yields the convergence of the iterates to a point that is $\mathscr{E}$-almost C-stationary for the MPEC problem.

Algorithm 1 (Outer Algorithm)

Data: y_d, f, α_0, ε_0.

1: Choose (y^0, u^0, p^0) and set $k := 0$.
2: **repeat**
3: Solve the first order system associated with (3.5) with $(\alpha, \varepsilon) = (\alpha_k, \varepsilon_k)$, to obtain $(y^{k+1}, u^{k+1}, p^{k+1})$ using initial values (y^k, u^k, p^k) for solution algorithm.
4: Choose $\alpha_{k+1} < \alpha_k$ and ε_{k+1}.
5: Set k:=k+1.
6: **until** some stopping rule is satisfied.

4.1. **Solving the subproblem by the full approximation scheme.** In the optimality system of (3.5) the control u can be eliminated. The resulting reduced nonlinear system reads

$$\begin{aligned} y + \mathcal{A}^* p + \tfrac{1}{\alpha} \max{}'_\varepsilon(0, -y)p &= y_d, \\ \mathcal{A}y - \tfrac{1}{\alpha} \max{}_\varepsilon(0, -y) - \tfrac{1}{\nu}p + \max(0, \tfrac{1}{\nu}p - b) - \max(0, -\tfrac{1}{\nu}p + a) &= f. \end{aligned} \tag{4.8}$$

For a given sequence of equidistant grids let h denote the size of the current grid and $H > h$ denote the mesh size of the next coarser grid. Furthermore let U_h and U_H denote the finite dimensional subspaces of $L^2(\Omega)$ corresponding to the mesh sizes h and H. Let $I_h^H : U_h \to U_H$ and $\hat{I}_h^H : U_h \to U_H$ denote the restriction operators using full weighting and straight injection, respectively, and let $I_H^h : U_H \to U_h$ denote the interpolation operator using linear interpolation. Let y_d^h, f^h denote the discretized data and let $h_{max} > 0$ be the grid size of the coarsest mesh, i.e., the mesh on which the system is solved exactly. Then the FAS-algorithm for solving the discrete optimality conditions is given by Algorithm 2.

For further details on the FAS scheme, such as the choice of the relaxation scheme, and numerical results we refer to [1]. Moreover, in this reference one also finds a comparison of the FAS-based solver with a solver relying on Hackbusch's multigrid method of the second kind. An alternative relaxation scheme for deriving first order conditions and an associated numerical scheme are studied in [2].

References

[1] M. Hintermüller and I. Kopacka, *A smooth penalty approach and a nonlinear multigrid algorithm for elliptic MPECs*, Comput Optim Appl, 2009, DOI 10.1007/s10589-009-9307-9.
[2] M. Hintermüller and I. Kopacka, *Mathematical Programs with Complementarity Constraints in function space: C- and strong stationarity and a path-following algorithm*, SIAM Journal on Optimization, 20 (2009), pp. 868-902.

Algorithm 2 (FAS-algorithm)

Data: (y_d^h, f^h), initial values (y^h, p^h).

1: **if** $h = h_{max}$ **then**
2: solve (4.8) exactly.
3: **else**
4: Do ν_{pre} pre-smoothing steps.
5: Compute residuals $r_a^h = y_d^h - y^h - (\mathcal{A}^h)^* p^h - \frac{1}{\alpha} \max_\varepsilon'(0, -y^h) p^h$ and $r_s^h = f^h - \mathcal{A}^h y^h + \frac{1}{\alpha} \max_\varepsilon(0, -y^h) - \frac{1}{\nu} p^h$.
6: Restrict residuals to coarser grid using **full weighting** $r_a^H = I_h^H r_a^h$, $r_s^H = I_h^H r_s^h$.
7: Restrict (y^h, p^h) to coarser grid using **straight injection** $y^H = \hat{I}_h^H y^h$, $p^H = \hat{I}_h^H p^h$.
8: Compute right hand sides for coarse problem $y_d^H = r_a^H + y^H + (\mathcal{A}^H)^* p^H + \frac{1}{\alpha} \max_\varepsilon'(0, -y^H) p^H$, $f^H = r_s^H + \mathcal{A}^H y^H - \frac{1}{\alpha} \max_\varepsilon(0, -y^H) - \frac{1}{\nu} p^H$.
9: Apply γ-times the FAS-algorithm to coarse grid problem with $h = H$, right hand side (y_d^H, f^H) and initial values (y^H, p^H) to compute new approximation $(\tilde{y}^H, \tilde{p}^H)$.
10: Coarse grid correction: $y^h = y^h + I_H^h(\tilde{y}^H - y^H)$, $p^h = p^h + I_H^h(\tilde{p}^H - p^H)$, where I_H^h denotes the interpolation operator using **linear interpolation**.
11: Do ν_{post} post-smoothing steps.
12: **end if**

Motion of phase boundaries by geometric evolution equations

Yoshihito Kohsaka
(joint work with Harald Garcke, Kazuo Ito)

The surface diffusion equation

$$V = -\Delta_\Gamma H$$

is a geometric evolution equation for an evolving hypersurface $\Gamma = \{\Gamma_t\}_{t \geq 0}$. Here, V is the normal velocity of the surface, H is the mean curvature of the surface, and Δ_Γ is the Laplace-Beltrami operator of the surface. This equation was introduced by Mullins [2] to model the motion of interfaces in the case that the motion of interfaces is governed purely by mass diffusion within the interfaces (for simplicity we set the diffusion constant to 1). Also, the surface diffusion equation is derived as the H^{-1}-gradient flow of the area functional for the surface (see [3]), so that an evolving hypersurface Γ has the property that the perimeter of the enclosed volume decreases whereas the volume is conserved. On the other hand, when viewing the surface diffusion equation as a partial differential equation (PDE), this equation is a fourth order nonlinear parabolic PDE. Thus, the maximum principle, which is a useful tool of analyzing second order parabolic PDEs, does not work.

In this paper we study the motion of three curves $\Gamma_t^i (i = 1, 2, 3)$ by surface diffusion. These three curves are contained in a bounded domain $\Omega \subset \mathbb{R}^2$ with

the conditions that each one of the end points of $\Gamma_t^i\,(i=1,2,3)$ is connected at a triple junction $p(t)\in\Omega$ and the other end points intersect with $\partial\Omega$. Then the motion of $\Gamma_t^i\,(i=1,2,3)$ are governed by

$$V^i=-m^i(\gamma^i\kappa^i)_{ss}\ \text{ on }\ \Gamma_t^i$$

with the boundary conditions at a triple junction $p(t)$

$$\text{(1)}\qquad \begin{cases} \angle(\Gamma_t^1,\Gamma_t^2)=\theta^3,\ \ \angle(\Gamma_t^2,\Gamma_t^3)=\theta^1,\ \ \angle(\Gamma_t^3,\Gamma_t^1)=\theta^2,\\ \gamma^1\kappa^1+\gamma^2\kappa^2+\gamma^3\kappa^3=0,\\ m^1(\gamma^1\kappa^1)_s=m^2(\gamma^2\kappa^2)_s=m^3(\gamma^3\kappa^3)_s, \end{cases}$$

and at $\Gamma_t^i\cap\partial\Omega$

$$\text{(2)}\qquad \Gamma_t^i\perp\partial\Omega,\quad (\gamma^i\kappa^i)_s=0.$$

Here, V^i is the normal velocity of Γ_t^i, κ^i is the curvature of Γ_t^i, and s is an arc-length parameter of Γ_t^i. Further, m^i and γ^i are positive constants concerning the mobility and the surface energy, respectively. In addition, θ^i are positive constants satisfying

$$\frac{\sin\theta^1}{\gamma^1}=\frac{\sin\theta^2}{\gamma^2}=\frac{\sin\theta^3}{\gamma^3},$$

which is called *Young's law*. The boundary conditions (1) and (2) are the natural boundary conditions when viewing the flow as the H^{-1}-gradient flow of the energy functional

$$E[\Gamma_t]:=\sum_{i=1}^3\gamma^iL[\Gamma_t^i],$$

where $\Gamma_t=\bigcup_{i=1}^3\Gamma_t^i$ and $L[\Gamma_t^i]$ is the length functional of Γ_t^i. Indeed, set

$$\mathfrak{M}(\Gamma):=\Big\{(u^1,u^2,u^3)\in\mathfrak{H}^1(\Gamma)\,\Big|\,u^1+u^2+u^3=0\ \text{ at triple junction},\ \int_{\Gamma^1}u^1\,ds=\int_{\Gamma^2}u^2\,ds=\int_{\Gamma^3}u^3\,ds\Big\}$$

with $\mathfrak{H}^1(\Gamma):=H^1(\Gamma^1)\times H^1(\Gamma^2)\times H^1(\Gamma^3)$. Then the H^{-1}-inner product corresponding to this system is given by

$$(\boldsymbol{v}_1,\boldsymbol{v}_2)_{-1}:=\sum_{i=1}^3m^i\int_{\Gamma^i}\partial_su^i_{\boldsymbol{v}_1}\partial_su^i_{\boldsymbol{v}_2}\,ds,$$

where $\boldsymbol{u}_{\boldsymbol{v}_j}=(u^1_{\boldsymbol{v}_j},u^2_{\boldsymbol{v}_j},u^3_{\boldsymbol{v}_j})\in\mathfrak{M}(\Gamma)\,(j=1,2)$ is a weak solution of

$$\text{(3)}\qquad \begin{cases} -m^i\partial_s^2u^i_{\boldsymbol{v}}=v^i\ \text{ on }\ \Gamma^i\ \ (i=1,2,3),\\ u^1_{\boldsymbol{v}}+u^2_{\boldsymbol{v}}+u^3_{\boldsymbol{v}}=0\ \text{ at triple junction},\\ m^1\partial_su^1_{\boldsymbol{v}}=m^2\partial_su^2_{\boldsymbol{v}}=m^3\partial u^3_{\boldsymbol{v}}\ \text{ at triple junction},\\ \partial_su^i_{\boldsymbol{v}}=0\ \text{ at }\Gamma^i\cap\partial\Omega\ \ (i=1,2,3) \end{cases}$$

for $\boldsymbol{v}_j = (v_j^1, v_j^2, v_j^3) \in \mathfrak{X}(\Gamma) := \big\{(v^1, v^2, v^3) \in (\mathfrak{H}^1)'(\Gamma) \,|\, \langle v^1, 1\rangle = \langle v^2, 1\rangle = \langle v^3, 1\rangle\big\}$. Here $\langle\cdot,\cdot\rangle$ is the duality pairing between $(H^1(\Gamma^i))'$ and $H^1(\Gamma^i)$. Since a Poincaré-type inequality holds for $\boldsymbol{u} \in \mathfrak{M}(\Gamma)$, we can prove that (3) has a unique weak solution for $\boldsymbol{v} \in \mathfrak{X}(\Gamma)$.

Our goal here is to obtain a linearized stability criterion of stationary curves. To mention it, we introduce some notation. Let $\Gamma_* = \bigcup_{i=1}^3 \Gamma_*^i$ be stationary curves. That is, Γ_*^i is a part of circle or a line segment. Then we denote by ℓ_*^i the length of Γ_*^i, by κ_*^i the curvature of Γ_*^i, and by h_*^i the curvature of $\partial\Omega$ at $\Gamma_*^i \cap \partial\Omega$. Now we are ready to state our results. Since space is lacking to explain fully, we show only one case. With regard to the other cases and details, see [1].

Theorem. Let $\gamma^1 = \gamma^2 = \gamma^3 = 1$, $\kappa_*^1 = 0$, $\kappa_*^2 = -\kappa_*^3 = -1/2$, $\ell_*^1 = \sqrt{3}$, and $\ell_*^3 = 4\pi/3$. Also, set

$$\Lambda(h_*^1, h_*^2, h_*^3) := a_{123}h_*^1h_*^2h_*^3 + a_{12}h_*^1h_*^2 + a_{23}h_*^2h_*^3 + a_{31}h_*^3h_*^1 + a_1h_*^1 + a_2h_*^2 + a_3h_*^3 + a_0,$$

where $a_{123}, a_{12}, \cdots, a_0$ are constants depending continuously on ℓ_*^2 and satisfying

$$4(a_ja_k - a_{jk}a_0)(a_{ki}a_{ij} - a_{123}a_i) - (a_{ki}a_j + a_{ij}a_k - a_{123}a_0 - a_{jk}a_i)^2 = 0,$$
$$a_{ki}a_{ij} - a_{123}a_i \geq 0$$

for $(i,j,k) = (1,2,3)$, $(2,3,1)$, $(3,1,2)$ and $0 < \ell_*^2 < 8\pi/3$. Further, let N_U be the number of positive eigenvalues for the linearized operator around Γ_*, and set

$$\mathfrak{R}_1 := \{(h_*^1, h_*^2, h_*^3) \in \mathfrak{R}_+ \,|\, h_*^i > h_{*,a}^i \,(i = 1,2,3)\}, \quad \mathfrak{R}_3 := \mathfrak{R}_+ \setminus \mathfrak{R}_1,$$
$$\mathfrak{R}_4 := \{(h_*^1, h_*^2, h_*^3) \in \mathfrak{R}_- \,|\, h_*^i < h_{*,a}^i \,(i = 1,2,3)\}, \quad \mathfrak{R}_2 := \mathfrak{R}_- \setminus \mathfrak{R}_4,$$

where $\mathfrak{R}_+ := \{(h_*^1, h_*^2, h_*^3) \,|\, \Lambda(h_*^1, h_*^2, h_*^3) > 0\}$, $\mathfrak{R}_- := \{(h_*^1, h_*^2, h_*^3) \,|\, \Lambda(h_*^1, h_*^2, h_*^3) < 0\}$, and $h_{*,a}^i := -a_{jk}/a_{123}$ for $(i,j,k) = (1,2,3)$, $(2,3,1)$, $(3,1,2)$. Then we obtain

(i) $N_U = 0$ if $(h_*^1, h_*^2, h_*^3) \in \mathfrak{R}_1$, (ii) $N_U = 1$ if $(h_*^1, h_*^2, h_*^3) \in \mathfrak{R}_2$,
(iii) $N_U = 2$ if $(h_*^1, h_*^2, h_*^3) \in \mathfrak{R}_3$, (iv) $N_U = 3$ if $(h_*^1, h_*^2, h_*^3) \in \mathfrak{R}_4$.

That is, in the case (i), Γ_* is linearly stable.

Remark. When (h_*^1, h_*^2, h_*^3) is included in $\mathfrak{S} := \{(h_*^1, h_*^2, h_*^3) \,|\, \Lambda(h_*^1, h_*^2, h_*^3) = 0\}$, zero eigenvalues of the linearized operator appear and their multiplicity is one except in the case $(h_*^1, h_*^2, h_*^3) = (h_{*,c}^1, h_{*,c}^2, h_{*,c}^3)$, where

$$h_{*,c}^i := -\frac{a_{ki}a_j + a_{ij}a_k - a_{123}a_0 - a_{jk}a_i}{2(a_{ki}a_{jk} - a_{123}a_i)}$$

for $(i,j,k) = (1,2,3)$, $(2,3,1)$, $(3,1,2)$. At $(h_{*,c}^1, h_{*,c}^2, h_{*,c}^3)$ the multiplicity of zero eigenvalue is two. Also, taking account of the sign of $h_{*,a}^i - h_{*,c}^i$ $(i = 1,2,3)$, we obtain that the configuration of $\mathfrak{S}$ is classified into two type (see Figure 1 & 2).

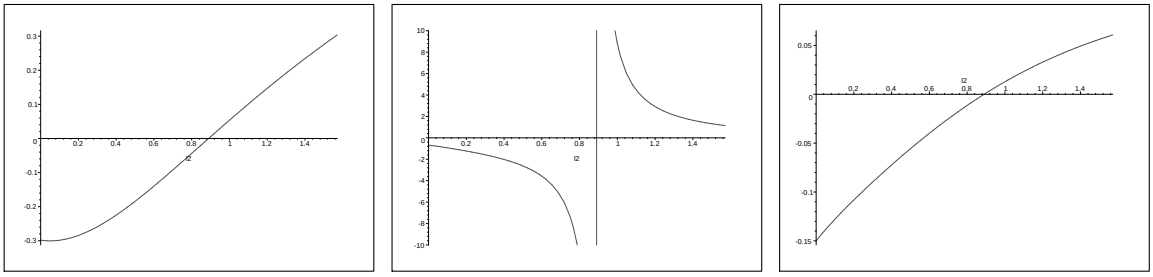

$h^1_{*,a} - h^1_{*,c}$ $h^2_{*,a} - h^2_{*,c}$ $h^3_{*,a} - h^3_{*,c}$

Figure 1 : The graphs of $h^i_{*,a} - h^i_{*,c}$ for the parameter ℓ^2.

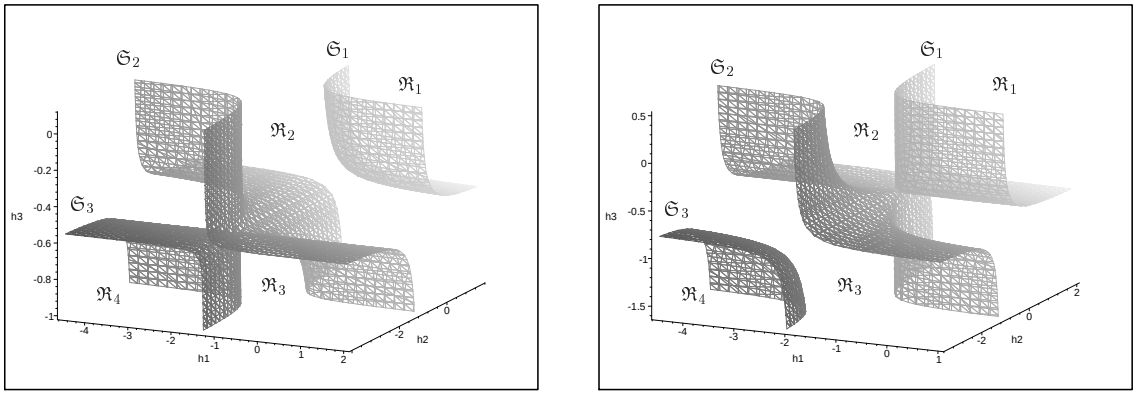

$h^i_{*,a} > h^i_{*,c}\,(i = 1, 2, 3)$ $h^i_{*,a} < h^i_{*,c}\,(i = 1, 2, 3)$

Figure 2 : The configuration of $\mathfrak{S}\,(= \mathfrak{S}_1 \cup \mathfrak{S}_2 \cup \mathfrak{S}_3)$.

References

[1] H. Garcke, K. Ito, and Y. Kohsaka, *Surface diffusion with triple junctions: A stability criterion for stationary solutions*, to appear in Advances in Differential Equations.
[2] W. W. Mullins, *Theory of thermal grooving*, J. Appl. Phys., **28** (1957), 333–339.
[3] J. E. Taylor and J. W. Cahn, *Linking anisotropic sharp and diffuse surface motion laws via gradient flows*, J. Stat. Phys. **77**, no.1-2 (1994), 183–197.

Nonsmooth Schur Newton Methods for Nonsmooth Saddle Point Problems

Ralf Kornhuber
(joint work with Carsten Gräser, Uli Sack)

The numerical simulation of the coarsening of binary alloys based on the Cahn-Larchè equations requires fast, reliable and robust solvers for Cahn-Hilliard equations with logarithmic potential. After semi-implicit time discretization as introduced by Blowey and Elliott 92, the resulting spatial problem can be reformulated as a non-smooth pde-constrained optimal control problem with cost functional induced by the Laplacian. The associated Karush-Kuhn-Tucker conditions take the form of a nonsmooth saddle point problem degenerating to a variational inclusion in the deep quench limit.

Our considerations are based on recent work of Gräser & Kornhuber 09 and the upcoming dissertation of Gräser 10. The starting point is the elimination of the primal variable leading to a nonlinear Schur complement which turns out to be the Frćhèt derivative of a convex functional. Now so-called nonsmooth Schur-Newton methods can be derived as gradient-related descent methods applied to this functional. In the discrete case we can show global convergence for an exact and an inexact version independent of any regularization parameters. Local quadratic convergence or finite termination can be shown for piecewise smooth nonlinearities or in the deep quench limit respectively. The algorithm can be reinterpreted as a preconditioned Uzawa method and generalizes the well-known primal-dual active set strategy by Kunisch, Ito, and Hintermüller 03. A (discrete) Allen-Cahn-type problem and a linear saddle point problem have to be solved (approximately) in each iteration step. In numerical computations we observe mesh-independent local convergence for initial iterates provided by nested iteration. In the deep quench limit, the numerical complexity of the (approximate) solution of the arising linear saddle point problem dominates the detection of the actual active set.

Recent related approaches to nonsmooth saddle point problems by Baňas & Nürnberg 09, Blank, Butz & Garcke 09, and Hintermüller, Hinze & Tber 09 were also discussed.

Self-similar rupture in thin films with slip

Barbara Niethammer
(joint work with A. Münch, D. Peschka)

We consider rupture of thin viscous films in the strong-slip regime with small Reynolds numbers in a model derived in [1]. Numerical simulations indicate self-similar behaviour near the rupture point. More precisely, they suggest that viscosity and van-der-Waals forces are dominant and that there are self-similar solutions of the second kind [2], that is the scaling in the spatial variable is not a-priori determined by a balance of force terms in the equation. More precisely, the film thickness h and the horizontal velocity u follow

$$h(t,y) \sim (t_*-t)^{\alpha} H(\eta) \qquad \text{and} \qquad u(t,y) \sim (t_*-t)^{\beta-1} U(\eta)\,,$$

where $\eta = (y-y_*)/(t_*-t)^{\beta}$ and y^*, t^* denote the point and time of rupture respectively. The scaling exponent α is $1/3$, while β is not determined by the balance of the dominant terms.

Second-kind similarity solutions also appear in simple models for inertialess jet pinch-off. In [5] convergence to these solutions is discussed. Under strong assumptions on the evolution of the jet the authors show that the selection of the self-similar solution in this model is solely determined by the behaviour of the initial data around their minimum. This behaviour is expected, but a rigorous analysis without a priori assumptions on the solutions has still been elusive.

Our goal in [3] is to provide such an analysis for viscosity dominated thin-film rupture that is also directly applicable to the model of jet pinch-off considered in

[5]. For a simplified model, where only terms accounting for viscous and van-der-Waals forces are kept, we rigorously establish finite time rupture in [2] following ideas of Renardy [4, 5] for jet pinch-off. In [3] we rigorously study the self-similar nature of the rupture. We show that for each $\beta > 0$ there exists a unique self-similar solution and equivalently these self-similar solutions can be uniquely characterized by their behaviour $\bar{H}(\eta) = \bar{H}_0 + \bar{H}_\rho \eta^\rho$ as $\eta \to 0$, where $\rho = \rho(\beta) \in (0, \infty)$. Next, we investigate whether solutions of the time-dependent problem converge to a self-similar shape and, in case they do, which self-similar solution, i.e. which ρ (or β), is selected. As expected, the long-time asymptotics are completely determined by the behaviour of the initial profile $h(0, y)$ at its minimum. We establish a necessary and sufficient condition for convergence to any of the self-similar solutions with $0 < \rho < 3/2$. The precise criterion is that the solution converges if and only if the data are regularly varying at their minimum with index ρ. The corresponding scaling is the one associated to the self-similar solution up to some slowly varying function given by the initial data. These results are very similar in nature to the dynamics in mean-field models for domain coarsening and coagulation, where the long-time behaviour depends sensitively on the tail of the initial distribution functions.

We can prove the analogous characterization of domains of attraction for every positive ρ under an additional assumption, namely that an associated nonlocal functional converges sufficiently fast. Presently we have no proof whether this assumption is satisfied for regularly varying data. Numerical results indicate that it is, but they also show that the situation is much more involved than in the case of $0 < \rho < 3/2$ and the details of the convergence proof must be different.

References

[1] A. Münch, B. Wagner, and T.P. Witelski. Lubrication models with small to large slip lengths. *Journal of Engineering Mathematics*, 53:359–383, Dec 2005.

[2] D. Peschka, A. Münch and B. Niethammer. Thin film rupture for large slip. *J. Eng. Math.*, 66(1-3):33-51 (2010).

[3] D. Peschka, A. Münch and B. Niethammer. Self-similar rupture of viscous thin films in the strong slip regime. *Nonlinearity*, 23(2):409-427 (2010)

[4] M. Renardy. A comment on self-similar breakup for inertialess Newtonian liquid jets. *IMA J. Appl. Math.*, 70(3):353–358, 2005.

[5] M. Renardy. Finite time breakup of viscous filaments. *Z. Angew. Math. Phys.*, 52(5):881–887, 2001.

Parametric approximation of geometric evolution equations and applications to the modelling of snowflake growth

Robert Nürnberg

(joint work with John W. Barrett, Harald Garcke)

Geometric evolution equations in general arise as gradient flows for a free energy for a curve or surface. In applications these hypersurfaces often play the role of an interface or a free boundary. In this talk, we review a variational formulation for

such geometric evolution laws that leads to discretizations with very good mesh properties, and we indicate how these formulations can be extended to situations where the interface evolution is coupled to a bulk equation.

Given a parameterization $\vec{x}(\rho,t) : I \times [0,T] \to \mathbb{R}^2$, $I := \mathbb{R}/\mathbb{Z}$, of the family of closed curves $\Gamma(t) \subset \mathbb{R}^2$, we note that the L^2- and H^{-1}-gradient flow of length, i.e. the curvature flow and the surface diffusion flow, respectively, can be written as

$$\vec{x}_t \,.\, \vec{\nu} = \begin{cases} \varkappa \\ -\varkappa_{ss} \end{cases}, \qquad \varkappa\,\vec{\nu} = \vec{x}_{ss}\,, \tag{1}$$

with $\varkappa$ the curvature of Γ and $\vec{\nu}$ a unit normal. Note that the formulation (1) is independent of the tangential component, $\vec{x}_t \,.\, \vec{x}_s$, of the velocity $\vec{x}_t$. However, when (1) is discretized with the help of piecewise linear finite elements, then the corresponding discrete tangential velocity is no longer arbitrary. In fact, the spatially discrete solutions are such that the polygonal curves $\Gamma^h(t)$, where they are not locally flat, are equidistributed at every time $t > 0$.

On introducing the appropriate spaces $\underline{V}^h$ and V^h of periodic piecewise linear vector- and scalar-valued parametric finite elements, we obtain the following semidiscrete continuous-in-time approximation of (1). Given $\Gamma^h(0)$, for $t \in (0,T]$ find $\Gamma^h(t) = \vec{X}^h(I,t)$, with $\vec{X}^h(t) \in \underline{V}^h$, and $\kappa^h(t) \in V^h$ such that

$$\langle \vec{X}^h_t, \chi\,\vec{\nu}^h\rangle^h_h - \begin{cases} \langle \kappa^h, \chi\rangle^h_h \\ \langle \kappa^h_s, \chi_s\rangle_h \end{cases} = 0 \qquad \forall\ \chi \in V^h, \tag{2a}$$

$$\langle \kappa^h\,\vec{\nu}^h, \vec{\eta}\rangle^h_h + \langle \vec{X}^h_s, \vec{\eta}_s\rangle_m = 0 \qquad \forall\ \vec{\eta} \in \underline{V}^h; \tag{2b}$$

where $\langle f,g\rangle_h := \int_{\Gamma^h(t)} f\,.\,g\,\mathrm{d}s = \int_I f\,.\,g\,|\vec{X}^h_\rho(t)|\,\mathrm{d}\rho$ with $\langle\cdot,\cdot\rangle^h_m$ the mass lumped inner product. It is now straightforward to show that (2b) implies that neighbouring elements of $\Gamma^h(t) = \vec{X}^h(I,t)$ have the same length or are parallel. When introducing fully discrete approximations, it is possible to use semi-implicit time stepping or a fully implicit approach. In the former case, we obtain linear schemes that intrinsically move mesh points tangentially so that e.g. numerical steady states are always equidistributed, while the latter leads to highly nonlinear approximations that truly equistribute at each time level; see [1, 2] and [9], respectively. Both variants are unconditionally stable.

An advantage of our scheme (2a,b), that follows from the formulation (1), is that other geometric evolution laws can be handled easily. For example, nonlinear curvature flow, including the inverse curvature flow, area preserving curvature flow, Willmore flow (or elastic flow) for curves, as well as higher codimension flows of curves in $\mathbb{R}^d$, $d \geq 3$, and geodesic flows of curves flowing on a given manifold, can all be considered; see [1, 2, 10] for details.

The approximation (2a,b) can also be generalized to cover the geometric evolution of curve networks, where different curves move by their given normal velocities and where certain conditions have to hold at triple junctions, where three curves

meet at a point. It turns out that the natural generalization of the weak formulation used to derive (2a,b) approximates all the necessary triple junction conditions correctly; see [1, 2].

Replacing the isotropic curve length $|\Gamma| := \int_\Gamma 1 \, \mathrm{d}s$ with a weighted length of the form $|\Gamma|_\gamma := \int_\Gamma \gamma(\vec{\nu}) \, \mathrm{d}s$, where $\gamma : \mathbb{R}^2 \setminus \{\vec{0}\} \to \mathbb{R}_{>0}$ is a given one-homogeneous anisotropy function, yields the anisotropic analogues of the geometric evolution equations of curvature flow and surface diffusion, i.e.

$$\vec{x}_t \,.\, \vec{\nu} = \begin{cases} \beta(\vec{\nu}) \, \varkappa_\gamma \\ -(\beta(\vec{\nu}) \, [\varkappa_\gamma]_s)_s \end{cases} , \qquad \varkappa_\gamma \, \vec{\nu} = [\gamma'(\vec{\nu})]_s^\perp \,, \tag{3}$$

where $\vec{\nu} = -\vec{x}_s^{\,\perp}$, $\varkappa_\gamma$ is the weighted curvature, and $\beta : S^1 \to \mathbb{R}_{>0}$ is an anisotropic mobility. The finite element approximations based on (2a,b) can now be extended to approximate the flows (3). The fully discrete schemes can be shown to be unconditionally stable for arbitrary smooth convex anisotropies, in the case of a fully implicit time discretization ([9]), and for anisotropies of the form

$$\gamma(\vec{p}) = \left[\sum_{\ell=1}^{L} [\gamma^{(\ell)}(\vec{p})]^r \right]^{\frac{1}{r}} = \left[\sum_{\ell=1}^{L} [\vec{p} \,.\, G^{(\ell)} \, \vec{p}]^{\frac{r}{2}} \right]^{\frac{1}{r}} , \tag{4}$$

where $G^{(\ell)} \in \mathbb{R}^{2\times 2}$, $\ell = 1 \to L$, are symmetric and positive definite, and $r \in [1, \infty)$; see [3, 10].

Moreover, the ideas presented above naturally generalize to the approximation of geometric evolution equations for hypersurfaces in $\mathbb{R}^3$. Examples are the mean curvature flow, nonlinear mean curvature flow and surface diffusion for isotropic (see [4]) and anisotropic surface energies (see [6]), the Willmore flow and Helfrich flow (see [5]), as well as the evolution of surface clusters with triple junction lines and quadruple junction points (see [7]). In all of the isotropic cases, we can show that our semidiscrete continuous-in-time approximations produce triangulations with very good mesh qualities, so called *conformal polyhedral surfaces*; see [4, §4] for details. Such surfaces are characterized by the fact that the two popular notions of discrete vertex normals, given by the directions of steepest descent of area and volume, respectively, coincide; which in turn means that the triangulation cannot be bad. Related properties can be derived for anisotropic surface energies.

Finally, we can also consider situations where the interface evolution is coupled to an equation that needs to hold in a bulk domain. For instance, the evolution of a solidifying front $\Gamma(t)$ in a Stefan problem with anisotropic Gibbs-Thomson law and kinetic undercooling can be expressed as

$$\rho \, (\vec{x}_t \,.\, \vec{\nu}) = \beta(\vec{\nu}) \, [\alpha \, \varkappa_\gamma - a \, u] \qquad \text{on } \Gamma(t), \tag{5}$$

where u, usually a rescaled temperature, satisfies a heat equation in the bulk domain Ω, with an energy balance at the interface leading to jumps in the gradient of u across $\Gamma(t)$. Coupling our natural parametric finite element approximation of (5) to a finite element approximation of the evolution of u in the bulk, we are able to introduce stable fully discrete schemes which mimic the underlying Lyapunov

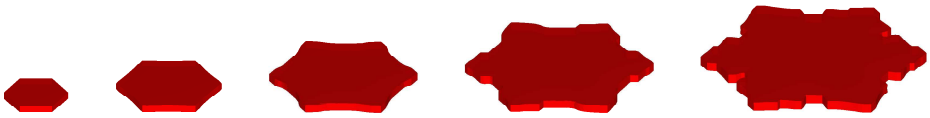

FIGURE 1. Solid plates and sectored plates.

structure of the continuous problem, see [8]. When u is interpreted as a concentration, then the studied Stefan problem can be used to model the solidification from a supersaturated solution, which is relevant for snowflake growth. An example computation, for a surface energy of the form (4) with a hexagonal prism Wulff shape, can be seen in Figure 1.

REFERENCES

[1] J.W. Barrett, H. Garcke, and R. Nürnberg, *A parametric finite element method for fourth order geometric evolution equations*, J. Comput. Phys. **222** (2007), 441–462.

[2] J.W. Barrett, H. Garcke, and R. Nürnberg, *On the variational approximation of combined second and fourth order geometric evolution equations*, SIAM J. Sci. Comput. **29** (2007), 1006–1041.

[3] J.W. Barrett, H. Garcke, and R. Nürnberg, *Numerical approximation of anisotropic geometric evolution equations in the plane*, IMA J. Numer. Anal. **28** (2008), 292–330.

[4] J.W. Barrett, H. Garcke, and R. Nürnberg, *On the parametric finite element approximation of evolving hypersurfaces in* $\mathbb{R}^3$, J. Comput. Phys. **227** (2008), 4281–4307.

[5] J.W. Barrett, H. Garcke, and R. Nürnberg, *Parametric approximation of Willmore flow and related geometric evolution equations*, SIAM J. Sci. Comput. **31** (2008), 225–253.

[6] J.W. Barrett, H. Garcke, and R. Nürnberg, *A variational formulation of anisotropic geometric evolution equations in higher dimensions*, Numer. Math. **109** (2008), 1–44.

[7] J.W. Barrett, H. Garcke, and R. Nürnberg, *Parametric approximation of surface clusters driven by isotropic and anisotropic surface energies*, 2009, Preprint No. 04/2009, University Regensburg.

[8] J.W. Barrett, H. Garcke, and R. Nürnberg, *On stable parametric finite element methods for the Stefan problem and the Mullins–Sekerka problem with applications to dendritic growth*, 2009, Preprint No. 21/2009, University Regensburg.

[9] J.W. Barrett, H. Garcke, and R. Nürnberg, *The approximation of planar curve evolutions by stable fully implicit finite element schemes that equidistribute*, 2009, Preprint No. 29/2009, University Regensburg.

[10] J.W. Barrett, H. Garcke, and R. Nürnberg, *Numerical approximation of gradient flows for closed curves in* $\mathbb{R}^d$, IMA J. Numer. Anal. **30** (2010), 4–60.

Level set method for spiral crystal growth and surface evolution

TAKESHI OHTSUKA

This is a brief introduction to a level set formulation for spiral patterns evolving by a mean curvature flow with driving force, and numerical simulations for crystal growth with aid of screw dislocations, which is called spiral crystal growth (see [1]). When partial displacements in the lattice of atoms, that is called screw dislocation, across the surface of a crystal, then steps are provided on the surface. The steps

evolve and climb up on the helical surface due to screw dislocations with drawing spiral patterns, and thus the crystal grows. According to the theory of [1] the velocity V of the steps is of the form

$$V = v_\infty(1 - \rho_c\kappa), \tag{1}$$

where κ is the curvature of the curve describing by spiral steps, v_∞ and ρ_c are constants denoting a velocity of a straight line step and critical radius, repectively. For the evolution of spiral patterns, phase field models are proposed by Karma–Plapp ([6]), Kobayashi [7], and a level set formulation is proposed by Smereka [9], repectively. However, Smereka's formulation is not convenience to describe, for example, a case of multiple spirals from single center. Thus, our goal is to propose a new level set formulation which is based on the idea of sheet structure functions due to [6] or [7]. We also give some numerical simulations for the growth rate of the crystal surface for the case of two screw dislocations with opposite orientations.

Let $\Omega \subset \mathbb{R}^2$ be a bounded domain denoting a evolving crystal surface. We denote a center of screw dislocations by $a_1, \dots, a_N \in \Omega$ and their closed neighborhoods $B_j \subset \Omega$, where $N \geq 1$. Assume that $B_i \cap B_j = \emptyset$ if $i \neq j$ and thus $W = \Omega \setminus \bigcup_{j=1}^N B_j$ has smooth boundary. We set a spiral pattern Γ_t by

$$\Gamma_t := \{x \in \overline{W};\ u(t,x) - \theta(x) \equiv 0 \mod 2\pi\mathbb{Z}\}, \tag{2}$$

where $\theta(x) = \sum_{j=1}^N m_j \arg(x - a_j)$, and $m_j \in \mathbb{Z} \setminus \{0\}$ for $j = 1, \dots, N$. We require that θ is a multiple valued function to describe a spiral pattern completely. However, θ is locally regarded as a single valued and smooth function in some neighborhood of Γ_t, and thus we define the orientation of steps $\vec{\mathbf{n}}$, which is a continuous unit normal vector field of Γ_t, is given by

$$\vec{\mathbf{n}} = -\frac{\nabla(u - \theta)}{|\nabla(u - \theta)|}. \tag{3}$$

The function θ is sheet structure function, which denotes a helical surface structure of the lattice of atoms, due to [7] or [6] for $N = 1$ with $\theta = \arg x$. The characteristic structure of our problem is that the spiral pattern has not only its evovling orientation $\vec{\mathbf{n}}$, but also rotational orientation with respect to each screw dislocations. We denote the rotational orientation by $\mathrm{sgn}(m_j)$. The number of steps attached to a_j is denoted by $|m_j|$. The sheet structure function is related to the crystal surface including the screw dislocations. In fact, by the dislocation theory and the linear elasticity the surface height $h(t,x)$ satisfies

$$\Delta h = -h_0 \mathrm{div}\delta_{\Gamma_t}\vec{\mathbf{n}}, \tag{4}$$

if the displacement of lattice is only in the vertical direction of the surface and small enough, where δ_{Γ_t} is the dirac's delta measure of Γ_t and h_0 is the unit height of the steps. In our case a branch of $(h_0/2\pi)\theta$ whose discontinuities are only on Γ_t is a solution of (4).

To determine the motion of spiral patterns we postulate the Neumann boundary condition for spiral patterns as $\Gamma_t \perp \partial W$. Then, by similar argument as the usual

level set method (see [5]) we obtain the level set equation as follows;

$$(5)\qquad \begin{cases} u_t - v_\infty |\nabla(u-\theta)| \left\{ 1 + \rho_c \mathrm{div} \dfrac{\nabla(u-\theta)}{|\nabla(u-\theta)|} \right\} = 0 & \text{in } (0,T)\times W, \\ \langle \vec{\nu}, \nabla(u-\theta)\rangle = 0 & \text{on } (0,T)\times \partial W, \\ u|_{t=0} = u_0 & \text{on } \overline{W}, \end{cases}$$

where $\vec{\nu}$ is the outer unit normal vector field of ∂W, $\langle\cdot,\cdot\rangle$ is the usual inner product in $\mathbb{R}^2$, and u_0 is an initial datum satisfying

$$(6)\qquad \Gamma_0 = \{x \in \overline{W};\ u_0(x) - \theta(x) \equiv 0 \mod 2\pi\mathbb{Z}\}.$$

We can define a viscosity solution to (5) in usual way (see [3]). The comparison, existence and uniqueness of viscosity solutions global-in-time for $u_0 \in C(\overline{W})$ is obtained by [8]. However, it is not clear the existence of $u_0 \in C(\overline{W})$ satisfying (6). Goto, Nakagawa and the author prove the existence of $u_0 \in C(\overline{W})$ for suitable initial pattern Γ_0. Moreover, they prove the uniqueness of Γ_t obtained from our level set formulation with respect to the initial pattern Γ_0. The basic strategy of the proofs are based on the method as in [2] or [4].

It is convenience for understanding our formulation to introduce a covering space which is based on θ. Formally we now introduce

$$\mathcal{X} := \{(x,z);\ z \equiv \theta(x) \mod 2\pi\mathbb{Z}\}.$$

Then we find that $\mathcal{X}$ is divided into three regions as follows;

$$\widetilde{\Gamma}_t := \{(x,z) \in \mathcal{X};\ u(t,x) - z = 0\},$$
$$\widetilde{I}_t := \{(x,z) \in \mathcal{X};\ u(t,x) - z > 0\},$$
$$\widetilde{O}_t := \{(x,z) \in \mathcal{X};\ u(t,x) - z < 0\}.$$

We observe that Γ_t is the image of $\widetilde{\Gamma}_t$ by the projection $(x,z) \mapsto x$, and also (3) is determined from $\widetilde{I}_t$ and $\widetilde{O}_t$; we consider steps evolve from $\widetilde{I}_t$'s side to $\widetilde{O}_t$'s side. The covering space is very convenient to remove the difficulties which come from the multiplicity of θ, that is the crucial difficulty of our problem. In particular, the uniqueness of Γ_t is obtained from the comparison of $\widetilde{I}_t$ and $\widetilde{O}_t$ between viscosity sub- and supersolution.

The covering space $\mathcal{X}$ is also useful to obtain the surface height $h(t,x)$. Once we obtain a solution u to (5), we set $\tilde{h}\colon [0,\infty)\times\mathcal{X} \to \mathbb{R}$ as

$$\tilde{\zeta}(t,x,z) = z - 2\pi k \quad \text{if } (x,z) \in \{(y,\eta) \in \mathcal{X};\ u(t,x) - z \in [2\pi k, 2\pi(k+1))\}.$$

Let $\Theta_j(x) \in [0,2\pi)$ is the principal value of $\arg(x-a_j)$ and $\Theta(x) = \sum_{j=1}^N m_j \Theta_j(x)$. We set

$$\zeta(t,x) = \tilde{\zeta}(t,x,\Theta(x)).$$

Then, we observe that $\zeta \equiv \theta \mod 2\pi\mathbb{Z}$ and the discontinuities of ζ lie only on Γ_t. Moreover, we obtain that $\widetilde{I}_t = \{(x,z) \in \mathcal{X};\ \zeta(t,x) + \pi - z > 0\}$. Consequently, we

set the height function h as

$$h(t,x) = \frac{h_0}{2\pi}(\zeta(t,x) + \pi).$$

The growth height of the surface is calculated as

$$R_h(t;t_0) = \frac{1}{|W|}\int_W [h(t,x) - h(t_0,x)]dx.$$

The growth rate of the surface is calculated as $R_h'(t;t_0)$ if R_h is smooth.

In this talk we propose a numerical results of the growth height in the case $N = 2$, $m_1 = -m_2 = 1$, and $W = \Omega \setminus (B_\rho(a_1) \cup B_\rho(a_2))$, where $B_\rho(a)$ is the closed disc whose center and radius is a and ρ, repectively. In [1] it is pointed out that the pair whose rotational orientations are opposite have no activity if $|a_1 - a_2| < 2\rho_c$. We call such a pair inactive pair. The existence of inactive pairs are not only verified numerically but also proved mathemtaically.

Theorem. Let Ω be a bounded domain such that $B_{4\rho_c}(0) \subset \Omega$. Let $W = \Omega \setminus (B_\rho(a_1) \cup B_\rho(a_2))$, $\theta(x) = \arg(x - a_1) - \arg(x - a_2)$, $a_1 = (-r, 0)$, $a_2 = (r, 0)$ with $r \in (0, \rho_c)$, and $\rho \in (0, \rho_c)$. Then, for any viscosity solution u to (5), there exists $M > 0$ such that $u(t,x) < M$ for $t > 0$ and $x \in \overline{W}$.

The idea of the proof is to construct a stationary solution to (5) by θ. We know that $C(b) := \{x \in \mathbb{R}^2;\ |x - b| = \rho_c\}$ for $b \in \mathbb{R}^2$ is a stationary solution of (1), and there exist $b \in \mathbb{R}^2$ and a part of $C(b)$ satisfying $\partial W \perp C(b)$ if $|a_1 - a_2| < 2\rho_c$. Then, we obtain that $\theta_{C(b)}$, that is one of branches of θ whose discontinuities are only on $C(b)$, is a viscosity solution of (5) by direct calculation.

References

[1] W. K. Burton, N. Cabrera and F. C. Frank, The growth of crystals and the equilibrium structure of their surfaces, Philos. Trans. Roy. Soc. London. Ser. A. **243**(1951), 299–358.

[2] Y.-G. Chen, Y. Giga and S. Goto, Uniqueness and existence of viscosity solutions of generalized mean curvature flow equation, J. Differential Geom. **33**(1991), 749–786.

[3] M. Crandall, H. Ishii and P.-L. Lions, User's guide to viscosity solutions of second order partial differential equations, Bull. Amer. Math. Soc. **27**(1992), 1–67.

[4] L. C. Evans and J. Spruck, Motion of level sets by mean curvature I, J. Differential Geom. **33**(1991), 635–681.

[5] Y. Giga, *Surface evolution equation –A level set approach*, Birkhäuser, 2006.

[6] A. Karma and M. Plapp, Spiral surface growth without desorption, Physical Review Letters **81**(1998), 4444–4447.

[7] R. Kobayashi, private communication.

[8] T. Ohtsuka, A level set method for spiral crystal growth, Adv. Math. Sci. Appl. **13**(2003), 225–248.

[9] P. Smereka, Spiral crystal growth, Physica D, **138**(2000), 282–301.

FEM approximation of the anisotropic mean curvature flow in higher codimension

P. Pozzi

Anisotropic mean curvature flow has been widely studied, both analytically and numerically. Much of the research concentrated so far on the case of codimension equal to one, i.e. on the flow for hypersurfaces. In this talk we present recent progress for the case of higher codimension.

After discussing the concept of anisotropic area functional, we consider the anisotropic mean curvature flow for parametric curves and two dimensional surfaces in $\mathbb{R}^n$ for arbitraty $n \geq 3$ and study its numerical approximation by finite elements.

Stabilization of a fluid – structure model

Jean-Pierre Raymond

We study a system coupling the incompressible Navier-Stokes equations in 2D bounded domains with a damped Euler-Bernoulli beam equation, where the beam is a part of the upper boundary of the domain occupied by the fluid. We also study similar systems in 3D domains, in that case the structure equation is a damped plate equation. Due to the deformation of the beam (or the plate in 3D) the fluid domain at time t depends on t. We are interested in exponential stabilization of such systems, locally about a stationary solution, by controls acting either in the fluid equation or in the beam equation.

These results are obtained by studying stabilizability results for linearized systems. In order to derive linearized systems, we first rewrite the nonlinear models in a cylindrical domain $\Omega \times (0,\infty)$, by using a change of variable defined thanks to the deformation of the structure. In the 2D case, the model linearized about the null solution reads as follows

$$
\begin{aligned}
&\mathbf{v}_t - \operatorname{div}\sigma(\mathbf{v},p) = \mathbf{f}\chi_{\mathcal{O}}, \qquad \operatorname{div}\mathbf{v} = 0 \quad \text{in } Q_\infty,\\
&\mathbf{v} = \eta_2\vec{e}_2 \ \text{ on } \Sigma^s_\infty, \quad \mathbf{v} = 0 \ \text{ on } \Sigma^0_\infty, \quad \mathbf{v}(0) = \mathbf{v}^0 \ \text{ in } \Omega,\\
&\eta_{1,t} = \eta_2, \quad \eta_{2,t} - \beta\eta_{1,xx} - \delta\eta_{2,xx} + \alpha M_s\eta_{1,xxxx} = M_s(\rho_1 p + g) \ \text{ on } \Sigma^s_\infty,\\
&\eta_1 = 0 \quad \text{and} \quad \eta_{1,x} = 0 \ \text{ on } \big\{0, L\big\} \times (0,\infty),\\
&\eta_1(0) = \eta_1^0 \quad \text{and} \quad \eta_2(0) = \eta_2^0 \ \text{ in } \Gamma_s,
\end{aligned}
\tag{1}
$$

where $Q_\infty = \Omega \times (0,\infty)$, Ω is a simply connected bounded domain with boundary Γ, for simplicity we assume that $\Omega \subset \{(x,y) \mid y < 1\}$, $\Gamma_s = (0,L)\times\{1\}$ is a flat part of the boundary Γ, $\vec{e}_2 = (0,1)^T$, $\Sigma^s_\infty = \Gamma_s \times (0,\infty)$, $\Sigma^0_\infty = \Gamma_0 \times (0,\infty)$, $\Gamma_0 = \Gamma \setminus \Gamma_s$, M_s is the orthogonal projection in $L^2(\Gamma_s)$ onto $L^2_0(\Gamma_s) = \{\eta \in L^2(\Gamma_s) \mid \int_{\Gamma_s} \eta = 0\}$, $\sigma(\mathbf{v},p) = \nu(\nabla\mathbf{v} + \nabla\mathbf{v}^T) - p\,I$, $\nu > 0$ is the fluid viscosity, $\alpha > 0$, $\beta \geq 0$, and $\delta > 0$ are the adimensional rigidity, stretching, and friction coefficients of the beam, ρ_1 is a positive constant related to the densities of the fluid and of the structure, $\mathbf{f}$ is a control acting in the fluid equation, $\chi_{\mathcal{O}}$ is the characteristic function of an open set

$\mathcal{O} \subset \Omega$, g is a control acting in the beam equation. To simplify the presentation, we assume that either Ω is of class C^2 or Ω is the rectangle $(0, L) \times (0, 1)$.

Let us introduce the spaces

$$L^2_0(\Omega) = \Big\{ p \in L^2(\Omega) \mid \textstyle\int_\Omega p = 0 \Big\}, \quad \mathcal{H}^\sigma(\Omega) = H^\sigma(\Omega) \cap L^2_0(\Omega) \quad \text{for } \sigma \geq 0,$$

$$\mathbf{V}^0_n(\Omega) = \Big\{ \mathbf{v} \in L^2(\Omega; \mathbb{R}^2) \mid \text{ div } \mathbf{v} = 0, \ \mathbf{v} \cdot \mathbf{n} = 0 \text{ on } \Gamma \Big\},$$

$$\mathbf{V}^0(\Omega) = \Big\{ \mathbf{v} \in L^2(\Omega; \mathbb{R}^2) \mid \text{ div } \mathbf{v} = 0 \Big\} \quad \text{and} \quad \mathbf{V}^2_n(\Omega) = H^2(\Omega; \mathbb{R}^2) \cap \mathbf{V}^0_n(\Omega).$$

We introduce the Leray projector $P : L^2(\Omega; \mathbb{R}^2) \mapsto \mathbf{V}^0_n(\Omega)$ and the Stokes operator $A_0 = \nu P \Delta$ with domain $\mathcal{D}(A_0) = H^2(\Omega; \mathbb{R}^2) \cap H^1_0(\Omega; \mathbb{R}^2) \cap \mathbf{V}^0_n(\Omega)$. We want to study system (1) when $\mathbf{v}^0 \in \mathbf{V}^0(\Omega)$, $\eta^0_1 \in H^2_0(\Gamma_s) \cap L^2_0(\Gamma_s)$, $\eta^0_2 \in L^2_0(\Gamma_s)$, $g \in L^2(0, \infty; L^2(\Gamma_s))$, $\mathbf{f} \in L^2(0, \infty; L^2(\Omega; \mathbb{R}^2))$, and when the initial data satisfy the compatibility condition

$$\mathbf{v}^0 \cdot \mathbf{n} = \eta^0_2 \, \chi_{\Gamma_s}. \tag{2}$$

For that, we have to study the semigroup corresponding to system (1). We denote by $N \in \mathcal{L}(H^{-1/2}(\Gamma), \mathcal{H}^1(\Omega))$ the Neumann operator defined by $N(g) = q$, where q is the solution of

$$\Delta q = 0 \quad \text{in } \Omega, \qquad \frac{\partial q}{\partial \mathbf{n}} = g \quad \text{on } \Gamma$$

($\mathbf{n}$ is the unit normal to Γ outward Ω), and by $D \in \mathcal{L}(H^{-1/2}(\Gamma; \mathbb{R}^2), \mathbf{V}^0(\Omega))$ the Dirichlet operator defined by $D(\mathbf{g}) = \mathbf{w}$, where $\mathbf{w}$ is the solution of

$$-\nu \Delta \mathbf{w} + \nabla \pi = 0, \quad \text{div } \mathbf{w} = 0 \text{ in } \Omega, \quad \mathbf{w} = \mathbf{g} \text{ on } \Gamma.$$

We also need $N_s(g) = N(g \, \chi_{\Gamma_s})$ and $\gamma_s(q) = M_s(q|_{\Gamma_s})$ (χ_{Γ_s} is the characteristic function of Γ_s). When $\mathbf{f} = 0$ and $g = 0$, we may rewrite system (1) in the form

$$\begin{aligned}
&P\mathbf{v}_t = A_0 P\mathbf{v} + (-A_0) P D(\eta_2 \vec{e}_2 \, \chi_{\Gamma_s}), \quad \mathbf{v}(0) = \mathbf{v}_0 \quad \text{in} \quad \Omega, \\
&(I - P)\mathbf{v} = (I - P) D(\eta_2 \vec{e}_2 \, \chi_{\Gamma_s}), \\
&\eta_{1,t} = \eta_2, \\
&(I + \gamma_s N_s)\eta_{2,t} - \beta \eta_{1,xx} - \delta \eta_{2,xx} + \alpha M_s \eta_{1,xxxx} = \gamma_s N(\Delta P\mathbf{v} \cdot \mathbf{n}) \ \text{ on } \Sigma^s_\infty, \\
&\eta_1 = 0 \quad \text{and} \quad \eta_{1,x} = 0 \ \text{ on } \big\{0, L\big\} \times (0, \infty), \\
&\eta_1(0) = \eta^0_1 \quad \text{and} \quad \eta_2(0) = \eta^0_2 \ \text{ in } \Gamma_s.
\end{aligned} \tag{3}$$

System (3) is of the form

$$\frac{\mathrm{d}}{\mathrm{d}t} \begin{pmatrix} P\mathbf{v} \\ \eta_1 \\ \eta_2 \end{pmatrix} = \mathcal{A} \begin{pmatrix} P\mathbf{v} \\ \eta_1 \\ \eta_2 \end{pmatrix}, \qquad (I - P)\mathbf{v} = (I - P) D(\eta_2 \vec{e}_2 \, \chi_{\Gamma_s}),$$

with

$$\mathcal{A} = \begin{pmatrix} I & 0 & 0 \\ 0 & I & 0 \\ 0 & 0 & (I+\gamma_s N_s)^{-1} \end{pmatrix} \begin{pmatrix} A_0 & 0 & (-A_0)PD \\ 0 & 0 & I \\ \gamma_s N(\Delta(\cdot)\cdot \mathbf{n}) & A_{\alpha,\beta} & \delta\Delta_s \end{pmatrix},$$

$$\mathcal{D}(A_{\alpha,\beta}) = H^4(\Gamma_s) \cap H_0^2(\Gamma_s) \cap L_0^2(\Gamma_s), \quad A_{\alpha,\beta}\eta = \beta\eta_{xx} - \alpha\eta_{xxxx}, \quad \Delta_s\eta = \eta_{xx},$$

and

$$\mathcal{D}(\mathcal{A}) = \Big\{ (P\mathbf{v}, \eta_1, \eta_2) \in \mathbf{V}_n^2(\Omega) \times (H^4 \cap H_0^2 \cap L_0^2)(\Gamma_s) \times (H_0^2 \cap L_0^2)(\Gamma_s) \\ \mid P\left(\mathbf{v} - D(\eta_2 \vec{e}_2\, \chi_{\Gamma_s})\right) \in H_0^1(\Omega;\mathbb{R}^2) \Big\}.$$

Theorem 1. The operator $(\mathcal{A}, \mathcal{D}(\mathcal{A}))$ is the infinitesimal generator of an analytic semigroup on $H = \mathbf{V}_n^0(\Omega) \times (H_0^2(\Gamma_s) \cap L_0^2(\Gamma_s)) \times L_0^2(\Gamma_s)$, and the resolvent of $\mathcal{A}$ is compact.

This type of result can be extended to the 3D case.

Theorem 2. (Exponential stabilization with an internal control acting in the fluid equation) Assume that Ω is of class C^2 and that $g = 0$. Then, for all $\omega > 0$, there exists a positive constant C_ω such that, for all $\mathbf{v}^0 \in \mathbf{V}^0(\Omega)$, $\eta_1^0 \in H_0^2(\Gamma_s) \cap L_0^2(\Gamma_s)$, $\eta_2^0 \in L_0^2(\Gamma_s)$ satisfying (2), there exists a control $\mathbf{f} \in L^2(0,\infty; L^2(\Omega;\mathbb{R}^2))$ for which the solution of system (1) obeys

$$\begin{aligned} &\|(\mathbf{v}(t), \eta_1(t), \eta_2(t))\|_{\mathbf{V}^0(\Omega)\times H_0^2(\Gamma_s)\times L_0^2(\Gamma_s)} \\ &\le C_\omega e^{-\omega t} \|(\mathbf{v}^0, \eta_1^0, \eta_2^0)\|_{\mathbf{V}^0(\Omega)\times H_0^2(\Gamma_s)\times L_0^2(\Gamma_s)}. \end{aligned} \tag{4}$$

The proof of Theorem 2 relies on Theorem 1 and on a unique continuation result proved in [1]. This type of result can be extended to the 3D case.

Theorem 3. (Exponential stabilization with a control acting in the structure equation) Assume that $\Omega = (0, L)\times(0, 1)$ and that $\mathbf{f} = 0$. Then, for all $\omega > 0$, there exists a positive constant C_ω such that, for all $\mathbf{v}^0 \in \mathbf{V}^0(\Omega)$, $\eta_1^0 \in H_0^2(\Gamma_s) \cap L_0^2(\Gamma_s)$, $\eta_2^0 \in L_0^2(\Gamma_s)$ satisfying (2), there exists a control $g \in L^2(0,\infty; L^2(\Gamma_s))$ for which the solution of system (1) obeys (4).

The proof of Theorem 3 relies on Theorem 1 and on a unique continuation result proved in [2]. This type of result can be extended to other domains in the 2D case by using unique continuation results proved in [3], but there is no similar result proved in the 3D case.

Thanks to Theorem 3, we can prove that the nonlinear system coupling the Navier-Stokes equations with the damped beam equation is exponentially stabilizable, locally about the null solution, with any prescribed decay rate, by a feedback control corresponding to a force term in the beam equation [4]. The feedback is applied on the whole structure and it is determined, via a Riccati equation, by solving an infinite time horizon control problem for the linearized model.

Thanks to Theorem 2, we can prove that the nonlinear system coupling the Navier-Stokes equations with the damped beam equation is exponentially stabilizable, locally about the null solution, with any prescribed decay rate, by a feedback

control corresponding to a force term in the fluid equation. We think that similar results could be obtained in the 3D case, but this is not yet done.

References

[1] C. Fabre, G. Lebeau, Régularité et unicité pour le problème de Stokes, Comm. Partial Differential Equations 27 (2002), 437–475.
[2] A. Osses, J.-P. Puel, Approximate controllability for a hydro-elastic model in a rectangular domain, ISNM 133 (1999), 231-243.
[3] A. Osses, J.-P. Puel, Unique continuation property near a corner and its fluid-structure controllability consequences, ESAIM Control, Optimization and Calculus of Variations, DOI: 10.1051/cocv:2008024.
[4] J.-P. Raymond, Feedback stabilization of a fluid - structure model, 2009, submitted to SIAM J. Control and Optim..

Numerical methods for surfactant transport in two-phase incompressible flows

Arnold Reusken
(joint work with P. Esser, J. Grande, S. Groß, M. Olshanskii)

1. A model for two-phase incompressible flows

We consider a two-phase flow problem with mass transport between the phases and transport of a surfactant ("surface active agent") on the interface between the phases. We briefly introduce a (standard) model for this type of flow problem.

Fluid dynamics. The domain $\Omega \subset \mathbb{R}^d$, $d = 2$ or $d = 3$, contains two different immiscible incompressible phases (fluid-fluid or fluid-gas) which may move in time and have different material properties ρ_i (density) and μ_i (viscosity), $i = 1, 2$. For each point in time, $t \in [0, T]$, Ω is partitioned into two open bounded subdomains $\Omega_1(t)$ and $\Omega_2(t)$, $\overline{\Omega} = \overline{\Omega}_1(t) \cup \overline{\Omega}_2(t)$, $\Omega_1(t) \cap \Omega_2(t) = \emptyset$, each of them containing one of the phases. These phases are separated from each other by the interface $\Gamma(t) = \overline{\Omega}_1(t) \cap \overline{\Omega}_2(t)$. We assume isothermal conditions and that both phases are pure substances. Furthermore, we do *not* consider reaction or phase transition. We introduce the normal velocity $V_\Gamma = V_\Gamma(x, t) \in \mathbb{R}$ which denotes the magnitude of the velocity of the interface Γ at $x \in \Gamma(t)$ in normal direction. The immiscibility assumption is modeled by the condition $V_\Gamma = \mathbf{u} \cdot \mathbf{n}_\Gamma$ at the interface, with $\mathbf{n}_\Gamma$ the unit normal on Γ pointing from Ω_1 to Ω_2. We consider the following standard model (in strong formulation) for the *fluid dynamics* of a two-phase incompressible

flow:

$$\text{(1)} \qquad \begin{cases} \rho_i\left(\dfrac{\partial \mathbf{u}}{\partial t} + (\mathbf{u}\cdot\nabla)\mathbf{u}\right) = \operatorname{div}\boldsymbol{\sigma}_i + \rho_i \mathbf{g} \\ \operatorname{div}\mathbf{u} = 0 \end{cases} \qquad \text{in } \Omega_i, \quad i = 1,2,$$

$$\text{(2)} \qquad [\boldsymbol{\sigma}\mathbf{n}_\Gamma] = -\tau\kappa\mathbf{n}_\Gamma - \nabla_\Gamma \tau \quad \text{on } \Gamma,$$

$$\text{(3)} \qquad [\mathbf{u}] = 0 \quad \text{on } \Gamma,$$

$$\text{(4)} \qquad V_\Gamma = \mathbf{u}\cdot\mathbf{n}_\Gamma \quad \text{on } \Gamma.$$

with the stress tensor $\boldsymbol{\sigma}_i = -p\mathbf{I} + \mu_i\big(\nabla\mathbf{u} + (\nabla\mathbf{u})^T\big)$. The density and viscosity, ρ_i and $\mu_i, i = 1,2$, are assumed to be constant in each phase. The operator ∇_Γ is the tangential gradient. The parameter τ is the surface tension coefficient and κ is the mean curvature of Γ, i.e., $\kappa(x) = \operatorname{div}\mathbf{n}_\Gamma(x)$ for $x \in \Gamma$. To make the problem well-posed one needs suitable initial and boundary conditions for $\mathbf{u}$.

Mass transport. We assume that one or both phases contain a dissolved species that is transported due to convection and diffusion and does not adhere to the interface. The concentration of this species is denoted by $c(x,t)$. This flow problem can be modeled by the equations (1)-(4) for the flow variables and a convection-diffusion equation for the concentration c. At the interface we need interface conditions for c. The first interface condition comes from mass conservation, which implies flux continuity. The second condition results from a constitutive equation known as Henry's law. The model is as follows:

$$\text{(5)} \qquad \begin{aligned} &\frac{\partial c}{\partial t} + \mathbf{u}\cdot\nabla c = \operatorname{div}(D_i\nabla c) \quad \text{in } \Omega_i,\ i = 1,2, \\ &[D_i\nabla c\cdot\mathbf{n}_\Gamma] = 0 \quad \text{on } \Gamma, \\ &c_1 = C_H c_2 \quad \text{on } \Gamma. \end{aligned}$$

The diffusion coefficient D_i is assumed to be piecewise constant. In the interface condition we use the notation c_i for $c_{|\Omega_i}$ restricted to the interface. The constant $C_H > 0$ is given (Henry's constant). In general $C_H \neq 1$, i.e. we have a discontinuity in c across Γ.

Surfactant transport. We assume that there is a species (called tenside or surfactant) which adheres to the interface and is transported on the interface due to convection (movement of the interface) and due to diffusion (molecular diffusion on the interface). For simplicity we assume that there are no adsorption and desorption effects. The concentration of this surfactant is denoted by $S(x,t)$, $x \in \Gamma(t)$. A partial differential equation for this quantity can be derived from the conservation of mass principle. This results in the convection-diffusion problem

$$\text{(6)} \qquad \dot{S} + S\operatorname{div}_\Gamma\mathbf{u} = \operatorname{div}_\Gamma(D_\Gamma\nabla_\Gamma S) \qquad \text{on } \Gamma.$$

Here $\dot{S}$ denotes the material derivative and $\operatorname{div}_\Gamma$ is the tangential divergence operator.

In the talk we presented an overview of numerical methods for treating the coupled model (1)-(6). Key ingredients are a level set method for interface capturing, finite element discretizations on a nested locally refined hierarchy of tetrahedral grids and problem adapted preconditioners. A detailed overview is given in [3]. A new finite element method for discretization of the surfactant transport equation (6) has been developed. The main idea is presented in section 2.

2. A new finite element method for the surfactant transport problem

We outline the main idea of a new Eulerian finite element method for discretization of the surfactant equation introduced in [1], for a simplified problem, namely the Laplace-Beltrami problem. In weak formulation this problem is as follows: For given $f \in L^2_0(\Gamma) := \{v \in L^2(\Gamma) \mid \int_\Gamma v\, ds = 0\}$, determine $u \in H^1_*(\Gamma) := \{v \in H^1(\Gamma) \mid \int_\Gamma v\, ds = 0\}$ such that

$$\int_\Gamma \nabla_\Gamma u \cdot \nabla_\Gamma v\, ds = \int_\Gamma f v\, ds \qquad \text{for all } v \in H^1_*(\Gamma). \tag{7}$$

We assume a stationary surface Γ and an approximation Γ_h of Γ. We assume that this approximate surface is constructed as follows. Let $\{\mathcal{T}_h\}_{h>0}$ be a family of tetrahedral triangulations of a *fixed* domain $\Omega \subset \mathbb{R}^3$ that contains Γ. These triangulations are assumed to be regular, consistent and stable. Take $\mathcal{T}_h \in \{\mathcal{T}_h\}_{h>0}$. We assume that Γ_h is a $C^{0,1}$ surface without boundary and Γ_h can be partitioned in planar segments, triangles or quadrilaterals, consistent with the outer triangulation $\mathcal{T}_h$. For any tetrahedron $S_T \in \mathcal{T}_h$ such that $\mathrm{meas}_2(S_T \cap \Gamma_h) > 0$ define $T = S_T \cap \Gamma_h$. We assume that each T is *planar*, i.e., either a triangle or a quadrilateral. Let $\mathcal{F}_h$ be the set of all triangles or quadrilaterals T such that $T = S_T \cap \Gamma_h$ is nonempty for some tetrahedron $S_T \in \mathcal{T}_h$ and $\Gamma_h = \cup_{T\in\mathcal{F}_h} T$.

The main new idea of the method is that for discretization of the problem (7) *we use a finite element space induced by the continuous linear finite elements on* $\mathcal{T}_h$. This is done as follows. We define a subdomain that contains Γ_h: $\omega_h := \cup_{T\in\mathcal{F}_h} S_T$. This subdomain in $\mathbb{R}^3$ is connected and partitioned in tetrahedra that form a subset of $\mathcal{T}_h$. We introduce the finite element space

$$V_h := \{\, v_h \in C(\omega_h) \mid v_{|S_T} \in P_1 \text{ for all } T \in \mathcal{F}_h \,\}.$$

This space induces the following space on Γ_h:

$$V_h^\Gamma := \{\psi_h \in H^1(\Gamma_h) \,|\, \exists\, v_h \in V_h :\, \psi_h = v_h|_{\Gamma_h}\,\}, \tag{8}$$

which is used for a Galerkin discretization of (7): determine $u_h \in V_h^\Gamma$ with $\int_{\Gamma_h} u_h\, ds = 0$ such that

$$\int_{\Gamma_h} \nabla_{\Gamma_h} u_h \nabla_{\Gamma_h} \psi_h\, ds = \int_{\Gamma_h} f_h \psi_h\, ds \qquad \text{for all } \psi_h \in V_h^\Gamma, \tag{9}$$

with f_h a suitable extension of f such that $\int_{\Gamma_h} f_h\, ds = 0$. Due the Lax-Milgram lemma this problem has a unique solution u_h. The paper [1] presents a discretization error analysis of this method that shows that under reasonable assumptions

we have *optimal error bounds*. In the talk we present these error bounds. Results of numerical experiments confirm the theoretical analysis. We remark that the family $\{\mathcal{T}_h\}_{h>0}$ is *shape-regular* but the family $\{\mathcal{F}_h\}_{h>0}$ in general is *not shape-regular*. In practice $\mathcal{F}_h$ contains a significant number of strongly deteriorated triangles that have very small angles. Moreover, neighboring triangles can have very different areas.

We briefly address the issue of conditioning of the mass and stiffness, investigated in [2]. Numerical experiments in two- and three-dimensional examples indicate that in the 3D case *both for the diagonally scaled mass and stiffness matrix* (effective) spectral condition numbers behave as $O(h^{-2})$ and in the 2D case the behaviour of these condition numbers is $O(h^{-3})$ and $O(h^{-2})$, respectively.

References

[1] M.A. Olshanskii, A. Reusken, J. Grande, *A Finite Element method for elliptic equations on surfaces*, SIAM J. Numer. Anal. **47** (2009), 3339–3358.

[2] M.A. Olshanskii, A. Reusken, *A finite element method for surface PDEs: Matrix properties*, Numerische Mathematik **114** (2010), 491–520.

[3] DROPS package for simulation of two-phase flows. //www.igpm.rwth-aachen.de/DROPS.

The Allen–Cahn action functional and forced mean curvature flow

Matthias Röger

(joint work with L. Mugnai)

For the stochastically perturbed Allen–Cahn equation

$$\varepsilon\partial_t u_\varepsilon^\delta \;=\; \varepsilon\Delta u_\varepsilon^\delta - \frac{1}{\varepsilon}F'(u_\varepsilon^\delta) + \delta\eta,$$

where η (formally) is a space-time white noise, the probability of being close to a deterministic path $u : [0,T]\times U \to \mathbb{R}$ is in the vanishing noise limit $\delta \to 0$ controlled by the *Allen–Cahn action functional*

$$\mathcal{S}_\varepsilon(u) \;:=\; \int_0^T \int_U \Big(\sqrt{\varepsilon}\partial_t u + \frac{1}{\sqrt{\varepsilon}}\big(-\varepsilon\Delta u + \frac{1}{\varepsilon}F'(u)\big)\Big)^2\, dx\, dt.$$

In the sharp interface limit $\varepsilon \to 0$ an asymptotic reduction was proposed [1]: For an evolution $\mathbf{\Gamma} = (\Gamma_t)_{t\in(0,T)}$ that is up to finitely many *nucleation times* a smooth evolution of smooth hypersurfaces Γ_t the *reduced action functional* is given by

$$\mathcal{S}_0\big(\mathbf{\Gamma}\big) \;=\; c_0 \int_0^T \int_{\Gamma_t} \big|v - H\big|^2\, d\mathcal{H}^{n-1}(x)\, dt \quad + 4c_0\mathcal{H}^{n-1}(\text{nucleated surface area}).$$

For small space dimensions $n = 2, 3$ we prove [2] the compactness of sequences u_ε that are uniformly bounded in action, give a generalized formulation of the reduced action functional, and show a general lower bound estimate.

In subsequent work [3] we used this result to prove a general convergence result for deterministically perturbed Allen–Cahn equations

$$\varepsilon\partial_t u_\varepsilon \;=\; \varepsilon\Delta u_\varepsilon - \frac{1}{\varepsilon}F'(u_\varepsilon) + g_\varepsilon,$$

with suitable initial and boundary conditions. Under the assumption that $n = 2, 3$ and that

$$\int_0^T \int_U \frac{1}{\varepsilon} g_\varepsilon(t,x)^2 \, dxdt \;\le\; \Lambda.$$

we prove that solutions u_ε converge to a generalized solution of forced mean curvature flow $H(t,\cdot) \;=\; v(t,\cdot) + g(t,\cdot)$. Here the limiting forcing term is given by

$$\lim_{\varepsilon\to 0} \int_{U_T} -\eta \cdot g_\varepsilon \nabla u_\varepsilon \;=\; \int_{U_T} \eta \cdot g \, d\mu^t \, dt, \quad \mu^t = \lim_{\varepsilon\to 0} \big(\frac{\varepsilon}{2}|\nabla u_\varepsilon|^2 + \frac{1}{\varepsilon}F'(u_\varepsilon)\big)(t,\cdot)\,\mathcal{L}^n.$$

The generalized formulations are in the sense of geometric measure theory, see [3].

References

[1] R. Kohn, F. Otto, M. G. Reznikoff, and E. Vanden-Eijnden. Action minimization and sharp-interface limits for the stochastic Allen-Cahn equation. *Comm. Pure Appl. Math.*, 60(3):393–438, 2007.

[2] L. Mugnai and M. Röger. The Allen-Cahn action functional in higher dimensions. *Interfaces Free Bound.*, 10(1):45–78, 2008.

[3] L. Mugnai and M. Röger. Convergence of perturbed Allen-Cahn equations to forced mean curvature flow. *Indiana Univ. Math. J.*, in press, 2010.

An Analysis of a Bar Code Deconvolution Problem

Fadil Santosa

(joint work with Selim Esedoḡlu)

In this work, we consider the problem of bar code reading using a laser-based scanner. The problem amounts to a deconvolution after we model the sensing process. The method discussed in this work could potentially be applied to analysis of camera-based scanners, with some modifications.

A bar code consists of black bars over a white back ground. A scanner sends out a narrow laser beam which moves across the bar code. The scanner is equipped with a light detector. Therefore, when the laser beam is on the black part of the bar, little light is reflected and so little light is detected. When the beam is on the white part, more light is detected. If the beam moves across the bar code at a constant speed, the amount of light detected, when converted into voltage, is a signal. The peaks of the signal occur when there is a lot of reflection (white parts of the bar code) and the valleys correspond to when there is little reflection (black parts of the bar code). Thus the signal is an imprint of the bar code.

The challenge comes from the fact that the laser beam is of finite width and has an intensity profile across the beam. Thus, the reading of the bar code by the

laser is "non-local". A simple model for the relationship between a bar code and its signal is a convolution.

We start by describing the bar code as a binary function, taking on values of 0 or 1

$$z(t) \in \{0, 1\},\ a.e., \quad z \in BV.$$

The effect of the laser on the bar code is modeled by a point-spread function. For simplicity, we will take it to be a scaled Gaussian

$$g_{\alpha,\sigma} = \frac{\alpha}{\sqrt{2\pi\sigma^2}} e^{-t^2/2\sigma^2}.$$

The parameters α captures how image intensity is converted to voltage, whereas σ describes the 'width' of the laser beam – smaller σ makes the beam have a smaller footprint while preserving the amount of energy. The signal recorded from a bar code $z(t)$ is

$$h(t) = \int g_{\alpha,\sigma}(t-\tau)z(\tau) + r(t), \tag{1}$$

where $r(t)$ is the noise. We will assume that the noise is bounded in L_2.

The inverse problem is to determine, to the extent possible, the bar code $z(t)$, and the scanner parameters α and σ given a signal $h(t)$.

Esedoḡlu [1] was the first to provide a mathematically rigorous study of the bar code inverse problem. In his work, he showed that under the above convolutional model, a bar code is uniquely determined by its signal. He further showed that the bar code reconstruction problem may be posed as a variational problem, and provided precise mathematical formulations which admits solutions. The paper presents a computational approach which is based on the Modica-Mortola, or the phase field, approximation of the bar code. The computational results contained in the paper demonstrated the effectiveness of this approach.

The computational approach put forward in [1] is based on minizing the following energy

$$E(u) = \int \epsilon|u'|^2 + \frac{1}{\epsilon}W(u) + \lambda\|g_{\alpha,\sigma} * u - h\|^2. \tag{2}$$

Here, ϵ is a small parameter, chosen by the user, and λ is a penalty parameter. The function $W(u)$ is a double potential given by

$$W(u) = u^2(1-u)^2.$$

Therefore, the first term, which can be recognized as the Modica-Mortola energy, enforces the binary nature of the solution u. The second term, which is referred to as the fidelity term, weighs the importance of fitting the data.

Esedoglu solves (2) for u, α and σ, using an alternating direction method consisting of a gradient flow for (α, σ) fixed, followed by updates of (α, σ) for u fixed. In this work, we will assume that $\alpha = 1$ and that σ is known. Thus, our simplified problem is just that of deconvolution of a binary signal.

Our analysis shows that the variational formulation recovers a smoothed version of the bar code. To be more precise, let

$$v = z * \phi_s$$

where $\phi_s(t)$ is a molifier with a smoothing characterized by the parameter s. We show that it is possible to choose penalty parameter $\lambda = O(1/\epsilon)$ and smoothing s such that the estimate

$$\|u - v\|^2 \leq Kn\epsilon$$

holds when the noise level $\|r\|^2 = O(\epsilon)$. Here K is some constant and n is the number of jumps (changes from white to black or from black to white) in the bar code.

The proof relies an integral identity due to Mortola [2], and on showing that the solution to the variational problem (2) for u is in BV. Details of the proof will appear in a separate publication.

References

[1] S. Esedoḡlu, *Blind deconvolution of bar code signals*, Inverse Problems **20** (2004), 121–135.
[2] L. Mortola, *The gradient theory of phase transitions and the minimal interface criterion*, Archives for Rational Mechanics and Analysis **98** (1987), 123–142.

Finite element simulation of solid-liquid phase transitions with a free melt surface

Alfred Schmidt

(joint work with Eberhard Bänsch, Thilo Moshagen, and Jordi Paul)

Introduction. The Collaborative Research Centre 747 "Micro cold forming" studies aspects of the production of micro components. Motivated by the engineering application of melting the end of thin wires by laser heating in order to accumulate material for a subsequent forming process, we study the melting and solidification of material with a free capillary melt surface. The model leads to a coupled system of Stefan and Navier-Stokes equations, where the solution of the Stefan problem defines the solid subdomain $\Omega_s(t)$ and the solution of Navier-Stokes with capillary boundary gives the shape of the liquid subdomain $\Omega_l(t)$. An Arbitrary Lagrangian Eulerian Finite Element method is presented that is able to compute a numerical solution without spurious oscillations.

Mathematical Model. The nondimensional system of equations for temperature θ, pressure p, velocity field u and time-dependent domain $\Omega(t) = \Omega_s(t) \cup \Omega_l(t) \cup \Gamma_S(t)$ (see Figure 1) consists of a Stefan problem for the temperature,

$$\frac{\partial}{\partial t}\theta + u \cdot \nabla\theta - \frac{1}{Re\,Pr}\Delta\theta = 0 \text{ in } \Omega_l(t), \quad \frac{\partial}{\partial t}\theta - \frac{1}{Re\,Pr}\frac{\kappa_s}{\kappa_l}\Delta\theta = 0 \text{ in } \Omega_s(t),$$

with Stefan boundary conditions on the solid-liquid interface $\Gamma_S(t) = \bar{\Omega}_l(t) \cap \bar{\Omega}_s(t)$

$$\theta = 0, \quad \frac{St}{Re\,Pr}\left[\partial_\nu \theta_{|\Omega_l} - \frac{\kappa_s}{\kappa_l}\partial_\nu \theta_{|\Omega_s}\right] = V_{\Gamma_S} \quad \text{on } \Gamma_S(t)$$

and heat flux condition including laser heating and radiation on the outer boundary

$$\partial_\nu \theta = La\, I_l + Em(\theta_a^4 - (\theta_m + \theta)^4) \quad \text{on } \partial\Omega(t),$$

coupled with Navier-Stokes equations in the liquid subdomain $\Omega_l(t)$

$$\frac{\partial}{\partial t}u + u \cdot \nabla u - \nabla \cdot \left(\frac{1}{Re}\mathbf{D}(u) - p\, I\right) = -\frac{Bo}{We}e_z + \frac{Gr}{Re^2}\theta\, e_z, \quad \nabla \cdot u = 0$$

with no-slip condition $u = 0$ on the solid-liquid interface $\Gamma_S(t)$ and capillary condition on the free melt surface $\Gamma_C(t) = \partial\Omega_l(t) \setminus \Gamma_S(t)$

$$u \cdot \nu = V_{\Gamma_C}, \quad \sigma\nu = \frac{1}{We}\mathcal{H}\nu, \quad \text{on } \Gamma_C(t).$$

Here, Re, Pr, Bo, We, Gr, and St denote the Reynolds, Prandtl, Bond, Weber, Grasshoff, and Stefan numbers, La and Em the laser power and emissivity constants, I_l is the intensity distribution of the laser heating, $\mathcal{H}$ the mean curvature of the capillary boundary.

Finite element methods. The finite element discretization of this system can be done separately for the Stefan problem in an enthalpy formulation as studied in [3] and for the Navier-Stokes system as in [1]. For an application *without* capillary boundary (Bridgman growth of a semiconducter crystal), the coupled numerical method was demonstrated sucessfully in [2]. There, on a fixed mesh, the discrete liquid subdomain is given by all mesh elements, where the temperature is above melting temperature (nondimensional, $\theta > 0$).

When the capillary boundary meets the phase boundary in a triple line (or point in 2D), a coupled method of the type mentioned above is possible, too, but can easily produce spurious velocity oscillations. This is due to the fact that whole mesh elements change from solid to liquid and thus parts of the outer boundary change from solid to capillary boundary. The capillary forces directly push the

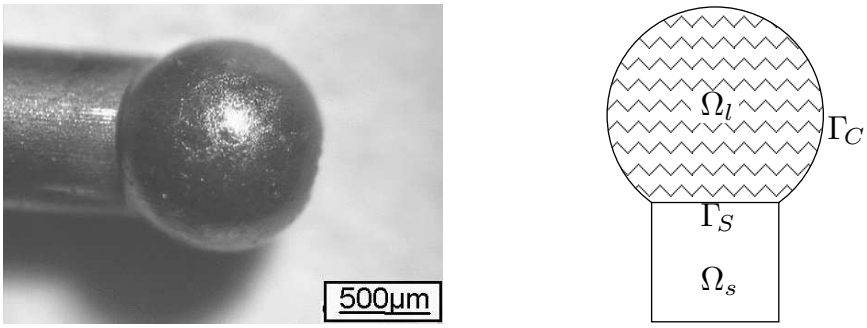

FIGURE 1. Left: material accumulation from experiment; right: solid and liquid subdomains Ω_s and Ω_l, interface Γ_S and capillary surface Γ_C.

boundary element into a different position, which produces a strong local velocity. Thus, a new approach had to be developed.

The new method presented here uses a representation of the phase boundary by mesh lines (in 2D, faces in 3D) and a front tracking method. Using the strong formulation of the Stefan problem, the velocity of the phase boundary can be computed from the jump of temperature gradients. Moving local mesh points by the velocity of the interface (which is a non-material velocity), we end up in an *Arbitrary Lagrangian Eulerian* (ALE) formulation of the coupled system. A similar approach is used for moving the mesh with the capillary surface. Special attention must be directed to the triple junction where capillary surface and solid-liquid interface meet.

As the moving mesh degenerates when the liquid subdomain changes much, as in our application, remeshing is necessary at certain times. In order to not reduce the resolution of free boundaries, we keep the mesh points on the capillary boundary and interface and generate a new mesh only for the interior of the solid and liquid subdomains.

Numerical results. Both a 2D and a 2D axial symmetric implementation of the algorithm were done based on the Navier code [1], the remeshing is done using by Triangle [5]. Figure 2 shows a zoom into the mesh around the solid-liquid interface at two different times from a 2D axial symmetric simulation. The interface lies in the light gray region. Mesh lines at the interface were moved together with it, and the bulk was remeshed between the two time instances.

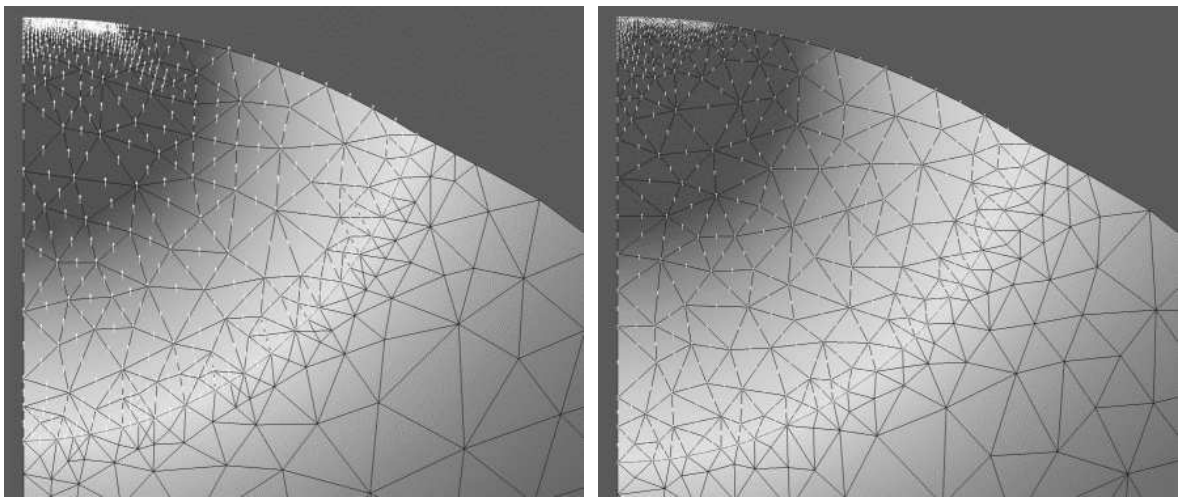

FIGURE 2. Meshes from two different time steps. Gray shade indicates temperature, the interface lies in the light region.

Work in progress. As the front tracking approach is applicable only when already some liquid pool exists, a combination with the enthalpy formulation FEM is needed in the beginning of the process, until some material is molten.

Some open questions and related future work regard the optimization of microstructure in the re-solidified material by a time-dependent control of laser power.

Acknowledgment. The authors thank the German Research Foundation (DFG) for funding this research via project A3 "Material Accumulation" of the Collaborative Research Centre 747 "Micro Cold Forming". We thank our partners from the Bremer Institut für angewandte Strahltechnik (BIAS) for cooperation.

References

[1] E. Bänsch: *Finite element discretization of the Navier-Stokes equations with a free capillary surface*, Numer. Math., **88** (2001), 203–235.

[2] G. Dziuk, S. Boschert, A. Schmidt, K. G. Siebert, E. Bänsch, K.-W. Benz, and T. Kaiser: *Simulation of industrial crystal growth by the vertical Bridgman method.* in W. Jäger and H.-J. Krebs, eds., Mathematics - Key Technology for the Future: Joint Projects between Universities and Industry, Springer (2003), 331–342.

[3] R. H. Nochetto, A. Schmidt, and C. Verdi: *A posteriori error estimation and adaptivity for degenerate parabolic problems*, Math. Comput. **69** (2000), 1–24.

[4] J. Paul: *Modellierung und Simulation eines Anschmelzvorganges mit freier Oberfläche*, Thesis, Univ. Bremen FB 3, 2009.

[5] J. R. Shewchuk: *Triangle: Engineering a 2D Quality Mesh Generator and Delaunay Triangulator*, in M. C. Lin and D. Manocha, eds., Applied Computational Geometry: Towards Geometric Engineering, Springer LNCS 1148 (1996), 203–222.

E. Bänsch and J. Paul: AM3, Department Mathematik, Universität Erlangen-Nürnberg,

T. Moshagen and A. Schmidt: Zentrum für Technomathematik, FB 3, Universität Bremen.

Large Scale Aerodynamic Shape Optimization

Stephan Schmidt

(joint work with Volker Schulz)

The talk presents the problem of aerodynamic shape optimization as a free boundary problem. Techniques from shape calculus are used to deform the interface between the fluid and the solid wall in such a manner that a given objective function is minimized. The Hadamard structure theorem states the existence of a gradient expression, which lives on the interface alone, enabling very fast numerical methods. Special emphasis also lies on higher order optimization methods, which results in the employment of a "Shape-Newton" method. To this end several fluid models are studied.

First, the incompressible Navier–Stokes equations are considered. The shape gradient in Hadamard form is derived for a wide array of possible objective functions. In the viscous limit of the Stokes equations, the shape Hessian is derived and its operator symbol is studied both analytically for the Stokes equations and numerically for the Navier–Stokes equations. The resulting Shape-Newton method is shown to show very fast convergence during the minimization of a fluid obstacle in a channel.

Next, the talk continous with aerodynamic design based on the compressible Euler equations as a model for the inviscid fluid. The optimization of both several airfoils and an Onera M6 flying wing is presented and the Shape-Newton method is used to deform the entire wing surface, i.e. the interface between the inviscid slip wall and the fluid. The flow and adjoint solution are computed using the DLR hybird finite volume flow solver TAU. The optimization of the wing is conducted using a multi-level discretization with adaptive mesh refinement, such that the coarse surface is discretized using $18,285$ nodes and the finer mesh features $36,806$ nodes. Each of these nodes defines the shape of the wing, i.e. the fluid interface, and is used as a design parameter during the optimization. Special attention is also given to the lift constraint, such that the optimized wing maintains its aerodynamic lift coefficient.

References

[1] K. Eppler, S. Schmidt, V. Schulz, and C. Ilic. Preconditioning the pressure tracking in fluid dynamics by shape Hessian information. *Journal of Optimization Theory and Applications*, 141(3):513–531, 2009.

[2] S. Schmidt, C. Ilic, N. Gauger, and V. Schulz. Shape gradients and their smoothness for practical aerodynamic design optimization. Technical Report Preprint SPP1253-10-03, DFG-SPP 1253, 2008. submitted (OPTE).

[3] S. Schmidt and V. Schulz. Impulse response approximations of discrete shape Hessians with application in CFD. *SIAM Journal on Control and Optimization*, 48(4):2562–2580, 2009.

[4] S. Schmidt and V. Schulz. Shape derivatives for general objective functions and the incompressible Navier–Stokes equations. Technical Report Preprint SPP1253-10-05, DFG-SPP 1253, 2009.

Analysis of Adaptive Finite Elements for Control Constrained Optimal Control Problems

Kunibert G. Siebert

(joint work with Kristina Kohls and Arnd Rösch)

Continuous Problem. We consider optimal control problems with constrained distributed control of the form

$$\min_{u\in\mathbb{U}^{\mathrm{ad}}} \frac{1}{2}\|y-y_d\|_{\mathbb{U}}^2+\frac{\alpha}{2}\|u\|_{\mathbb{U}}^2 \quad \text{subject to} \quad \mathcal{B}[y,\,v]=\langle u,\,v\rangle_{\mathbb{U}} \quad \forall\, v\in\mathbb{Y}. \tag{1}$$

Hereafter, $\mathbb{Y}$ is an L^2 based Hilbert space over a bounded, polygonal domain $\Omega\subset\mathbb{R}^d$, $\emptyset\neq\mathbb{U}^{\mathrm{ad}}\subset\mathbb{U}:=L^2(\Omega;\mathbb{R}^n)\subset\mathbb{Y}^*$ is a convex and bounded set of admissible controls for suitable $n\geq 1$, $y_d\in\mathbb{U}$ is a desired state, $\alpha>0$ is a cost parameter, and $\mathcal{B}\colon\mathbb{Y}\times\mathbb{Y}\to\mathbb{R}$ is a continuous bilinear form satisfying the inf-sup condition

$$\inf_{\substack{v\in\mathbb{Y}\\ \|v\|_{\mathbb{Y}}=1}}\sup_{\substack{w\in\mathbb{Y}\\ \|w\|_{\mathbb{Y}}=1}}\mathcal{B}[v,\,w]=\inf_{\substack{w\in\mathbb{Y}\\ \|w\|_{\mathbb{Y}}=1}}\sup_{\substack{v\in\mathbb{Y}\\ \|v\|_{\mathbb{Y}}=1}}\mathcal{B}[v,\,w]=\gamma>0. \tag{2}$$

The inf-sup condition (2) is equivalent to solvability of the state equation

$$\bar{y}\in\mathbb{Y}: \qquad \mathcal{B}[\bar{y},\,v]=\langle f,\,v\rangle \qquad \forall\, v\in\mathbb{Y} \tag{3}$$

for any $f \in \mathbb{Y}^*$ as well as solvability of the dual problem

$$\bar{p} \in \mathbb{Y}: \qquad \mathcal{B}[w, \bar{p}] = \langle g, w\rangle \qquad \forall\, w \in \mathbb{Y} \tag{4}$$

for any $g \in \mathbb{Y}^*$ [7, 8].

For given $p \in \mathbb{Y}$ let $\Pi(p)$ be the the best approximation of $-\frac{1}{\alpha}p$ in $\mathbb{U}^{\rm ad}$. Then the unique solution $(\hat{u}, \hat{y}) = (\Pi(\hat{p}), \hat{y})$ of (1) is characterized by the *reduced first order optimality system*

$$\begin{aligned} \mathcal{B}[\hat{y}, v] &= \langle \Pi(\hat{p}), v\rangle \qquad \forall\, v \in \mathbb{Y}, \\ \mathcal{B}[w, \hat{p}] &= \langle \hat{y} - y_d, w\rangle \qquad \forall\, w \in \mathbb{Y}, \end{aligned} \tag{5}$$

compare with [3, 10].

Discrete Problem. Let $\mathcal{T}$ be a conforming triangulation of Ω and let $\mathbb{Y}(\mathcal{T}) \subset \mathbb{Y}$ be a piecewise polynomial conforming finite element space over $\mathcal{T}$ such that

$$\inf_{\substack{V\in\mathbb{Y}(\mathcal{T})\\ \|V\|_{\mathbb{Y}}=1}} \sup_{\substack{W\in\mathbb{Y}(\mathcal{T})\\ \|W\|_{\mathbb{Y}}=1}} \mathcal{B}[V, W] = \inf_{\substack{W\in\mathbb{Y}(\mathcal{T})\\ \|W\|_{\mathbb{Y}}=1}} \sup_{\substack{V\in\mathbb{Y}(\mathcal{T})\\ \|V\|_{\mathbb{Y}}=1}} \mathcal{B}[V, W] \geq \underline{\gamma} > 0.$$

The discrete solution $(\hat{Y}, \hat{P}, \hat{U})$ is given as the unique solution of the *discretized reduced first order optimality system*

$$\begin{aligned} \mathcal{B}[\hat{Y}, V] &= \langle \Pi(\hat{P}), V\rangle \qquad \forall\, V \in \mathbb{Y}(\mathcal{T}), \\ \mathcal{B}[W, \hat{P}] &= \langle \hat{Y} - y_d, W\rangle \qquad \forall\, W \in \mathbb{Y}(\mathcal{T}). \end{aligned} \tag{6}$$

The discrete control $\hat{U} = \Pi(\hat{P})$ is in general not a finite element function. Efficient solution techniques for (6) are described in [2].

Examples. We next give two examples of spaces $\mathbb{Y}$ and bilinear forms $\mathcal{B}$. The variational formulation of the Poisson problem

$$-\Delta y = f \quad \text{in } \Omega, \qquad y = 0 \quad \text{on } \partial\Omega$$

utilizes on $\mathbb{Y} = H^1_0(\Omega)$ the *coercive* and continuous bilinear form

$$\mathcal{B}[v, w] = \int_\Omega \nabla v \cdot \nabla w \, dx.$$

Coercivity of $\mathcal{B}$ implies the inf-sup condition (2). The standard discretization of the Poisson problem utilizes Lagrange finite elements of order $\ell \in \mathbb{N}$. Coercivity of $\mathcal{B}$ on $\mathbb{Y}$ is inherited to any subspace.

The weak form of the Stokes problem

$$-\Delta \boldsymbol{y} + \nabla \pi = \boldsymbol{f} \quad \text{in } \Omega, \qquad \nabla \cdot \boldsymbol{y} = 0 \quad \text{in } \Omega, \qquad \boldsymbol{y} = \boldsymbol{0} \quad \text{on } \partial\Omega$$

is formulated in $\mathbb{Y} = H^1_0(\Omega; \mathbb{R}^d) \times L^2_0(\Omega)$ with the continuous bilinear form

$$\mathcal{B}[(\boldsymbol{v}, r), (\boldsymbol{w}, q)] := \int_\Omega \nabla \boldsymbol{v} : \nabla \boldsymbol{w} \, dx - \int_\Omega r \, \nabla \cdot \boldsymbol{w} \, dx - \int_\Omega \nabla \cdot \boldsymbol{v} \, q \, dx,$$

which satisfies an inf-sup condition. We discretize the Stokes problem with the Taylor-Hood element of order $\ell \geq 2$, which is a stable stable discretization, i. e., the bilinear form $\mathcal{B}$ satisfies a uniform inf-sup condition in $\mathbb{Y}(\mathcal{T})$ on any shape-regular triangulation $\mathcal{T}$.

A typical example for $\mathbb{U}^{\rm ad}$ are box-constraints, namely

$$\mathbb{U}^{\rm ad} := \{u \in L^2(\Omega;\mathbb{R}^n) \mid a \le u \le b \text{ in } \Omega\},$$

where $a \le b$ are given functions in $L^2(\Omega;\mathbb{R}^n)$. In case of the Poisson problem we let $n = 1$ and for the Stokes problem we use $n = d$. In the later case the constraint $a \le u \le b$ has to be read component-wise. For the Stokes problem we could also use a norm constraint

$$\mathbb{U}^{\rm ad} := \{u \in L^2(\Omega;\mathbb{R}^d) \mid |u|_2 \le r \text{ in } \Omega\}.$$

A Posteriori Error Analysis. The a posteriori error analysis for optimal control problems was initiated by Liu and Yan at the beginning of this century [4], compare also with [1, 5]. We next present a unified framework for the a posteriori error analysis of (1) solely based on estimators for the linear problems (3) and (4). We would like to stress that there exists a well-established theory of different kinds of estimators for a huge class of linear problems.

Denote by $\bar{Y}, \bar{P} \in \mathbb{Y}(\mathcal{T})$ the Galerkin approximations to the solutions $\bar{y}, \bar{p} \in \mathbb{Y}$ of the linear problems (3) respectively (4) with given right hand sides f and g. Furthermore, let $\mathcal{E}_{\mathcal{T}}(\bar{Y}, f; \mathcal{T})$ and $\mathcal{E}^*_{\mathcal{T}}(\bar{P}, g; \mathcal{T})$ be reliable and efficient estimators for the primal respectively dual problem, i. e.,

$$\begin{aligned}\|\bar{Y} - \bar{y}\|_{\mathbb{Y}} &\preccurlyeq \mathcal{E}_{\mathcal{T}}(\bar{Y}, f; \mathcal{T}) \preccurlyeq \|\bar{Y} - \bar{y}\|_{\mathbb{Y}} + \operatorname{osc}_{\mathcal{T}},\\ \|\bar{P} - \bar{p}\|_{\mathbb{Y}} &\preccurlyeq \mathcal{E}^*_{\mathcal{T}}(\bar{P}, g; \mathcal{T}) \preccurlyeq \|\bar{P} - \bar{p}\|_{\mathbb{Y}} + \operatorname{osc}^*_{\mathcal{T}}.\end{aligned}$$

Hereafter, $\operatorname{osc}_{\mathcal{T}}, \operatorname{osc}^*_{\mathcal{T}}$ are the typical oscillation terms in the lower bound. Note, that the constants hidden in '$\preccurlyeq$' only depend on the bilinear form $\mathcal{B}$ and the shape regularity of $\mathcal{T}$ but not the right hand sides f and g. We then prove that the sum of these estimators give a reliable and efficient estimator for the optimal control problem (1), i. e., if $(\hat{y}, \hat{p})$ is the solution of (5) and $(\hat{Y}, \hat{P})$ the solution of (6) then there hold with $\hat{u} = \Pi(\hat{p})$ and $\hat{U} = \Pi(\hat{P})$ the error bounds

$$\begin{aligned}\|(\hat{Y}, \hat{P}, \hat{U}) - (\hat{y}, \hat{p}, \hat{u})\|_{\mathbb{Y}\times\mathbb{Y}\times\mathbb{U}} &\preccurlyeq \mathcal{E}_{\mathcal{T}}(\hat{Y}, \hat{U}; \mathcal{T}) + \mathcal{E}^*_{\mathcal{T}}(\hat{P}, \hat{Y} - y_d; \mathcal{T})\\ \mathcal{E}_{\mathcal{T}}(\hat{Y}, \hat{U}; \mathcal{T}) + \mathcal{E}^*_{\mathcal{T}}(\hat{P}, \hat{Y} - y_d; \mathcal{T}) &\preccurlyeq \|(\hat{Y}, \hat{P}, \hat{U}) - (\hat{y}, \hat{p}, \hat{u})\|_{\mathbb{Y}\times\mathbb{Y}\times\mathbb{U}} + \widetilde{\operatorname{osc}_{\mathcal{T}}}.\end{aligned}$$

The oscillation term $\widetilde{\operatorname{osc}_{\mathcal{T}}}$ depends on $\operatorname{osc}_{\mathcal{T}}$ and $\operatorname{osc}^*_{\mathcal{T}}$ and an additional term that encodes the approximability of $\hat{u}$ in a suitable finite element space over $\mathcal{T}$.

Convergence Analysis. Using the standard adaptive iteration

$$\text{(7)} \qquad \mathsf{SOLVE} \longrightarrow \mathsf{ESTIMATE} \longrightarrow \mathsf{MARK} \longrightarrow \mathsf{REFINE}$$

we obtain a sequence $\{(\hat{Y}_k, \hat{P}_k, \hat{U}_k)\}_{k\ge 0}$ of discrete solutions. Applying the techniques from [6, 9] we finally show under very mild assumptions on the modules of (7) convergence, i. e., there holds

$$\lim_{k\to\infty} \|(\hat{Y}_k, \hat{P}_k, \hat{U}_k) - (\hat{y}, \hat{p}, \hat{u})\|_{\mathbb{Y}\times\mathbb{Y}\times\mathbb{U}} = \lim_{k\to\infty} \mathcal{E}_k(\hat{Y}_k, \hat{U}_k; \mathcal{T}_k) + \mathcal{E}^*_k(\hat{P}_k, \hat{Y}_k - y_d; \mathcal{T}_k) = 0.$$

References

[1] *M. Hintermüller, R. H. Hoppe, Y. Iliash, and M. Kieweg*, *An a posteriori error analysis of adaptive finite element methods for distributed elliptic control problems with control constraints*, ESAIM, Control Optim. Calc. Var., 14 (2008), pp. 540–560.

[2] *M. Hinze and M. Vierling*, *Variational discretization and semi-smooth Newton methods; implementation, convergence and globalization in PDE constrained optimization with control constraints*. Hamburger Beiträge zur Angewandten Mathematik No. 2009-13, 2009.

[3] *J. L. Lions*, *Optimal Control of Systems Governed by Partial Differential Equations*, vol. 170 of Die Grundlehren der mathematischen Wissenschaften, Springer-Verlag, 1971.

[4] *W. Liu and N. Yan*, *A posteriori error estimates for distributed convex optimal control problems*, Adv. Comput. Math, 15 (2001), pp. 285–309.

[5] *W. Liu and N. Yan*, *A posteriori error estimates for control problems governed by Stokes equations*, SIAM J. Numer. Anal., 40 (2002), pp. 1850–1869.

[6] *P. Morin, K. G. Siebert, and A. Veeser*, *A basic convergence result for conforming adaptive finite elements*, Math. Models Methods Appl. 18 (2008), 18 (2008), pp. 707–737.

[7] *J. Nečas*, *Sur une méthode pour resoudre les équations aux dérivées partielles du type elliptique, voisine de la variationnelle*, Ann. Sc. Norm. Super. Pisa, Sci. Fis. Mat., III. Ser., 16 (1962), pp. 305–326.

[8] *R. H. Nochetto, K. G. Siebert, and A. Veeser*, *Theory of adaptive finite element methods: An introduction*, in Multiscale, Nonlinear and Adaptive Approximation, R. A. DeVore and A. Kunoth, eds., Springer, 2009, pp. 409–542.

[9] *K. G. Siebert*, *A convergence proof for adaptive finite elements without lower bound*, 2009. Preprint Universität Duisburg-Essen No. 694, to appear in IMA J. of Numer. Anal.

[10] *F. Tröltzsch*, *Optimal Control of Partial Differential Equations. Theory, Methods and Applications*, vol. 112 of Graduate Studies Series in Mathematics, AMS, Providence, 2010.

Technical and Mathematical Problems in the Czochralski Growth of Single Crystals

Jürgen Sprekels

(joint work with Wolfgang Dreyer (WIAS Berlin), P.-E. Druet (WIAS Berlin), O. Klein (WIAS Berlin), F. Tröltzsch (TU Berlin), I. Yousept (TU Berlin))

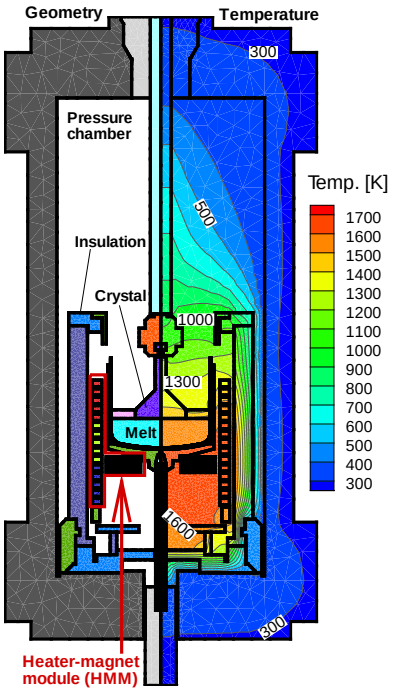

The most important industrial technique for growing bulk semiconductor single crystals (GaAs, Si, Ge) from the melt is the *Czochralski method*. In this method, a rotating crystal seed is dipped into the melt that is contained in a rotating crucible. The seed is then slowly pulled out of the melt, and a single crystal solidifies.

A typical growth apparatus is depicted in the figure; here, the left side shows the geometry, while the right side shows the temperature distribution during a growth run calculated with the software `WIAS-HiTNIHS` developed at the Weierstrass Institute for Applied Analysis and Stochastics (WIAS) in Berlin.

In the Czochralski process, the melt flow is turbulent, which creates the problem that impurities can find their way into the crystal, lowering its quality. Also, crystal growers want the solid–liquid interface to have a certain shape, and the temperature oscillations below the crystal should have small amplitudes and not too small frequencies. Since the melt is electrically conducting, electromagnetic fields can play the role of a *control*, since a Lorentz force is induced into the melt in their presence.

In the project KRIST$\widetilde{MAG}^{®}$ of the Technologiestiftung Berlin, a consortium was formed in which a technological breakthrough was achieved by demonstrating that *traveling magnetic fields* can be successfully applied for the task of controlling the turbulent melt. Several patents were filed, and the groundbreaking nature of these developments was recognized when the KRIST$\widetilde{MAG}^{®}$ consortium was awarded the *Innovation Prize Berlin–Brandenburg 2008*.

An important role for the success of the KRIST$\widetilde{MAG}^{®}$ project played *mathematical modeling and simulation*. This part was covered by members of the Weierstrass Institute for Applied Analysis and Stochastics (WIAS) in Berlin.

From the mathematical point of view, an extremely complicated system of partial differential equations had to be solved, namely:

- Maxwell's equations for the electromagnetic fields
- the equations of temperature-dependent magnetohydrodynamics in the melt
- the balance of energy in the whole growth apparatus.

The complexity of the mathematical problem was increased by the fact that

- due to temperatures of up to 2000 K, many of the physical constants depend on temperature,
- physical coefficients and boundary conditions jump between the different materials,
- the geometry of the apparatus is very complex,
- the main energy transport in the gas cavities is due to radiation.

The latter complication presents a particular challenge, since it leads to both nonlocal and nonlinear boundary conditions for the temperature in the gas cavities.

In a series of papers (see [1, 2, 3]), P.-E. Druet studied the full problem sketched above, culminating in an existence proof for weak solutions. Associated optimal control aspects were treated in [4, 7, 8], and the results of numerical simulations were presented in [5, 6].

References

[1] P.-E. Druet, *Weak solutions to a stationary heat equation with nonlocal radiation boundary condition and right-hand side in L^p*, Math. Meth. Appl. Sci. **32** (2008), 135–166.

[2] P.-E. Druet, *Existence of weak solutions to the time-dependent MHD equations coupled to the heat equation with nonlocal radiation boundary conditions*, Nonlin. Anal. RWA **10** (2009), 2914–2936.

[3] P.-E. Druet, *Analysis of a coupled system of partial differential equations modeling the interaction between melt flow, global heat transfer and applied magnetic fields in crystal growth*, PhD Thesis, Humboldt-Universität zu Berlin, 2009.

[4] P.-E. Druet, O. Klein, J. Sprekels, F. Tröltzsch, and I. Yousept, *Optimal control of 3D state-constrained induction heating problems with nonlocal radiation effects*, to appear in SIAM J. Control Optim.

[5] O. Klein, P. Philip, and J. Sprekels, *Modelling and simulation of sublimation growth in SiC bulk single crystals*, Interfaces Free Bound. **6** (2004), 295–314.

[6] O. Klein, Ch. Lechner, P.-E. Druet, P. Philip, J. Sprekels, Ch. Frank-Rotsch, F. M. Kießling, W. Miller, U. Rehse, and P. Rudolph, *Numerical simulation of Czochralski crystal growth under the influence of a traveling magnetic field generated by an internal heater-magnet module (HMM)*, J. Crystal Growth **310** (2008), 1523–1532.

[7] C. Meyer, P. Philip, and F. Tröltzsch, *Optimal control of a semilinear PDE with nonlocal radiation interface conditions*, SIAM J. Control Optim. **45** (2006), 699–721.

[8] C. Meyer and I. Yousept, *Regularization of state-constrained optimal control of semilinear elliptic equations with nonlocal radiation interface conditions*, SIAM J. Control Optim. **48** (2009), 734–755.

Preconditioning for Allen-Cahn variational inequalities with non-local constraints

Martin Stoll
(joint work with Lavinia Sarbu, Luise Blank)

Recently, Blank *et al.* [1] proposed the use of the semi-smooth Newton method to solve Allen-Cahn variational inequalities with mass constraints. Problems of this type arise in a variety of applications (see [6, 3]). In the scalar case, the Allen-Cahn equation with interface thickness ε

$$\varepsilon \partial_t u = \gamma \varepsilon \triangle u - \frac{\gamma}{\varepsilon} \psi'(u) \tag{1}$$

with homogeneous Neumann boundary conditions on $\partial\Omega$ has to be solved with the additional condition of mass conservation, i.e., under the constraint that $\fint_\Omega u = m$, where $\fint_\Omega f(x)dx := \frac{1}{|\Omega|}\int_\Omega f(x)dx$ with $|\Omega|$ being the Lesbesque measure of Ω. In the vector-valued case a similar constraint for each phase is introduced. The discretization using finite elements and the use of the semi-smooth Newton method leads in both cases to the solution of a linear system in saddle point form, which in the scalar case has the following form

$$\mathcal{K} := \begin{bmatrix} (\frac{\varepsilon^2}{\tau} - \gamma)M + \varepsilon^2 \gamma K & -\mathbf{m} \\ -\mathbf{m}^T & 0 \end{bmatrix} \tag{2}$$

where K is the stiffness and M the mass matrix, $\mathbf{m}$ is the moment vector, τ the time-step and γ an interfacial energy parameter. The efficient solution of this

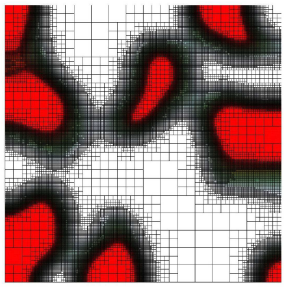

(A) An intermediate solution of the Allen-Cahn equation with mass constraints and adaptive mesh refinement.

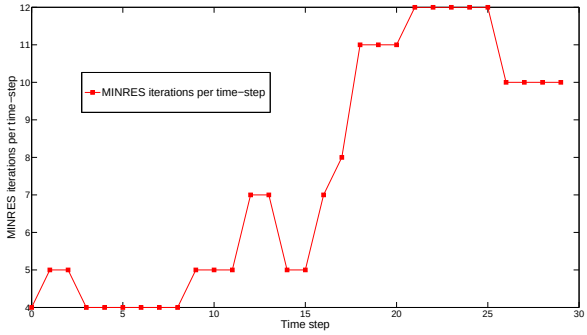

(B) Scalar-case: Average number of MINRES iterations for each time step for the first 30 time steps.

linear system typically is at the bottleneck for the fast solution of the variational inequality. We propose to employ Krylov subspace methods, namely the Minimal

Residual method (MINRES) [4], in combination with a block-diagonal preconditioner

$$\mathcal{P} = \begin{bmatrix} \tilde{L} & 0 \\ 0 & 1 \end{bmatrix} \tag{3}$$

where $\tilde{L}$ is an approximation to the matrix $(\frac{\varepsilon^2}{\tau} - \gamma)M + \varepsilon^2\gamma K$. Typically, a good choice for $\tilde{L}$ is a geometric or algebraic multigrid method for L. Also, other Krylov subspace methods such as a non-standard conjugate gradients (CG) method can be applied [2, 5] to the system $\mathcal{K}$.

References

[1] *L. Blank, H. Garcke, L. Sarbu, and V. Styles*, *Primal-dual active set methods for Allen-Cahn variational inequalities with non-local constraints*, Preprint SPP1253-09-01.

[2] *J. H. Bramble and J. E. Pasciak*, *A preconditioning technique for indefinite systems resulting from mixed approximations of elliptic problems*, Math. Comp, 50 (1988), pp. 1–17.

[3] *H. Garcke, B. Nestler, B. Stinner, and F. Wendler*, *Allen-Cahn systems with volume constraints*, Math. Models Methods Appl. Sci., 18 (2008), pp. 1347–1381.

[4] *C. C. Paige and M. A. Saunders*, *Solutions of sparse indefinite systems of linear equations*, SIAM J. Numer. Anal, 12 (1975), pp. 617–629.

[5] *T. Rees and M. Stoll*, *Block triangular preconditioners for PDE constrained optimization*, Numer. Linear Algebra Appl. to appear, (2009).

[6] *J. E. Taylor and J. W. Cahn*, *Linking anisotropic sharp and diffuse surface motion laws via gradient flows*, J. Statist. Phys., 77 (1994), pp. 183–197.

Finite element methods for interface flows with surfactants

Lutz Tobiska

(joint work with Sashikumaar Ganesan)

The accurate numerical computation of two-phase flows is a challenging task. An important issue is the precise inclusion of the surface force which compresses the surface/interface tension and the local curvature on the free surface/interface. Surfactants are surface active agents which lower the surface/interfacial tension on the liquid-gas/liquid-liquid interface. In addition, nonuniform distributions of surfactants on the surface/interface induce Marangoni forces. Adsorption and desorption of surfactants between the interface and the bulk phase may take place in the soluble surfactant case. Thus, the presents of surfactants influences the dynamics of the free surface/interface [5, 7, 8].

We consider a mathematical model for two-phase flows consisting of the incompressible Navier-Stokes equation

$$\begin{aligned}
\rho_k \left(\frac{\partial u}{\partial t} + (u \cdot \nabla) u \right) - \nabla \cdot \mathbb{S}_k(u,p) &= \rho_k e && \text{in } \Omega_k(t) \subset \mathbb{R}^3, \\
\nabla \cdot u &= 0 && \text{in } \Omega_k(t) \subset \mathbb{R}^3, \\
[u] = 0, \quad \nu \cdot [\mathbb{S}(u,p)] \cdot \nu + \sigma(c_\Gamma)\,\mathcal{K} &= 0 && \text{on } \Gamma_F(t), \\
u = w, \quad \tau_i \cdot [\mathbb{S}(u,p)] \cdot \nu - \tau_i \cdot \nabla \sigma(c_\Gamma) &= 0 && \text{on } \Gamma_F(t),
\end{aligned}$$

a transport equation for the surfactant concentration in the outer phase

$$\begin{aligned} \frac{\partial C}{\partial t} + (u \cdot \nabla)C = D_c \Delta C \qquad & \text{in } \Omega_1(t) \subset \mathbb{R}^3, \\ -D_c(\nu \cdot \nabla C) = S(c_\Gamma, C) \qquad & \text{on } \Gamma_F(t), \end{aligned}$$

with appropriate boundary conditions on the remaining part of the boundary, and a transport equation for the surfactant concentration on the interface

$$\frac{\partial c_\Gamma}{\partial t} + U \cdot \underline{\nabla} c_\Gamma + c_\Gamma \underline{\nabla} \cdot u = D_s \underline{\Delta} c_\Gamma + S(c_\Gamma, C) \qquad \text{on } \Gamma_F(t).$$

The coupling term $S(c_\Gamma, C)$ is often modeled by

$$S(c_\Gamma, C) = k_a C \left(1 - \frac{c_\Gamma}{c_{\Gamma,\infty}}\right) - k_d c_\Gamma.$$

Following notations have been used above: $\mathbb{S}_k(u,p) = \mu_k \mathbb{D}(u) - p\mathbb{I}$, $e = (0,0,-g)$, u - velocity, U-tangential velocity, p - pressure, t - time, ρ_k - density, μ_k - dynamic viscosity, σ - surface tension, g - gravity. C - surfactant in outer phase, D_c - diffusion coefficient of C, c_Γ - surfactant on interface, D_s - diffusion coefficient of c_Γ, k_a - adsorption coefficient, k_d - desorption coefficient, $c_{\Gamma,\infty}$ - maximum surface packing surfactant concentration.

The Navier-Stokes equations are solved together with the bulk and interface concentration equations using the coupled ALE-Lagrangian method in 3D-axisymmetric configuration [4]. Contrary to Eulerian methods, the interface in the arbitrary Lagrangian-Eulerian (ALE) approach is resolved by the computational mesh and tracked over time by a moving mesh. Thus, the surface/interface force can be incorporated more accurately. In our numerical scheme, we replace the curvature in the surface force by the Laplace-Beltrami operator. Then, applying integration by parts we reduce one order of differentiation associated with the curvature [6]. Suppressing the spurious velocities is another challenge in computing interface flows. By choosing an appropriate finite element spaces for the discretization of pressure in an interface resolved mesh, we can suppress the spurious velocities up to machine precision. A detailed study on the choice of different finite element spaces for the pressure and different approximations of the curvature in computations of interface flows has been done in [1].

In our numerical scheme, we use continuous, piecewise polynomials of second order enriched by cubic bubble functions and discontinuous, piecewise polynomials of first order (P_2^b/P_1^{disc}) for the discretization of the velocity and pressure, respectively. Continuous, piecewise polynomials of second order (P_2) have been used to discretize the bulk and interface concentrations. Further, the fractional step-ϑ scheme has been used for the temporal discretization of these equations. To handle the moving mesh, the elastic-solid technique has been applied [2]. The numerical scheme has been validated for the free surface flows with a constant surface tension in [3] and with insoluble surfactants in [4]. The influence of surfactants on a freely oscillating bubble has been also studied in [4].

This work has been partially supported by the German Research Foundation (DFG) through grant TO 143/9-1.

References

[1] S. Ganesan, G. Matthies, L. Tobiska, *On spurious velocities in incompressible flow problems with interfaces*, Comput. Methods Appl. Mech. Engrg. **196** (2007), 1193–1202.

[2] S. Ganesan, L. Tobiska, *An accurate finite element scheme with moving meshes for computing 3D-axisymmetric interface flows*, Intern. Journal Numer. Methods Fluids **57** (2008), 119–138.

[3] S. Hysing, S. Turek, D. Kuzmin, N. Parolini, E. Burman, S. Ganesan, L. Tobiska, *Quantitative benchmark computations of two-dimensional bubble dynamics*, Intern. Journal Numer. Methods Fluids **60** (2009), 1259–1288.

[4] S. Ganesan, L. Tobiska, *A coupled arbitrary Lagrangian-Eulerian and Lagrangian method for computation of free surface flow with insoluble surfactants*, Journal of Computational Physics **228** (2009), 2859–2873.

[5] M. Muradoglu, G. Tryggvason, *A front-tracking method for the computation of interfacial flows with soluble surfactants*, Journal of Computational Physics **227** (2008), 2238–2262.

[6] G. Dziuk, *Finite elements for the Beltrami operator on arbitrary surfaces*, in: S. Hildebrandt, R. Leis, Partial Differential Equations and Calculus of Variations, Springer, Berlin, 1988, 142–155.

[7] A.J. James, J. Lowengrub, *A surfactant-conserving volume-of-fluid method for interfacial flows with insoluble surfactant*, Journal of Computational Physics **201** (2004), 685–722.

[8] Y.Y. Renardy, M. Renardy, V. Cristini, *A new volume-of-fluid formulation for surfactants and simulations of drop deformation under shear at a low viscosity ratio*, Eur. J. Mech. B **21** (2002), 49-59.

Anisotropic adaptive finite element methds for interface problems

Ningning Yan

(joint work with Duan Wang and Ruo Li)

In the singular or nearly singular problems, the structures of singularity often exhibit "low-dimensional" feature that the solutions vary significantly in some directions but mildly in other directions. To numerically approximate such solutions efficiently, no doubt we prefer anisotropic meshes, which are of different length scales in different directions so that to fit the anisotropic feature of the solutions. Numerous examples, including interface discontinuities, have shown the efficiency of anisotropic elements in reducing computational cost and improving approximation accuracy.

The main focus of this talk is to discuss the approximations of the elliptic interface problem with homogeneous and non-homogeneous jump conditions, which attracts a lot of interests as it is omnipresent in many scientific and engineering problems, including multi-phase flows, nano-electronic devices, electromagnetic wave propagation in heterogeneous waves, implicit solvent models in structural biology, biological membrane, etc.

To resolve this layer anisotropy, we develop an anisotropic adaptive finite element method, which can be effective not only for the interface problem, but also for problems with global anisotropy. Compared with isotropic elements, the indicators of anisotropic meshes adaptivity need more information. Take two-dimensional triangular element as example, its anisotropy should be measured in two main aspects. One is orientation, which is roughly the direction of its longest

side. The other is the aspect ratio, which measures how thin the triangle is. The first quantity is supposed to be more crucial to the success of the anisotropic finite element methods, a wrong direction may lead to non-convergence.

In order to construct an efficient and useful anisotropic adaptive finite element methods, we proposed an indicator for anisotropic adaptive mesh refinement, which depends on only the first order derivatives of $u(u_h)$. The new indicator provides the information to mark not only the preferred refinement elements, but also the preferred refinement edges (or faces). For each element with indicator above the given tolerance, one edge is chosen as the preferred refinement edge.

For a posteriori error estimates, the affine map from the reference element to the actual element plays an essential role in anisotropic error analysis. In [1], Formaggia et al proved that the sum of error gradient projection onto two principal axes of the affine map is an upper bound of the element error. And in [2], a posteriori error estimators are provided based on the anisotropic error analysis. Different with these methods, we project the error gradient onto the element edges to search the preferred refinement edge. Since the Jacobian matrix of the affine map can be expressed by edge vectors when we use the unit reference triangle, the sum of error gradient projection onto the three edges is again an upper bound of the element error. To reduce this upper bound error estimate, the most efficient mesh adaptation is to refine the edge with the maximal contribution to the estimate. As an application, we consider a 2nd order elliptic immersed-interface problem with homogeneous and non-homogeneous jump conditions. In this case, the simple recovery-type Zienkiewicz-Zhu error estimator [4] is adopted as the adaptation indicator.

Based on the theoretical analysis, we provide some numerical examples in the talk. The standard conforming finite element methods are used, and the a posteriori error estimator provided in the talk is applied for adaptive mesh refinement. It is shown that the new schemes are more efficient than the adaptive isotropic finite element methods for the interface problems, almost optimal convergence orders are obtained in our numerical examples.

References

[1] L. Formaggia and S. Pertto, *New anisotropic a priori error estimates*, Numer. Math., **89** (2001), 641-667.

[2] M. Picasso, *Adaptive finite elements with large aspect ratio based on an anisotropic error estimator involving first order derivatives*, Comput. Methods Appl. Mech. Engrg., **196** (1996), 14-23.

[3] D. Wang, R. Li and N. Yan, *An edge-based anisotropic mesh refinement algorithm and its application to interface problems*, accepted by Communications in Computational Physics.

[4] O.C. Zienkiewicz and J.Z. Zhu, *A Simple error estimator and adaptive procedure for practical engineering analysis*, Int. J. Numer. Methods Engrg., **24** (1997), 337-357.

A diffuse-interface approach for solving coupled bulk/surface PDEs in complex evolving domains

Axel Voigt
(joint work with Sebastian Aland, Andreas Rätz, John Lowengrub)

Many problems in the biological, physical and engineering sciences involve systems of equations that need to be solved in evolving domains with complex shapes. In addition, the solution in the bulk domain may couple with the surface through adsorption of mass from the bulk to the surface and desorption from the surface to the bulk. Furthermore, the evolution of the domain boundary may depend on the distribution of the surface concentration through the modification of interfacial forces. Examples include biomembranes where transmembrane proteins play an important role in intra- and extra-cellular dynamics, epitaxially grown thin films where adsorbing/desorbing adatoms affect the dynamics and coarsening of the thin film, electrochemical dissolution of binary alloys where one component is removed selectively and dissolved in an electrolyte solution, and two-phase flow with surfactants, where amphiphilic organic compounds may adsorb to and desorp from a liquid/liquid or liquid/gas interface and lower the surface tension of the interface.

From a numerical point of view, solving a coupled bulk/surface system of equations on a moving, complex domain is highly challenging; the domain boundary may strech, break-up or coalesce with other interfaces. The available numerical methods for solving these problems can roughly be divided into two categories: interface tracking and interface capturing methods, where the first use either a seperate grid for the interface, or a set of interconnected points to mark the interface, while the second defines the interface only implicitly, which decouples the solution from the underlying grid and thus greatly simplifies gridding, discretization, and handling of topological changes.

Within a diffuse-interface approach, which is a interface capturing method, the complex domain is represented implicitly by a phase-field function, which is an approximation of the characteristic function of the domain. The domain boundary is replaced by a narrow diffuse interface layer such that the phase-field function rapidly transitions from one inside the domain to zero in the exterior of the domain. The boundary can thus be represented as an isosurface of the phase-field function. The bulk and surface PDEs are then extended on a larger, regular doamin with additional terms that approximate the adsorption-desorption flux boundary conditions and source terms for the bulk and surface equations, respectively.

General diffuse-interface methods have been developed for solving PDEs on stationary surface [1], evolving surface [2, 3] and for solving PDEs in complex evolving domains with Dirichlet, Neumann and Robin boundary conditions [4].

Combining these approaches allows to solve coupled bulk/surface systems of equations on moving, complex domains in a straight forward manner. As an

exampel we consider the following coupled bulk/surface system:

$$f_t + \nabla_\Gamma \cdot (\mathbf{u}f) = \Delta_\Gamma f + j \qquad \text{on } \Gamma(t) \tag{1}$$

$$F_t + \nabla \cdot (\mathbf{u}F) = \Delta F \qquad \text{in } \Omega_1(t) \tag{2}$$

$$\nabla F \cdot \mathbf{n} = -j = r_a F - r_d f \qquad \text{on } \Gamma(t) \tag{3}$$

with f a surface concentration on Γ, which is assumed to be constantly extended in normal direction. F a bulk concentration in Ω_1 and r_a and r_d attachment and detachment coefficients modeling the coupling between f and F. $\mathbf{u}$ is the velocity field, which is here assumed to be given for simplicity. Formulating this problem within the diffuse-domain approach reads on the time-independent domain Ω:

$$(B(c)f)_t + \nabla \cdot (B(c)\mathbf{u}f) = \nabla \cdot (B(c)\nabla f) + B(c)j \qquad \text{in } \Omega \tag{4}$$

$$(cF)_t + \nabla \cdot (c\mathbf{u}F) = \nabla \cdot (c\nabla F) - |\nabla c|j \qquad \text{in } \Omega \tag{5}$$

$$-j = r_a F - r_d f \qquad \text{in } \Omega \tag{6}$$

$$c_t + \mathbf{u} \cdot \nabla c = \nabla \cdot (M(c)\nabla \mu) \qquad \text{in } \Omega \tag{7}$$

$$\mu = G'(c) - \epsilon^2 \Delta c \qquad \text{in } \Omega \tag{8}$$

with a phase-field function c approximating Ω_1, a function $B(c) = 4G(c)$ approximating δ_Γ, $M(c) = \sqrt{B(c)}$ a mobility function and $G(c) = 0.25c^2(1-c)^2$ a double well potential. ϵ is a parameter measuring the width of the diffuse interface. Using matched asymptotics the convergence of the system to the original system can be shown for $\epsilon \to 0$. For details on the numerical solution of this system and convergence studies see [5].

The described approach is applicable to a wide range of applications and allows to reformulate complicated coupled bulk/surface problems into a system of PDEs in a time-independent domain, which can be solved using standard tool.

References

[1] A. Rätz, A. Voigt, *PDEs on surface - a diffuse interfac eapproach*, Comm. Math. Sci. **4** (2006), 575–590.

[2] A. Rätz, A. Voigt, *A diffuse-interface approximation for surface diffusion including adatoms*, Nonlin. **20** (2007), 177–192.

[3] C.M. Elliott, B. Stinner, *Analysis of a diffuse interface approach to an advection diffusion equation on a moving surface*, Math. Mod. Meth. Appl. Sci. **19** (2009), 787-802

[4] X. Li, J. Lowengrub, A. Rätz, A. Voigt, *Solving PDEs in complex geometries: a diffuse domain approach*, Comm. Math. Sci. **7** (2009), 81–107.

[5] K.E. Teigen, X. Li, J. Lowengrub, F. Wang, A. Voigt, *A diffuse-interface approach for modeling transport, diffusion and adsorption/desorption of material quantities on a deformable interface*, Comm. Math. Sci. **7** (2009), 1009–1037.

Reporter: Charles M. Elliott, Yoshikazu Giga, Michael Hinze, Vanessa Styles

Participants

Dirk Abbeloos
Departement Computerwetenschappen
Katholieke Universiteit Leuven
Celestijnenlaan 200A
B-3001 Heverlee

Prof. Dr. Helmut Abels
Fakultät für Mathematik
Universität Regensburg
93040 Regensburg

Prof. Dr. Hans Wilhelm Alt
Institut für Angewandte Mathematik
Universität Bonn
Endenicher Allee 60
53115 Bonn

Dr. Tomoro Asai
Graduate School of
Mathematical Sciences
University of Tokyo
3-8-1 Komaba, Meguro-ku
Tokyo 153-8914
JAPAN

Prof. Dr. John Barrett
Department of Mathematics
Imperial College London
Huxley Building
GB-London SW7 2AZ

Prof. Giovanni Bellettini
Dipartimento di Matematica
Universita di Roma Tor Vergata
Via della Ricerca Scientif. 1
I-00133 Roma

Martin Bernauer
Fakultät für Mathematik
Technische Universität Chemnitz
09107 Chemnitz

PD Dr. Luise Blank
Naturwissenschaftliche Fakultät I
Mathematik
Universität Regensburg
93040 Regensburg

Prof. Dr. Dieter Bothe
Center of Smart Interfaces
Technische Universität Darmstadt
Petersenstr. 32
64287 Darmstadt

Prof. Dr. Eduardo Casas
Dept. de Matematica Aplicada
E.T.S.I. Industriales y Telecom.
Av. Los Castros s/n
E-39071 Santander

Prof. Dr. Klaus Deckelnick
Institut für Analysis u. Numerik
Otto-von-Guericke-Universität
Magdeburg
Universitätsplatz 2
39106 Magdeburg

Prof. Dr. Gerhard Dziuk
Abteilung für Angewandte Mathematik
Universität Freiburg
Hermann-Herder-Str. 10
79104 Freiburg

Prof. Dr. Charles M. Elliott
Mathematics Institute
University of Warwick
Gibbet Hill Road
GB-Coventry CV4 7AL

Prof. Dr. Xiaobing Feng
Department of Mathematics
University of Tennessee
121 Ayres Hall
Knoxville , TN 37996-1300
USA

Hans Fritz
Abteilung f. Angewandte Mathematik
Universität Freiburg
Eckerstr. 1
79104 Freiburg

Prof. Dr. Harald Garcke
NWF-I Mathematik
Universität Regensburg
93040 Regensburg

Prof. Dr. Yoshikazu Giga
Graduate School of
Mathematical Sciences
University of Tokyo
3-8-1 Komaba, Meguro-ku
Tokyo 153-8914
JAPAN

Andreas Günther
Konrad-Zuse-Zentrum für
Informationstechnik Berlin (ZIB)
Takustr. 7
14195 Berlin

Prof. Dr. Roland Herzog
Fakultät für Mathematik
TU Chemnitz
Reichenhainer Str. 41
09126 Chemnitz

Prof. Dr. Michael Hintermüller
Fachbereich Mathematik
Humboldt-Universität Berlin
Unter den Linden 6
10117 Berlin

Prof. Dr. Michael Hinze
Department Mathematik
Universität Hamburg
Bundesstr. 55
20146 Hamburg

Prof. Dr. Yoshihito Kohsaka
Muroran Institute of Technology
27-1 Mizumoto
Muroran 050-8585
JAPAN

Prof. Dr. Ralf Kornhuber
Institut für Mathematik
Freie Universität Berlin
Arnimallee 6
14195 Berlin

Prof. Dr. Karl Kunisch
Institut für Mathematik und
wissenschaftliches Rechnen
Karl-Franzens-Universität Graz
Heinrichstr. 36
A-8010 Graz

Prof. Dr. Barbara Niethammer
Mathematical Institute
Oxford University
24-29 St. Giles
GB-Oxford OX1 3LB

Dr. Robert Nürnberg
Department of Mathematics
Imperial College London
Huxley Building
GB-London SW7 2AZ

Prof. Dr. Takeshi Ohtsuka
Meiji Institute for Advanced Study
of Mathematical Sciences
1-1-1 Higashimita, Tamaku
Kawasaki 214-8571
JAPAN

Prof. Dr. Rene Pinnau
Fachbereich Mathematik
T.U. Kaiserslautern
Erwin-Schrödinger-Straße
67653 Kaiserslautern

Dr. Paola Pozzi
Abteilung für Angewandte Mathematik
Universität Freiburg
Hermann-Herder-Str. 10
79104 Freiburg

Prof. Dr. Jean-Pierre Raymond
Institut de Mathematiques de Toulouse
Universite Paul Sabatier
118, route de Narbonne
F-31062 Toulouse Cedex 9

Dr. Philipp Reiter
Abteilung für Angewandte Mathematik
Universität Freiburg
Hermann-Herder-Str. 10
79104 Freiburg

Prof. Dr. Arnold Reusken
Institut für Geometrie und
Praktische Mathematik
RWTH Aachen
Templergraben 55
52061 Aachen

Prof. Dr. Jose-Francisco Rodrigues
CMAF & University of Lisbon
Centro de Matematica e Aplicacoes
Fundamentais
Av. Prof. Gama Pinto, 2
P-Lisboa 1649-003

Prof. Dr. Matthias Röger
Fachbereich Mathematik
Technische Universität Dortmund
Vogelpothsweg 87
44227 Dortmund

Prof. Dr. Piotr Rybka
Institute of Applied Mathematics
Warsaw University
ul. Banacha 2
02-097 Warsaw
POLAND

Prof. Dr. Ekkehard Sachs
Abteilung Mathematik
Fachbereich IV
Universität Trier
54286 Trier

Prof. Dr. Fadil Santosa
School of Mathematics
University of Minnesota
127 Vincent Hall
206 Church Street S. E.
Minneapolis MN 55455-0436
USA

Lavinia Sarbu
Department of Mathematics
University of Sussex
Falmer
GB-Brighton BN1 9QH

Prof. Dr. Alfred Schmidt
Zentrum für Technomathematik
FB3
Universität Bremen
Postfach 330 440
28334 Bremen

Dipl.Math. Stephan Schmidt
Fachbereich IV - Mathematik
Numerik - Optimierung, partielle
Differentialgleichungen
Universität Trier
54286 Trier

Prof. Dr. Kunibert G. Siebert
Fakultät für Mathematik
Universität Duisburg-Essen
Campus Duisburg
Forsthausweg 2
47057 Duisburg

Prof. Dr. Jürgen Sprekels
Weierstraß-Institut für
Angewandte Analysis und Stochastik
im Forschungsverbund Berlin e.V.
Mohrenstr. 39
10117 Berlin

Dr. Björn Stinner
Mathematics Institute
University of Warwick
Gibbet Hill Road
GB-Coventry CV4 7AL

Prof. Dr. Martin Stoll
Mathematical Institute
Oxford University
24-29 St. Giles
GB-Oxford OX1 3LB

Dr. Vanessa Styles
Department of Mathematics
University of Sussex
Falmer
GB-Brighton, East Sussex BN1 9RF

Prof. Dr. Endre Süli
Computing Laboratory
Oxford University
Wolfson Building
Parks Road
GB-Oxford OX1 3QD

Prof. Dr. Lutz Tobiska
Institut für Analysis und Numerik
Otto-von-Guericke-Universität
Magdeburg
Postfach 4120
39016 Magdeburg

Prof. Dr. Fredi Tröltzsch
Institut für Mathematik
Technische Universität Berlin
Sekr. MA 4-5
Strasse des 17. Juni 136
10623 Berlin

Prof. Dr. Boris Vexler
Zentrum Mathematik
TU München
Boltzmannstr. 3
85748 Garching bei München

Morten Vierling
Department Mathematik
Universität Hamburg
Bundesstr. 55
20146 Hamburg

Prof. Dr. Axel Voigt
Abteilung Mathematik
Technische Universität Dresden
Mommsenstr. 13
01069 Dresden

Thorben Weiner
Department Mathematik
Universität Hamburg
Bundesstr. 55
20146 Hamburg

Prof. Dr. Ningning Yan
Academy of Mathematics and
Systems Science
Chinese Academy of Sciences
Beijing 100 080
CHINA